

**Synthesis and Exploration of Functionalized
Zinc(II) and Terbium(III) complexes
as Molecular Probes**

Dissertation

zur Erlangung des Doktorgrades der Naturwissenschaften

(Dr. rer. nat.)

an der Fakultät Chemie und Pharmazie

der Universität Regensburg



vorgelegt von

Mouchumi Bhuyan

aus

Assam (Indien)

2012

The experimental part of this work was carried out between October 2008 and March 2012 under the supervision of Prof. Dr. Burkhard König at the Institute for Organic Chemistry, University of Regensburg, Regensburg/Germany.

The PhD thesis was submitted on: 24th April, 2012

The colloquium took place on: 25th May, 2012

Board of Examiners:	Prof. Dr. Robert Wolf	(Chairman)
	Prof. Dr. Burkhard König	(1st Referee)
	Prof. Dr. Hans-Achim Wagenknecht	(2nd Referee)
	Prof. Dr. Arno Pfitzner	(Examiner)

Acknowledgements

Through my career in chemistry so far, I have learnt a lot from almost everybody I have had interaction with. However when it comes to this thesis, my greatest debt rests with my supervisor Prof. Dr. Burkhard König. I want to express my sincere gratitude to him for giving me an opportunity to visit Germany and work in his research group and also for all kinds of help he offered me throughout these years.

I am very thankful to Prof. Dr Hans-Achim Wagenknecht and Prof. Dr. Arno Pfitzner for being the doctoral committee members of my thesis. I thank Prof. Dr. Robert Wolf for being Chairman in my PhD defence.

I express my gratitude to Prof. Dr. Itaru Hamachi, Prof. Dr. Olaf Prante and Dr. Sabine Amslinger for the collaborative projects.

I thank all members of the central analytical department, especially Annette Schramm, Georgine Stühler, Fritz Kastner, Dr. Thomas Burgemeister, Dr. Ilya Shenderovich for recording 2D NMR spectra, Wolfgang Söllner and Joseph Kiermaier for recording mass spectra, Dr. Manfred Zabel and Sabine Stempfhuber for providing X-ray crystal structure.

I would like to thank Dr. Rudi Vasold and Simone Strauß for HPLC, Ernst Lautenschlager for his help in all technical questions. I thank Susanne Schulze for being so nice and fast regarding chemical order lists. I would like to thank Dita Fritsch for Western Bolt.

I am grateful to Evonik Degussa foundation and Bayerischen Forschungsstiftung for the financial assistance during my Ph.D period.

I would like to thank all my present and past co-workers, who made my stay in Regensburg colourful and exciting, especially my lab mates Dr. Michael Egger, Alexandra Bila, Andreas Hohenleutner, Susanna Schmidbauer and Christoph Stanglmair. I thank Thomas Zanni for being so joyous, cooperative and friendly during our collaborative project. It was great fun working with him.

I thank Natascha Kuzmanovic, Maria Cherevatskaya, Josef Herrmann, Stefan Balk, Michael Dobmeier, Dr. Tatiana Mitkina for all fun moments in our kitchen, some of which were although tiny but absolutely funny. It was an immense pleasure to work with all of you.

I thank all my Indian friends that I have met during my stay at Regensburg: Amilan, Anand, Suva, Durga, Sudipta, Supratim, Senthil are only a few to name and especially I thank Tapan and Anu for being so supportive and helpful during my accident.

On a very personal front, gratitude goes to my grandma (Aaita), my mom, my parents in laws and my friends especially Arkaprava Basu, Anamitra Roychoudhury and Moitree Laskar. They are parts of my life. Arka has been a constant source of encouragement, amusement, and friendship. I will always cherish his encouraging and reviving comments throughout these years. Without their friendship life wouldn't have been such fun. I would also thank my friend Pankaj Barah, for many practical discussions, debates and jokes. It is a pleasure to thank Borun for everything, among them his friendship, encouragement and love. My life is greatly enriched by his companionship.

Last but definitely not least, I would like to thank myself for finally finishing my thesis.

Dedicated to Aaita

উৎসৰ্গা

সাদৰী আইতাৰ চেনেহী কোলাত

*“Where Nature ceases to produce its own species,
Mankind begins, using natural things,
and with the aid of this very Nature,
creates an infinity of species...”*

– Leonardo da Vinci

Table of Contents

Chapter 1

1. Rigid Luminescent bis-Zinc(II)-bis-Cyclen Complexes for the Detection of Phosphate Anions and Non-covalent Protein Labeling in Aqueous Solution

	1
1.1. General Introduction	2
1.1.1. Selective labeling of proteins: Background	2
1.1.2. Recognition of biologically relevant phosphates in aqueous solution: Snippets	3
1.2. Outline of the chapter	5
1.3. Results and discussions	5
1.3.1. Synthesis of Zn(II)-cyclen complexes	5
1.3.2. UV-visible and luminescent properties of Zn(II)-cyclen complexes	9
1.3.3. Coordination of tetra-aspartate (Boc-D ₄ -NH ₂) and tetra-glutamate (Boc-E ₄ -NH ₂) peptides sequence	11
1.3.4. Coordination of phosphate anions	13
1.4. Concluding remarks	15
1.5. Experimental Section	16
1.6. Supporting Data	24
1.7. References	37

Chapter 2

2. Rigid Amphiphilic Molecular Receptors, Bioconjugates and Radiopharmaceuticals based on Metal-cyclen complexes via Click chemistry

	39
2.1. General Introduction	40
2.1.1. The “Click” Philosophy	40
2.1.2. The Click reaction: An efficient strategy for bioconjugations	41
2.2. Outline of the Chapter	44
2.3. Design and synthesis of bioconjugates based on a Zn(II)-bis-cyclen complex: introduction to potential applications, results and discussions	44

2.3.1. Synthesis of bis-cyclen azide	44
2.3.2. Biotin bioconjugate of a Zn(II)-bis-cyclen complex for potential applications in activity based proteomics	45
2.3.2.1. Introduction and aim of the project	45
2.3.2.2. Design and synthesis of biotin bioconjugate of Zn(II)-bis-cyclen complex	45
2.3.2.3. Selective recognition of phosphorylated protein in gel phase	46
2.3.2.4. Concluding remarks	47
2.3.3. Modified cyclen based precursor for potential radiopharmaceuticals for Positron Emission Tomography (PET)	47
2.3.3.1. Introduction and aim of the project	47
2.3.3.2. Synthesis of precursor for potential Radiopharmaceuticals for Positron Emission Tomography (PET)	48
2.3.3.3. Concluding remarks	49
2.3.4. Design and synthesis of rigid amphiphilic modified Zn(II)-cyclen based receptors for a template guided cooperative self-assembly of nucleotides at interfaces	50
2.3.4.1. Introduction and aim of the project	50
2.3.4.2. Design and synthesis of rigid Zn(II)-bis-cyclen based amphiphilic receptors	51
2.3.4.3. Concluding remarks	54
2.4. Experimental Section	54
2.5. Supporting Data	65
2.6. References	72

Chapter 3

3. Phosphorescent Small Unilamellar Vesicles with embedded Amphiphilic Lanthanide complexes

	75
3.1. General Introduction	76
3.1.1. Lanthanides: Relevance	76
3.1.2. Sensitized Lanthanide Luminescence: Principles and Advantages	76
3.1.3. Phospholipid based Liposomes: Introduction	78
3.1.4. Liposomal stability and surface modification chemistry	79

3.1.5. Lanthanide complexes and liposomes	83
3.2. Outline of the chapter	84
3.3. Temperature responsive phosphorescent small unilamellar vesicles	85
3.3.1. Introduction	85
3.3.2. Results and discussions	86
3.3.2.1. Synthesis of amphiphilic Tb(III) complex	86
3.3.2.2. Preparation of the Tb(III) containing vesicular systems (LNT)	87
3.3.2.3. Temperature dependent measurements	89
3.3.3. Concluding remarks	92
3.3.4. Experimental Section	93
3.3.5. Supporting Data	97
3.4. Nano-sized Vesicular Membranes with Amphiphilic Binding Sites and Lanthanide complex with Delayed Luminescence as Reporter Dye	101
3.4.1. Introduction	101
3.4.2. Results and Discussions	101
3.4.2.1. Anion recognition site and reporter dye	101
3.4.2.2. Vesicle Preparation and Characterization of vesicle dispersions	102
3.4.2.3. Enhancement of lanthanide luminescence by self assembly	103
3.4.2.4. Attempts to use lanthanide based complex as reporter dye: Experimental observations	104
3.4.3. Concluding remarks	106
3.5. References	107
Summary	112
Zusammenfassung	113
Abbreviations	114
Appendix	

Chapter 1

Rigid Luminescent bis-Zinc(II)-bis-Cyclen Complexes for the Detection of Phosphate Anions and Non-covalent Protein Labeling in Aqueous Solution

“Beyond molecular chemistry based on the covalent bond, there lies the field of Supramolecular Chemistry, whose goal is to gain control over the intermolecular interactions”

-Jean Marie Lehn

1.1 General Introduction

1.1.1 Selective labeling of proteins: Background

Protein labeling with chemically modified small molecular probe is an important tool for sensing and visualizing protein dynamics, localization, functions and protein-protein interaction *in vivo*. It is an invaluable technique to understand protein functions and networks in living cells. Genetically encoded fluorescent protein (FPs and GFPs) is the most popular technique for protein labeling^[1] in protein research and this has allowed a wide range of studies in living cells with high labeling specificity.^[2]

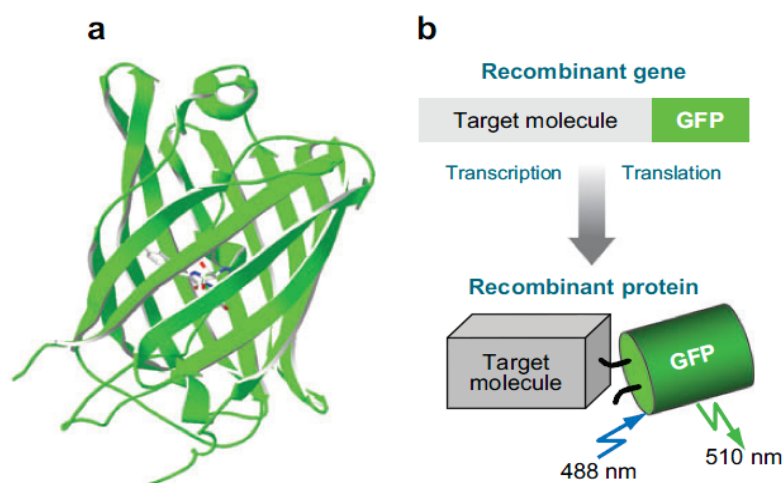


Figure 1: The principle of GFP labeling. (a) The structure of GFP. (b) Schematic representation of a recombinant gene containing cDNA of a target molecule fused to that of GFP. The expression of the recombinant gene in cells allows the observation of the recombinant protein with excitation and emission wavelengths of GFP at 488 and 510 nm, respectively [Reprinted with permission from the quoted reference]^[3]

However this technique has some potential disadvantages. First is, these fluorescent proteins are large enough to interfere with the localization, structure or activity of the proteins to which they are fused and second, these fluorescent proteins are poor probes for environmental cues like pH, hydrophobicity and ion concentrations.^[4] All these led to the current efforts to develop alternate technique of proteins by chemically modified small luminescent markers or affinity tags. Based on binding mechanisms, most chemical labeling techniques can be classified into two major categories; enzymatic labeling and affinity labeling. Enzymatic labeling involves covalent labeling while affinity labeling deals with non-covalent methods to label proteins. There are several reports of enzymatic labeling on protein research and some remarkable examples include: covalent modification of fusion proteins on cell surface like acyl carrier protein (ACP) by phosphopantetheine transferase (PPTase),^[5]

site specific introduction of genetically encoded aldehyde tag into formylglycine generating enzyme,^[6] sequential labeling of fusion proteins of O⁶-alkylguanine-DNA alkyltransferase (AGT) with different fluorophores in mammalian cells,^[7] selective labeling of farnesylation motif proteins by using protein farnesyltransferase (PFTase).^[8] Although the permanence of covalent labeling allows unambiguous analyses of the protein after labeling,^[9] this method is irreversible and also often the covalent modifications of proteins involves tedious synthesis. Non-covalent labeling of protein is free from the limitations of covalent labeling and reversibility of this method can be considered as the primary advantage. The non-covalent methods include several high affinity snap tags, antibodies and metal chelation methods.^[10]

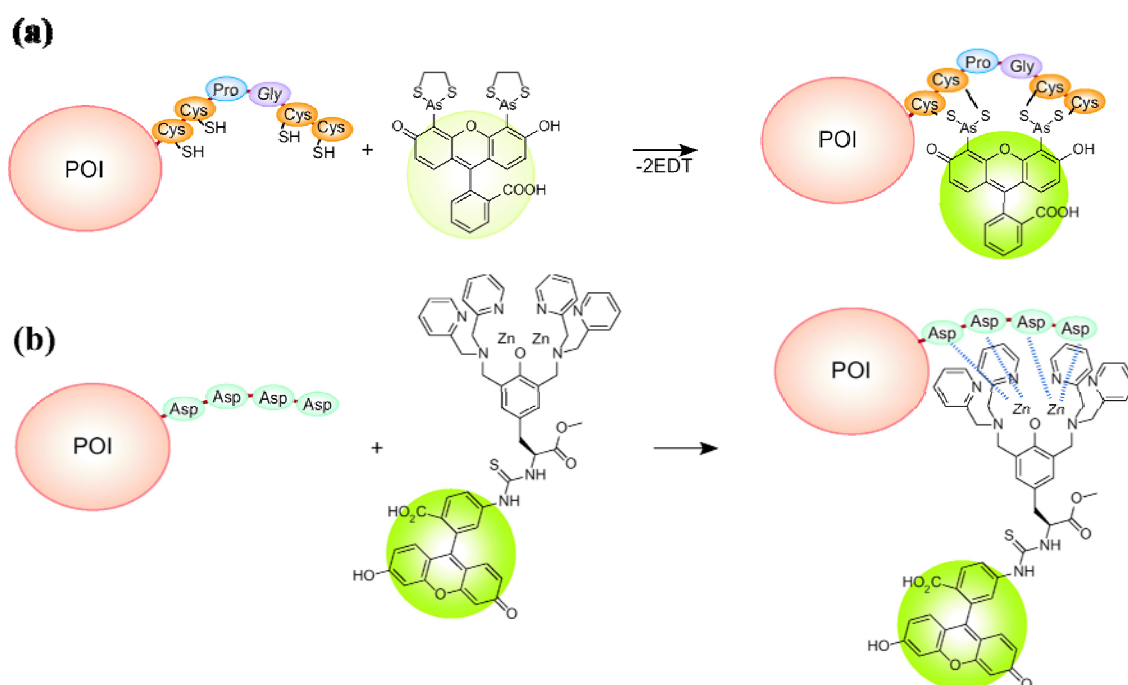


Figure 2: Chemical labeling of proteins of interest (POI) with small fluorescent molecules based on metal-chelation (a) tetracysteine/biarsenical system (b) oligo-aspartate/zinc-complex system [adapted from the quoted reference]^[1]

1.1.2 Recognition of biologically relevant phosphates in aqueous solution: Snippets

Phosphates are ubiquitously present in nature and they are an integral part of recognition events involving proteins, nucleic acids, cofactors, and antibodies. Phosphates are vividly present in RNA and DNA, in phosphorylated saccharides and phosphorylated proteins.^[11] Protein phosphorylation plays a significant role in a wide range of cellular processes. The nucleotide, adenosine triphosphate (ATP), is the universal energy currency for metabolism and involved in

intracellular energy transport for various metabolic processes including biosynthetic reactions, mobility, and cell division. The hydrolysis of ATP in cells produces pyrophosphate (PPi) along with AMP and it plays an important role in intracellular signaling.^[12] Hence development of artificial phosphate anion receptors is of immense importance to understand numerous biological processes.

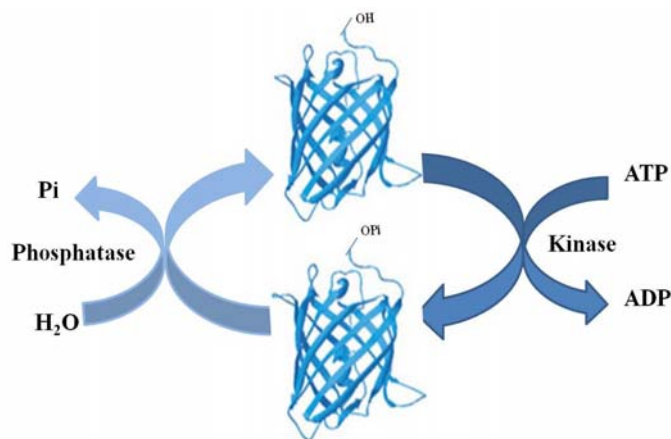


Figure 3: Schematic representation of reversible protein phosphorylation by kinase [adapted from the quoted reference]^[13]

Transition metal complexes with vacant coordination sites are well suited to serve as phosphate ion binding sites.^[14] Some metal complexes were reported to show selective binding to biologically relevant phosphates and were used as binding receptor moieties in phosphate recognition: Zinc(II)-dipicolylamine (Dpa) complexes as demonstrated by Hamachi,^[15] Hong^[16] and Smith^[17] and macrocyclic 1,4,7,10- tetraazacyclododecane (cyclen) transition metal complexes reported by Kikuchi^[18] and Kimura.^[19]

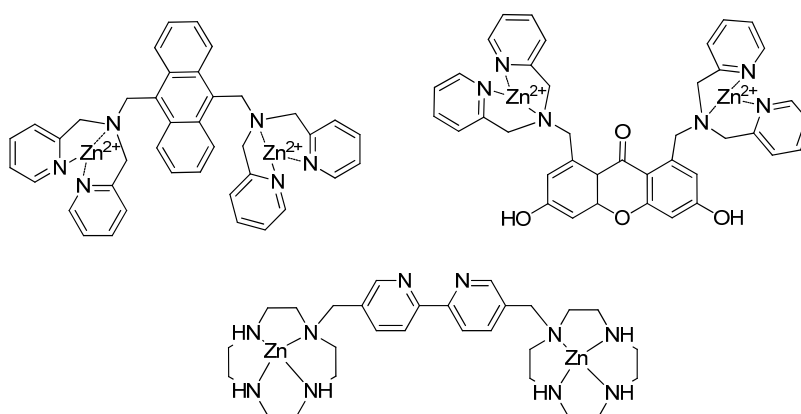


Figure 4: Some of the metal complexes widely used as binding receptors in phosphate recognition ^[15, 19]

1.2 Outline of the chapter¹

In this chapter the synthesis of a series of water soluble bis- and tetrakis-Zn(II)-cyclen complexes with rigid structures is reported, which were designed to enhance the carboxylate and phosphate ion binding response in contrast to analogues with less confined molecular structure. Boc-protected 6-chloro-1, 3, 5-triazine-bis cyclen was coupled to different aryl and alkyl moieties in moderate to high yields and subsequently converted into the corresponding bis- or tetrakis-Zn(II)-cyclen complexes. The bis-Zn(II)-cyclen moiety is known for its affinity to anions. Depending on the arene substituent some of the synthesized synthetic receptors are luminescent. They were studied by absorption and emission spectroscopy for their response to the presence of phosphate anions of biological relevance in buffered aqueous solution at neutral pH and for their affinity to the genetically encodable oligo-aspartate and glutamate sequences (D₄- and E₄-tag) recently introduced by Hamachi et al. The rigid structures of the compounds enhance the electronic coupling between the metal complex binding site and the reporter dye. This leads to an increased anion binding response in homogeneous aqueous solution.

1.3 Results and Discussions²

1.3.1 Synthesis of Zn(II)-cyclen complexes

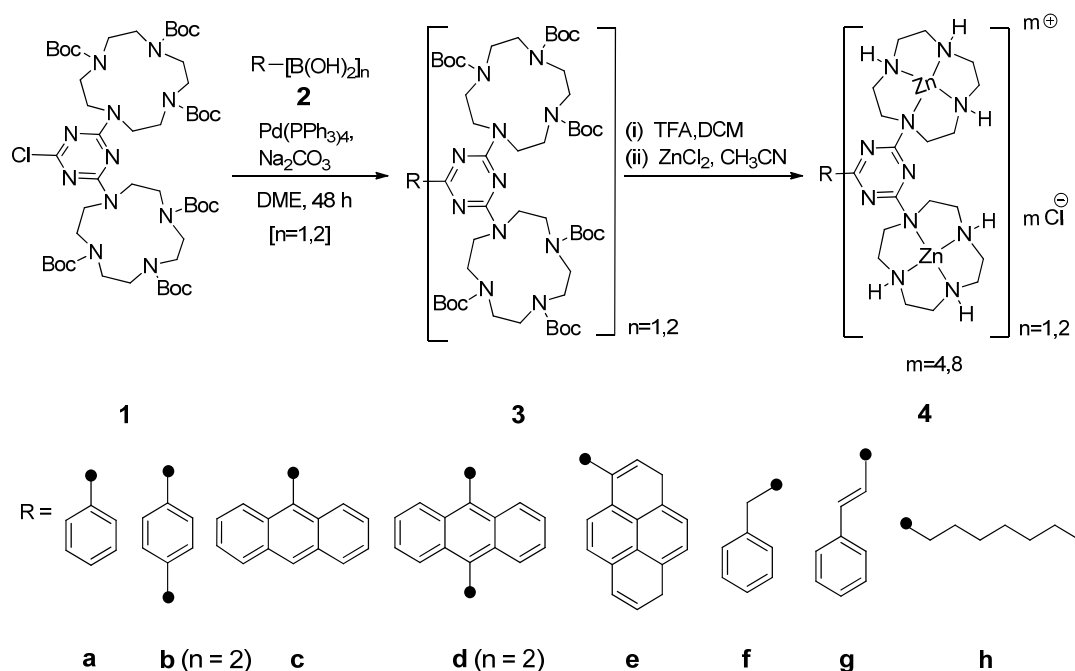
The rigid bis-Zn(II)-cyclen based receptors are synthesized mainly by using Suzuki-Miyaura cross coupling reactions as shown in Scheme 1.

Threefold Boc-protected bis-cyclen and compound **1** were synthesized following an earlier reported procedure.^[20] The protection of the cyclen azamacrocycle reduces polarity and prevents multi-N-substitution. Trichlorotriazine reacts with two equivalents of threefold Boc-protected cyclen yielding **1** in a clean twofold nucleophilic aromatic substitution. The remaining chloro substituent of the triazine bis-cyclen **1** was then used for coupling with different boronic acids **2** via palladium catalyzed Suzuki-Miyaura reaction. The synthesized ligands **3** are listed in the Table 1 with their isolated yields. The obtained Boc-protected cyclen ligands **3** were deprotected with trifluoroacetic acid to give the corresponding ammonium salts in quantitative yields. Finally, complexation of the azamacrocyclic amines with ZnCl₂ gave the Zn(II)-cyclen complexes **4**.

¹ M. Bhuyan, E. Katayev, S. Stadlbauer, H. Nonaka, A. Ojida, I. Hamachi, B. König *Eur. J. Org. Chem.* **2011**, 2011, 2807.

² All compounds were synthesized at University of Regensburg by Mouchumi Bhuyan. The peptide tags used were provided by the group of Itaru Hamachi, Kyoto University, Japan. All the investigations were carried out at University of Regensburg.

Complex **4c** was characterized with the help of single crystal diffraction analysis. In order to obtain suitable crystals a small excess of zinc(II) chloride present in the aqueous solution was used for crystallization. This conditions led to the formation of complex $[(\mathbf{4c}-2\text{Cl})^{2+}][\text{ZnCl}_4^{2-}]$ (Figure 1). The cyclen moieties coordinate to zinc cations with typical Zn-N distances of 2.1 Å to the three aliphatic nitrogen atoms and one longer Zn-N distance of 2.6 Å to the triazine nitrogen. The anthracene ring is twisted from the triazine plane by a torsion angle of 68°.



Scheme 1: The synthesis of triazine bis-Zn (II)-cyclen complexes **4a – h**

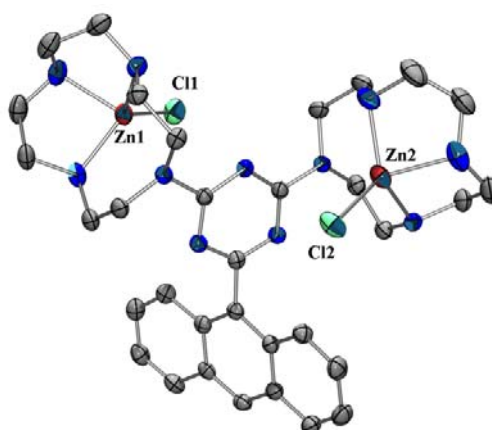
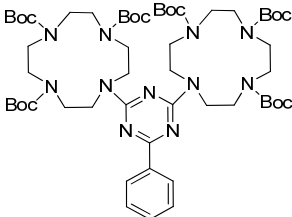
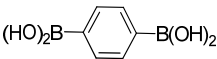
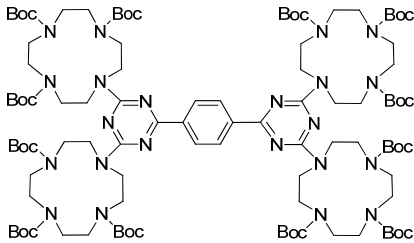
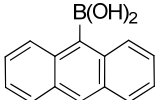
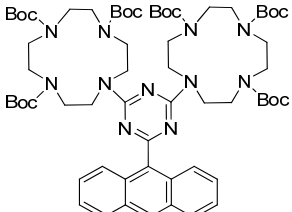
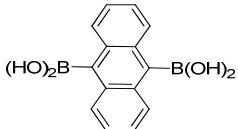
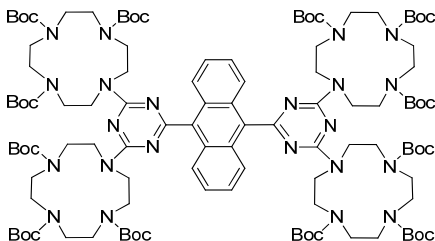


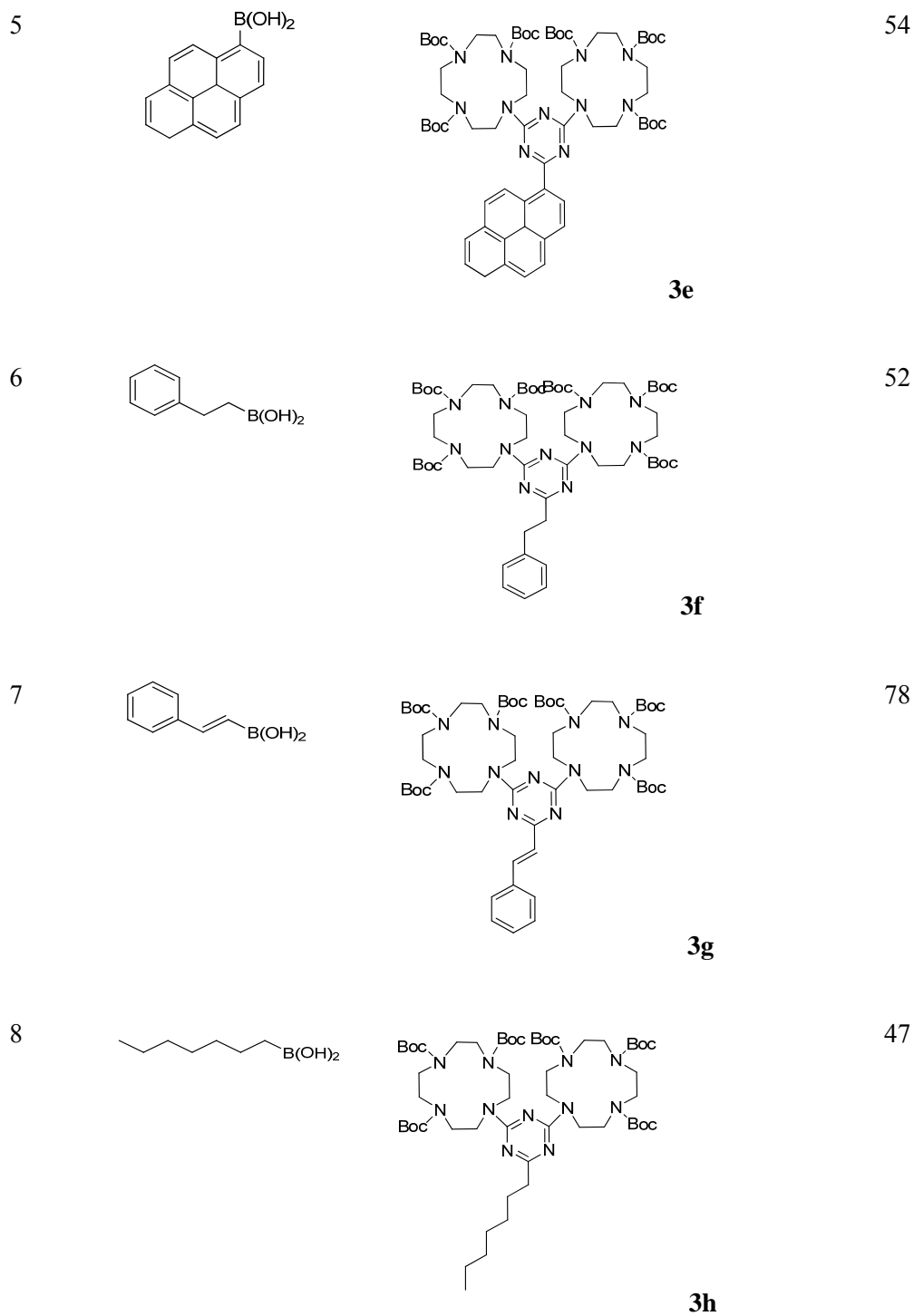
Figure 5: ORTEP rendered view of the molecular structure of complex **4c**. Hydrogen atoms, methanol and the ZnCl_4^{2-} anion are omitted for clarity. Ellipsoids are shown in 50% probability level.

1. Rigid Luminescent bis-Zinc(II)-bis-Cyclen Complexes for the Detection of Phosphate Anions and non-covalent Protein Labeling in Aqueous Solution

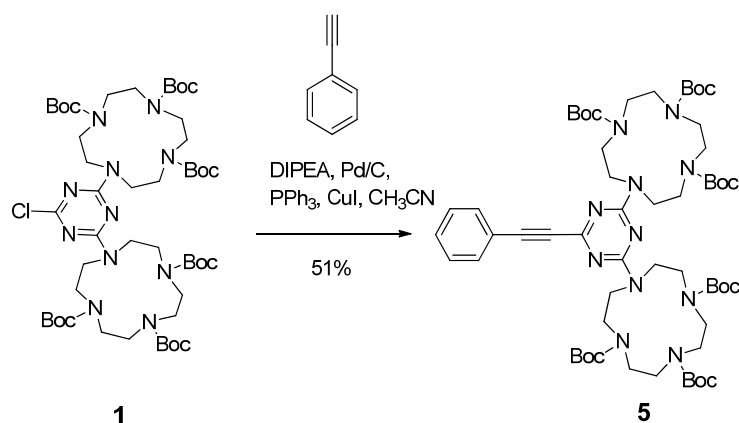
Table 1: Structures and isolated yields of the synthesized bis- and tetrakis Boc-protected cyclen ligands **3a-h** obtained by Suzuki-Miyaura cross coupling strategy

Entry	Boronic acids 2	Protected Ligands 3	Isolated Yield [%]
1		 3a	50
2		 3b	31
3		 3c	50
4		 3d	30

1. Rigid Luminescent bis-Zinc(II)-bis-Cyclen Complexes for the Detection of Phosphate Anions and non-covalent Protein Labeling in Aqueous Solution



In the attempts to include rigidity in bis-Zn(II)-cyclen complexes, apart from Suzuki-Miyaura cross coupling strategy, Sonogashira cross coupling has also been tried (Scheme 2), but this strategy has not been further developed due to the unsatisfactory chemical yields.



Scheme 2: The synthesis of modified triazine bis-cyclen ligand **5**, for potential metal complexation using Sonogashira cross coupling strategy

1.3.2 UV-visible and luminescent properties of Zn(II)-cyclen complexes

Some of the synthesised complexes **4** bear fluorophores and their UV-visible and luminescent properties were investigated. The data are summarized in Table 2.

Complexes	Absorption ^[a]			Emission ^[b]	
	λ_{max}	$\log \epsilon$	$\lambda_{\text{excitation}}$ [nm]	λ_{max} [nm]	Φ_{rel} (%) ^[c]
4a	224	4.44	230	457	0.02
4b	285	4.53	290	385	0.2
4c	365	3.90	364	455	2.0
4d	370	3.36	372	456	20
4e	350	4.16	354	453	5.9
4g	220	4.10	220	424	0.02

^[a] Measured in HEPES buffer at a concentration of $c = 10^{-4}$ mol/L. ^[b] Measured in HEPES buffer at a concentration of $c = 10^{-5}$ mol/L. ^[c] Relative quantum yields were determined using quinine sulphate ($\Phi_{\text{Quinine sulphate}} = 58\%$).^[21]

Table 2: Absorption and emission data of the synthesized complexes **4a-e** and **4g** [All compounds have similar emission maxima in HEPES buffer] The emission quantum yields of the synthesised complexes were measured in methanol as solvent with quinine sulphate as reference to explore variations of the photo physical properties.

Highest quantum yields are observed for compounds **4b-4e**. These compounds were studied in detail using fluorescence titrations in 25 mM HEPES buffer, pH 7.4 at 25°C and binding affinities for carboxylates and phosphates were determined. The concentration of HEPES buffer was chosen to cover the range of binding affinities which are characteristic for complexes **4b-4e**. We were interested

to compare the selectivities of binding and emission responses of rigid bis- and tetra-Zn(II) complexes arising from the interaction with different anions. The studies performed by the Hamachi group using Zn(II)-Dpa-Tyr and a series of oligo-aspartate peptides (Boc-D_n-NH₂, n = 2 – 5) and oligo-glutamate peptides (Boc-E_n-NH₂, n = 3, 4) revealed that D₄-tag (n= 4) has the highest affinity.^[22] Based on the reported results, we selected D₄- and E₄-tag sequences for our investigations. The derived binding affinities of the complexes with the carboxylates, pyrophosphate (PPi) and O-phospho-L-serine are shown in Table 3. Analysis of fluorescence responses (F/F₀) in Table 3 reveals that in most cases the coordination of a guest to a zinc complex leads to an increase of emission. This is in good agreement with reports on Zn²⁺-DPA complexes.^{16d}

	Boc-E₄-NH₂	Boc-D₄-NH₂	PPi	O-Phospho-L-serine
4d	logβ ₂₁ =13.46(12) logβ ₁₁ =7.21(6)	logβ ₂₁ =16.22(8) logβ ₁₁ > 7	^[b]	logβ ₁₁ <3
H:G ratio, F/F ₀ ^[a]	1:1, 6.8	1:1, 4.8	1:2, 5.5	1:1, 1.21
4b	logβ ₂₁ =12.24(8) logβ ₁₁ =6.74(3)	logβ ₁₁ > 7 logβ ₁₂ =13.38(8)	^[b]	^[c]
H:G ratio, F/F ₀ ^[a]	1:1, 2.2	1:2, 1.3	1:2, 0.1	
4c	logβ ₁₁ =3.41(1)	logβ ₁₁ =3.31(1)	^[b]	^[c]
H:G ratio, F/F ₀ ^[a]	1:1, 1.3	1:1, 1.8	1:1, 3.4	
4e	logβ ₁₁ < 3	logβ ₁₁ < 3	logβ ₂₁ =11.05(7) logβ ₂₂ =16.55(12)	^[c]
H:G ratio, F/F ₀ ^[a]	1:1, 0.9	1:1, 0.9	1:1, 1.2	

^[a] Stoichiometry of host (H) : guest (G) ration was determined according to Job's method; F/F₀ = changes in fluorescence of zinc complex upon addition of one equivalent of a guest. ^[b] Good fitting of the experimental curve was not possible; each stepwise binding constant was of the range of > 10⁶ M⁻¹. ^[c] Changes in fluorescence response upon titration with guest were negligible.

Table 3: Binding characteristics of complexes **4b–e** measured as 0.01–0.05 mM solutions in 25 mM HEPES buffer, pH 7.4, 25 °C

According to our ESI mass spectroscopy investigations, at the concentration required for fluorescence measurement some di- and tri-nuclear zinc complexes are formed from the parent tetranuclear zinc complexes. They are weakly fluorescent due to quenching by photoinduced electron transfer (PET) from the uncomplexed aliphatic nitrogens. The coordination of an anion induces complete Zn²⁺-cation

coordination to the nitrogen ligand and thus decreases PET quenching,^[23] which results in a turn-on response. The presence of this mechanism was proved by addition of an excess of zinc (II) chloride to complexes, in this case slight increase (1.1-1.4 fold) of fluorescence was observed. However, the coordination of E₄- and D₄-tag to complex **4d** led to much larger increase of fluorescence - 6.8 and 4.8, respectively. This data indicate that another turn-on mechanism is also present: The coordination of a guest rigidifies the structure leading to a significant emission increase.

1.3.3 Coordination of tetra-aspartate (Boc-D₄-NH₂) and tetra-glutamate (Boc-E₄-NH₂) peptides sequences

Coordination of D₄ or E₄ peptide sequences to bis-Zn(II) complexes **4c** and **4e** is rather weak and only small changes in fluorescence are observed upon addition of ca. 10 equivalents of a guest. The tetra-Zn(II) complexes have much higher binding affinities for both E₄- and D₄-tags with stepwise binding constants of ca. 10⁷ M⁻¹. Such a dramatic increase is explained by the increased coulombic interaction in a host-guest complex. The characteristic changes in emission and the binding isotherm for tetra-Zn(II) complex **4d** are shown in Figure 6.

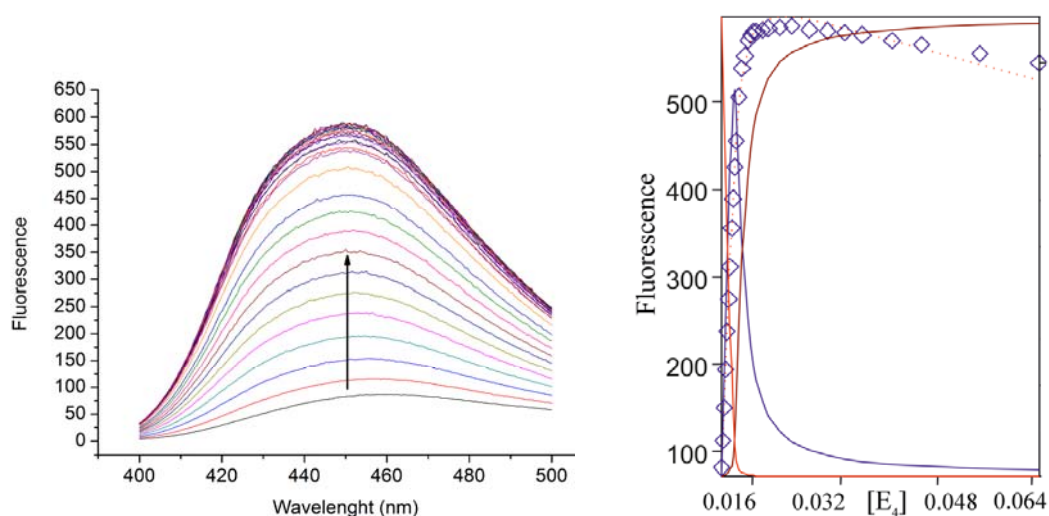


Figure 6: Changes of fluorescence of tetra-Zn(II) complex **4d** upon addition of the E₄-tag. Experimental points on the binding isotherm are shown as rhombuses. The titrations were carried out in 25 mM HEPES buffer, pH 7.4, at 25°C, excitation wavelength λ_{ex} =320 nm.

Binding isotherms were fitted to a model of stepwise 2:1, 1:1 and 1:2 binding. Aggregate formation with a 2:1 stoichiometry appears only due to the addition of a mM solution of the guest to the μM solution of a host. During first additions the complex is in large excess, thus several molecules of the later can coordinate to the tetracarboxylate. The other binding stoichiometries were observed in

solution and confirmed by ESI spectrometry. Comparison of the calculated and experimentally found isotope distribution of the molecular ions is shown in Figure 7.

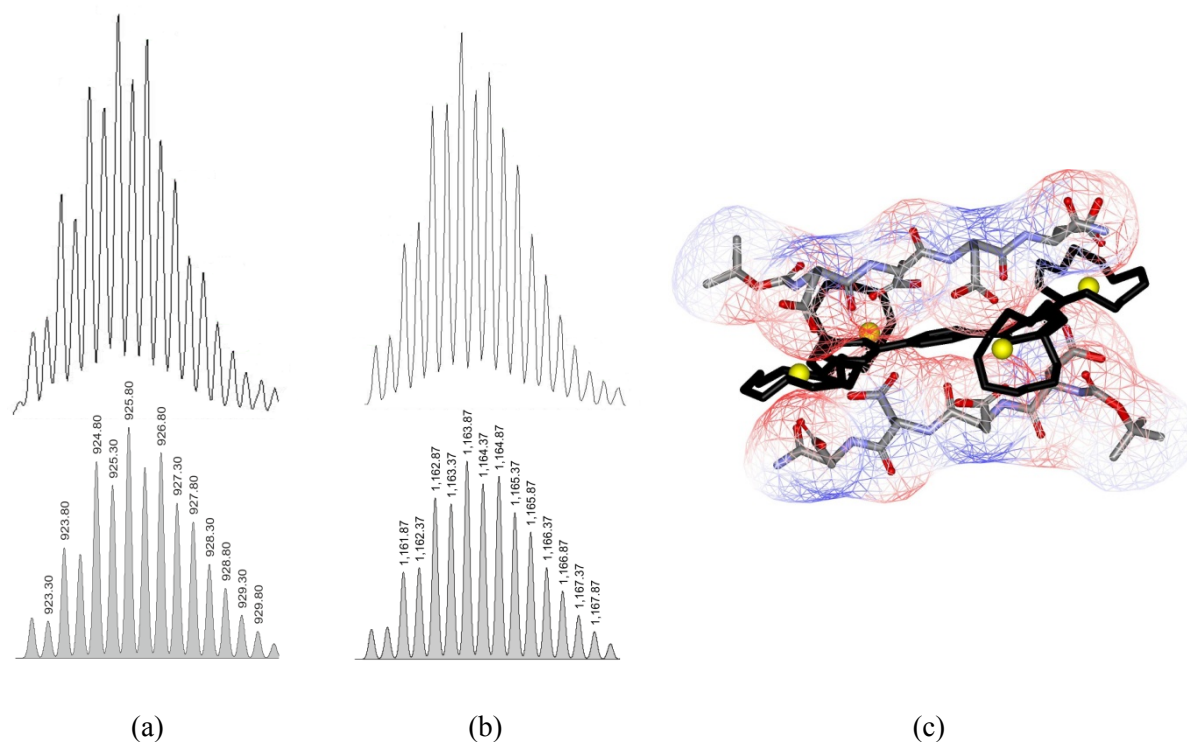


Figure 7: Comparison of the calculated (lower) and observed (upper) isotope distribution for ions: (a) $m/z=923$ [**4d**-8Cl+D₄-6H]²⁺ and (b) $m/z=1160$ [**4b**-8Cl+2D₄-6H]²⁺ (c) Proposed geometry of receptor–peptide tag aggregate of **4b** with two molecules of D₄-tag.

In order to understand the mode of interactions between the oligopeptide and the tetrazine complexes we have conducted DFT (B3LYP, 6-31G*) calculations using Spartan'06 (Wavefunction Inc.). According to the calculations the scaffold of the two benzene linked binuclear Zn(II)-cyclen complexes (**4b**) perfectly matches the oligo peptide tags (D₄, E₄) structure and charge distribution. In a sandwich-like aggregate of **4b** and the tag protein strong electrostatic interactions are likely, resulting in the observed high apparent binding affinity. The electrostatic potential surface is displayed as wired mesh of the D₄-tag in Figure 7. The red colour indicates a high density of negative charges at the carboxylate residues of the tag. The cationic Zn(II)-cyclen favourably interacts with the anionic carboxylate residues. The figure shows a sandwich-like 1:2 receptor–peptide tag aggregate formation of **4b** and the D₄-tag. The energy minimized structure of **4d** shows that unlike **4b**, where benzene and triazine moieties are in plane, the plane of anthracene is perpendicular to the plane of the triazine. This creates steric hindrance, which may be responsible for the observed 1:1 receptor to peptide binding stoichiometry in case of **4d**. The predicted twisted conformation of the triazine

anthracene moiety of complex **4d** is in a good agreement with the crystal structure of bis-Zn(II)-anthracene complex **4c**.

1.3.4 Coordination of phosphate anions

Bis-Zn(II)-cyclen complexes show high affinity for phosphate anions in aqueous solution, which is of interest for potential applications in biological phosphate recognition. However, the so far developed bis-Zn(II)-cyclen based synthetic receptors have flexible spacers between the receptor moiety and the signalling unit. Due to this flexibility, the luminescent group cannot respond effectively to the binding event by a change in its emission properties. Figure 8 shows one of our previously reported complexes with flexible linker between fluorophore and the receptor and its negligible change emission properties in presence of analytes in homogeneous solution.^[24]

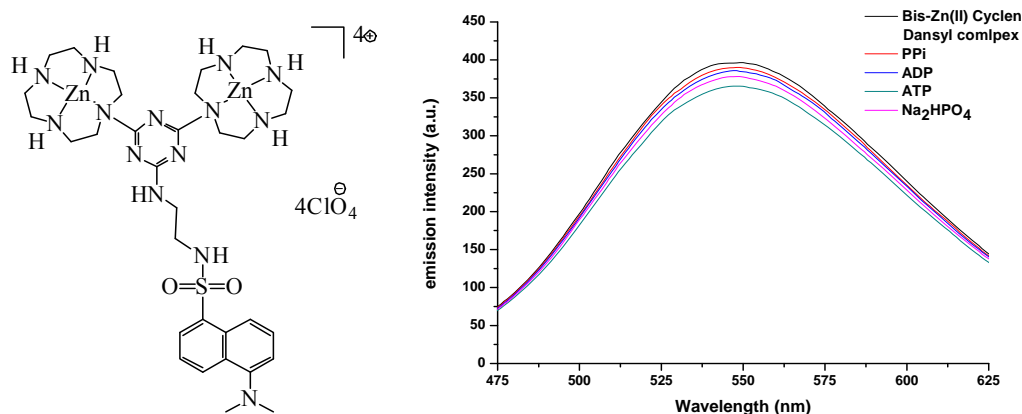


Figure 8: Dinuclear Zn(II)-cyclen dansyl complex with flexible linker between receptor and fluorophore (left); emission intensity changes of binuclear Zn(II)-cyclen dansyl complex (80 μ M in HEPES buffer, pH 7.4, $\lambda_{\text{ex}} = 330$ nm, 25 $^{\circ}$ C) upon addition of various nucleotides and phosphates (right).

In the here reported synthesised bis-Zn(II)-cyclen complexes, the rigid molecular structure and the direct conjugation of the central triazine unit to the arenes allows the transmission of the anion binding event at the cyclen complex to the signalling unit, which response by changes of the emission properties (Table 3). The affinities of the complexes for monophosphate anions such as phenylphosphate or O-phospho-L-serine are rather small, but excellent for polyphosphates. The most efficient response was observed for bis-Zn(II)-anthracene containing complex **4c**, whose fluorescence is 3.4 fold increased upon addition of one equiv. of pyrophosphate. The sensitivity for pyrophosphate is even higher for tetra-Zn(II) complexes: 5.5 and 0.1 fold change in fluorescence for anthracene (**4d**) and benzene (**4b**) containing complexes, respectively (Table 3). Complexes **4b** and **4d** have opposite

responses: the presence of pyrophosphate quenches the fluorescence of **4b**, but strongly increases the fluorescence of **4d** (Figure 9).

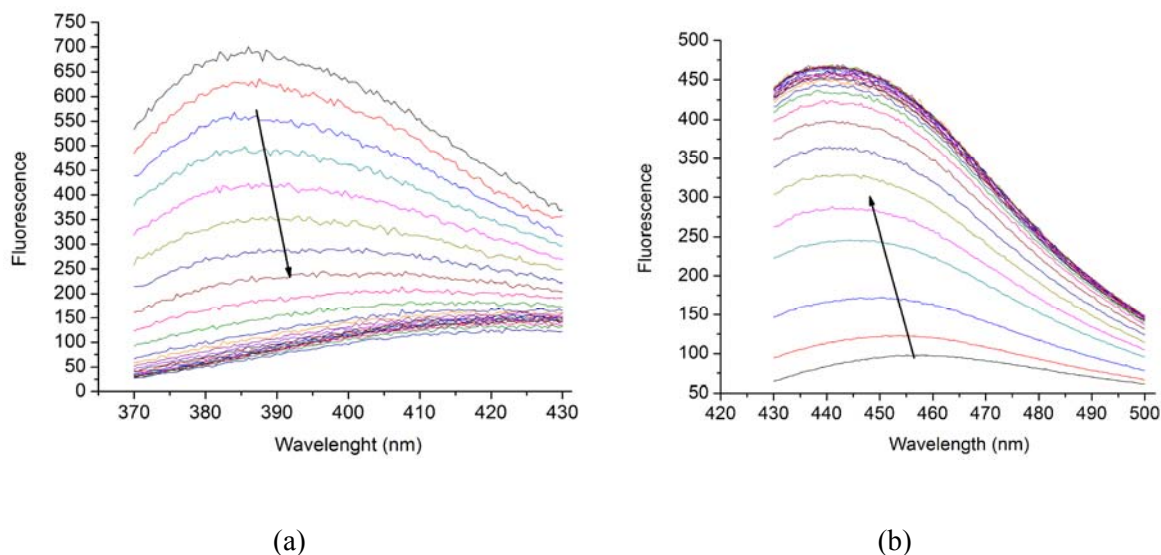


Figure 9: Fluorescence response upon addition of sodium pyrophosphate to the solution of (a) complex **4b** and solution of (b) complex **4d**. Titrations were carried out in 25 mM HEPES buffer, pH 7.4, at 25°C.

Though the affinities of tetra-Zn(II) complexes for pyrophosphate were good it was difficult to fit binding isotherms with typical models. Job's plot analysis showed that tetra-Zn(II) complexes bind pyrophosphate in a 1:2 stoichiometry. Using this model we were able to obtain a stepwise binding constant in the order 10^7 M^{-1} (Table 3). The binding isotherm of bis-Zn(II) complex **4c** was successfully fitted using a 2:1 and 2:2 stepwise binding model. Additional proof for the formation of the complex with a 2:2 stoichiometry were obtained using ESI mass spectrometry, where the complex with the composition $[(\mathbf{4c}\text{-}4\text{Cl}^-\text{+}2\text{PPi}^{4-}\text{+}2\text{Na}^+)]^{2+}$ was one of the major peaks (Supporting data, Figure 19). Thus, coordination of pyrophosphate to **4c** induces dimerization of the complex. This observation led us to suggest that strong quenching of the fluorescence of complex **4b** upon interaction with pyrophosphate can arise from a similar dimerization resulting in π - π stacking interactions of planar benzene-triazine moieties (Figure 10(c)). This could not be the case for anthracene-containing tetra-Zn(II) complex, because it does not have a planar structure according to DFT calculations of **4d** and the X-ray structure of **4c**, thus close interaction of the anthracene rings is not sterically favourable. To prove the dimerization of **4b** we have conducted ESI measurements of both complexes **4b** and **4d** in the presence of excess of pyrophosphate in aqueous solution. Though the major peaks for both complexes corresponded to $[\mathbf{4b}\text{-}8\text{Cl}^-\text{+}2\text{PPi}^{4-}\text{+}2\text{Na}^+]^{2+}$ and $[\mathbf{4d}\text{-}8\text{Cl}^-\text{+}2\text{PPi}^{4-}\text{+}2\text{Na}^+]^{2+}$, the presence of the dimer $[(\mathbf{4b}\text{-}8\text{Cl}^-\text{+}2\text{PPi}^{4-}\text{+}2\text{Na}^+)_2]^{2+}$ was clearly observed allowing to compare the isotope distribution with the predicted one (Figure 10). For the anthracene containing tetra-Zn(II) complex **4d**

the corresponding dimer was also observed, but with much lower intensity not allowing to resolve experimentally the isotope distribution.

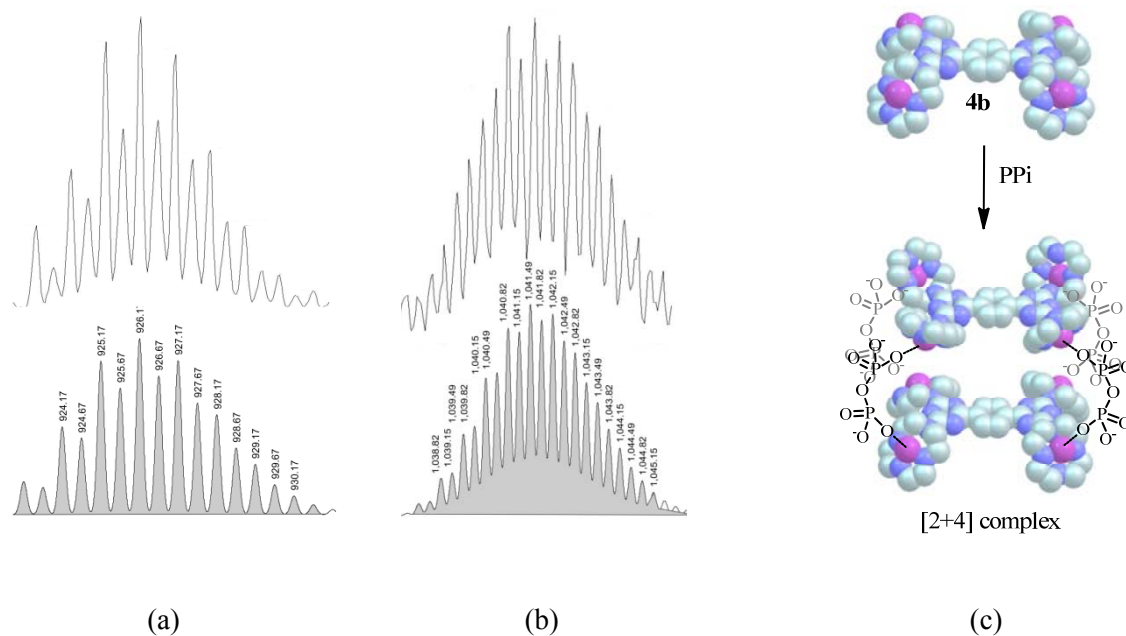


Figure 10: Isotope distribution for ions: (a) $m/z=923$ $[(4c-4Cl+PPi^4+Na^+)_2]^{2+}$, (b) $m/z = 1036$ $[(4b-8Cl+2PPi^4+Na^+)_2 + Na^+]^{3+}$ and (c) proposed structure of dimer $[4b-8Cl+2PPi^4]_2$.

1.4 Concluding remarks

We have obtained luminescent synthetic receptors based on 1, 3, 5-triazine bis-Zn(II)-cyclen binding sites and arenes by transition metal mediated cross coupling reactions. The synthesized complexes are rigid in structure and show excellent analyte response in buffered aqueous solution. Complexes **4b**, **4c** and **4d** have high affinities for pyrophosphate and oligocarboxylates (Boc-D₄-NH₂, Boc-E₄-NH₂) anions with changes in emission response reaching one order of magnitude. Though the coordination geometry of Zn(II)-cyclen is different in comparison with Zn(II)-Dpa, the affinities for the target anions are comparable. Thus, our complexes can be considered as alternative probes for polyphosphates and polycarboxylates.

1.5 Experimental Section

General methods and materials

All reagent grade chemicals were used without purification unless otherwise specified. Phenyl boronic acid, benzene-1, 4-diboronic acid, phenyl acetylene, cyanuric chloride, ATP, ADP, O-phospho-L-serine, phenyl phosphate were obtained from Aldrich and used as received.

UV-visible absorption spectra were recorded using a Cary 50 Bio spectrophotometer and emission spectroscopy was performed using a Varian Cary Eclipse fluorescence spectrophotometer.

Except for phenylboronic acid (**2a**) and benzene-1, 4-diboronic acid (**2b**), all other boronic acids (**2c-2h**) were synthesized following reported procedures.^{[25], [26]}

NMR Spectra

NMR spectra were measured with Bruker Avance 600 (1H: 600.1 MHz, 13C: 150.1 MHz, T = 300 K), Bruker Avance 400 (1H: 400.1 MHz, 13C: 100.6 MHz, T = 300 K), Bruker Avance 300 (1H: 300.1 MHz, 13C: 75.5 MHz, T = 300 K). The chemical shifts are reported in δ [ppm] relative to external standards (solvent residual peak). The spectra were analysed by first order, the coupling **S-1** constants are given in Hertz [Hz]. Characterisation of the signals: s = singlet, d = doublet, t = triplet, q = quartet, m = multiplet, br = broad, dd = double doublet. Integration is determined as the relative number of atoms. The solvent used is reported for each spectrum.

Mass Spectra

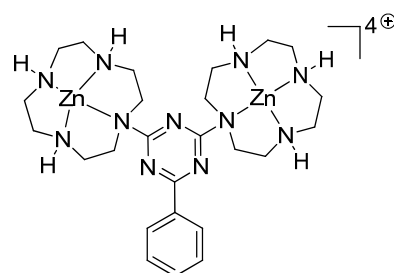
Mass spectra were obtained with Varian CH-5 (EI), Finnigan MAT 95 (CI; FAB and FD), Finnigan MAT TSQ 7000 (ESI). Xenon serves as the ionisation gas for FAB.

IR Spectra

IR spectra were recorded with a Bio-Rad FTS 2000 MX FT-IR and Bio-Rad FT-IR FTS 155

General procedure for the synthesis of complexes 4: To a mixture of Boc-protected bis-cyclen chloro-triazene **1** (100 mg, 0.1mmol) and Pd(PPh₃)₄ (10 mg, 0.012mmol, 12 mol %) in DME, the required aryl boronic acid **2** (1.5 eq. of monoboronic acid and 0.5 eq. of diboronic acid) was added, which was immediately followed by aqueous Na₂CO₃ (2M, 2ml). The mixture was refluxed for 48 h under N₂ atmosphere. After cooling, the solvent was evaporated under reduced pressure to dryness. THF was added and the suspension was shortly placed in an ultra sonication bath. The mixture was then filtered, washed thoroughly with THF and the filtrate was evaporated under reduced pressure. The residue was purified by column chromatography on silica gel using ethyl acetate and petrol ether solvent mixture as eluent, to afford the pure products **3** as solids.

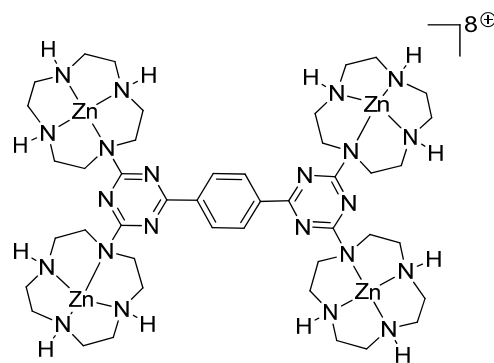
The obtained ligand **3** was Boc-deprotected with 14 equivalents of trifluoroacetic acid per Boc group and passed through a basic ion exchange column. The Boc-deprotected azamacrocycles, except in the case of **4d**, were dissolved in acetonitrile, anhydrous ZnCl_2 (2.5 eq. for **4a**, **4c**, **4e-4h** and 4.5 eq. for **4b**, **4d**) dissolved in methanol was slowly added to it leading to the formation of a white precipitate. For the synthesis of **4d**, the Boc-deprotected **3d** was dissolved in methanol/water (4:1) mixture, anhydrous ZnCl_2 (4.5 eq.) dissolved in methanol was slowly added to it. The reaction mixture was refluxed overnight, which dissolved the precipitate. The hot solution is then decanted in a conical flask. Upon cooling a white precipitate is obtained, which was filtered and analyzed by NMR spectroscopy. The individual reaction and characterization details are described below.



Compound 4a: The Boc-protected ligand **3a** was obtained as a colorless solid (53 mg, 50%) (R_f = 0.68, EE/PE 50:50). It was then Boc deprotected using TFA yielding the free base (23 mg, 97%) followed by zinc-complexation (30 mg, 100%).

3a: $^1\text{H NMR}$ (300MHz, CDCl_3) δ [ppm]: 1.44 (s, 54H, CH_3 -BOC), 3.41-3.91 (br, m, 32H, CH_2 -cyclen), 8.441 (d, 2H, $J = 6.9$), 7.469 (t, 1H), 7.438 (t, 2H); $^{13}\text{C NMR}$ (75MHz, CDCl_3) δ [ppm]: 27.5 (+, CH_3 -BOC), 49.1, 49.7, 50.2 (-, CH_2 -cyclen), 76.5, 78.9 (C_{quart} , C-BOC), 156.4, 157.0 (C_{quart} , C=O BOC), 168.6 (C_{quart} , triazine- $\text{C}_{\text{Aryl-N}}$), 126.9, 127.430, 130.2, 135.5 (benzene). **MS** (ES-MS) (DCM/MeOH +10mM NH_4OAc) m/z (%) = 1094 (100) (MH^+).

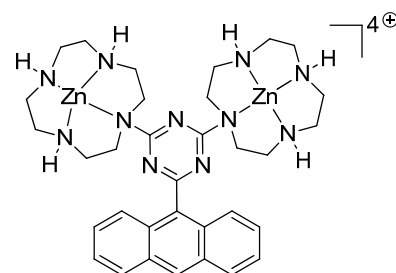
4a: $^1\text{H NMR}$ (300 MHz, CDCl_3) δ [ppm]: 8.492 (t, 2H), 7.512-7.623 (m, 3H), 4.433-4.508 (m, 2H), 4.149 (br, s, 2H), 2.721-3.554 (m, 28H), $^{13}\text{C NMR}$ (75 MHz, CDCl_3) δ [ppm]: 42.4, 43.3, 44.5, 45.5, 45.6, 46.4, 47.6, 47.9 (-, CH_2 -cyclen), 128.1, 128.5, 132.2, 132.4, 135.1, 135.3, 170.3, 170.8. - **MS** (ESI-MS) (DCM/MeOH +10mM NH_4OAc) m/z (%) = 372.6 (100) ($\text{M}^{4+} + 2\text{CH}_3\text{COO}^-$) $^{2+}$. **M.P.** 235-238 °C; **IR** (ATR) [cm^{-1}]: $\tilde{\nu} = 3100, 2940, 1350, 1154, 968, 820$; **UV** (HEPES pH 7.4, 25mM): λ_{max} ($\log \epsilon$) = 224 nm (4.4) **MF:** $[\text{C}_{25}\text{H}_{43}\text{N}_{11}\text{Zn}_2]^{4+} 4\text{ClO}_4^-$. **FW:** 1026.25 g/mol.



Compound 4b: The Boc-protected compound **3b** was obtained as a colorless solid (64 mg, 31%) (R_f = 0.68, EE/PE 50:50). It was then Boc-deprotected using TFA (27 mg, 96%) followed by Zn-complexation (41 mg, 100 %).

3b: $^1\text{H NMR}$ (300MHz, CDCl_3) δ [ppm]: 1.391 (s, 108H, CH_3 -BOC), 3.370-3.594 (br, m, 64H, CH_2 -cyclen), 8.368 (s, 4H); $^{13}\text{C NMR}$ (300MHz, CDCl_3) δ [ppm]: 28.52 (+, CH_3 -Boc), 50.24 (-, CH_2 -cyclen), 79.91 (C_{quart} , C-Boc), 128.11, 156.62, 169.46. **MS** (ES-MS) (DCM/MeOH +10mM NH_4OAc) m/z (%) = 1060 (100) ($\text{M}+2\text{H}^+$) $^{2+}$, 1010 (50) ($\text{M}+2\text{H}^+$ -BOC) $^{2+}$, 2119.2 (10) (MH^+)

4b: $^1\text{H NMR}$ (300MHz, DMSO-d_6) δ [ppm]: 1.042-1.992 (br, m, 58H), 2.925 (br, 6H), 6.878 (s, 4H); $^{13}\text{C NMR}$ (75MHz, DMSO-d_6) δ [ppm]: 44.2, 46.3, 129.5, 140.5, 168.9, 171.4; **MS** (ES-MS) ($\text{H}_2\text{O}/\text{MeOH}$ +10mM NH_4OAc) m/z (%) = 490.7 (100) ($\text{M}^{8+}+5\text{CH}_3\text{COO}^-$) $^{3+}$. **M.P.:** 255-257°C; **IR** (ATR) [cm^{-1}]: ν = 3398, 2933, 1680, 1524, 1347, 1193, 1132, 1087, 971, 813, 723. – **UV** (HEPES pH 7.4, 25mM): λ_{max} ($\log \epsilon$) = 285 nm (4.530). **MF:** $[\text{C}_{44}\text{H}_{92}\text{N}_{22}\text{Zn}_4]^{8+}\text{Cl}_8$. – **FW:** 1474.50 g/mol.

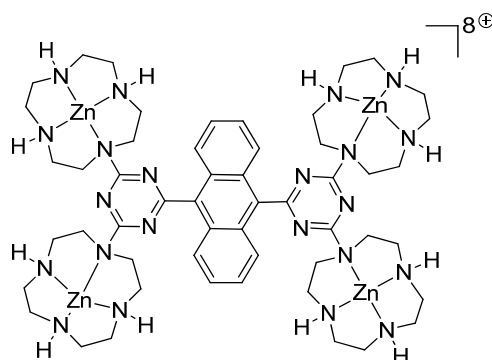


Compound 4c: The Boc-protected compound was obtained as a colorless solid (56mg, 50%) (R_f = 0.68, EE/PE 50:50). It was then Boc deprotected using TFA. (25mg, 95%) followed by Zn-complexation (36 mg, 100%).

3c: $^1\text{H NMR}$ (300MHz, CDCl_3) δ [ppm]: 1.451 (s, 54H, CH_3 -BOC), 3.440-3.661 (br, m, 32H, CH_2 -cyclen), 7.316-7.439 (m, 4H), 7.903 (br, d, 2H), 8.003 (d, 2H), 8.445 (s, 1H); $^{13}\text{C NMR}$ (75MHz, CDCl_3) δ [ppm]: 22.88, 26.30, 26.87, 27.48, 28.43, 48.95, 49.99, 79.05, 123.93, 124.28, 125.17,

126.12, 127.31, 127.82, 130.27, 133.22; **MS** (ES-MS) (DCM/MeOH +10mM NH₄OAc) *m/z* (%) = 1023 (100) (M+2H⁺)²⁺, 1199 (65) (MH⁺), 1053 (35) (M+2H⁺-BOC)²⁺.

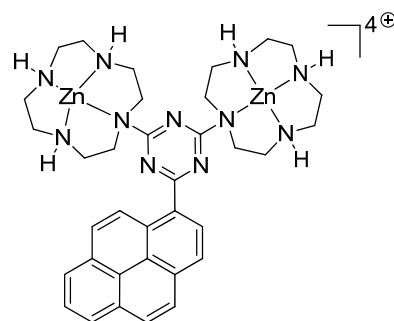
4c: ¹H NMR (300MHz, DMSO-d₆) δ [ppm]: 2.647-3.231 (br, m, 32H), 4.249 (br, s, 2H), 4.815 (br, s, 4H), 7.445-7.573 (m, 4H), 8.025 (d, 2H), 8.168 (d, 2H), 8.725 (s, 1H); ¹³C NMR(150MHz, DMSO-d₆) δ [ppm]: 30.6, 44.8, 46.8(CH₂ Cyclen), 125.4, 126.2, 128.1, 130.7, 132.8, 133.1, (CH, aromatic), 158.0, 169.2, 172.5, 173.0; **MS** (ES-MS) (H₂O/MeOH +10mM NH₄OAc) *m/z* (%) = 423.6 (100) (M⁴⁺+2CH₃COO⁻)²⁺. **M.P.**: 274-282°C; **IR** (ATR) [cm⁻¹]: ν[~] = 3090, 2943, 1345, 1087, 1130, 963, 825; **UV** (HEPES pH 7.4, 25mM): λ_{max} (log ε)=365 nm (3.9) **MF**: [C₃₃H₄₇N₁₁Zn₂]⁴⁺Cl₄⁻. **FW**: 870.37 g/mol.



Compound 4d: The Boc-protected compound was obtained as a colorless solid (65mg, 30%) (*R_f* =0.68, EE/PE 50:50). It was then Boc deprotected using TFA. (12mg, 95%) followed by Zn-complexation (18mg, 100%)

3d:¹H NMR (300MHz, CDCl₃) δ [ppm]: 1.457 (s, 108H, CH₃-Boc), 3.441-3.653 (br, m, 64H, CH₂-cyclen), 7.283-7.317 (dd, 4H), 7.834-7.868 (br, 4H); ¹³C NMR (300MHz, CDCl₃) δ [ppm]: 27.5 (+, CH₃-Boc), 48.9 (-, CH₂-cyclen), 79.0 (C_{quart}, C-Boc); **MS** (ES-MS) (DCM/MeOH +10mM NH₄OAc) *m/z* (%) = 1110.6 (100) (M+2H⁺)²⁺, 2220 (6) (MH⁺)

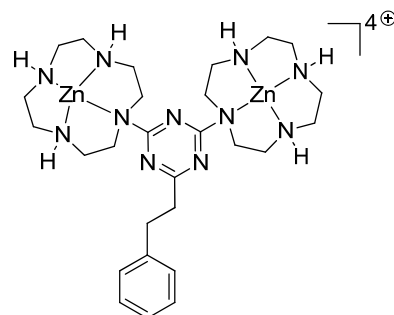
4d: ¹H NMR (300MHz, D₂O) δ [ppm]: 2.667-2.965 (m, 46H), 2.987-3.011 (br, 3H), 3.192-3.337 (br, 18H), 7.4921-7.953 (dd, 4H), ¹³C NMR (150 MHz, D₂O) δ [ppm]: 43.6, 44.8, 46.1, 47.6, 113.4, 115.3, 117.2, 119.2, 169.8, 173.9; **MS** (**ES-MS**) (H₂O/MeCN) *m/z* (%) = 355.0(M⁸⁺+4Cl⁻)⁴⁺(100), 485.2 (M⁸⁺+5Cl⁻)³⁺(50). **M.P.**: 292-296 °C; **IR** (ATR) [cm⁻¹]: ν[~] = 3025, 2893, 1640, 1585, 1125, 980, 720; **UV** (HEPES pH 7.4, 25mM): λ_{max} (log ε) = 370 nm (3.36) **MF**: [C₅₂H₈₄N₂₂Zn₄]⁸⁺Cl₈⁻. **FW**: 1562.52 g/mol.



Compound 4e: The Boc-protected compound was obtained as a colorless solid (62mg, 54%) (R_f = 0.68, EE/PE 50:50). It was then Boc deprotected using TFA. (30mg, 96%) followed by Zn-complexation (43mg, 100%)

3e: $^1\text{H NMR}$ (300MHz, CDCl_3) δ [ppm]: 1.466(s, 54H, CH_3 -BOC), 3.150-3.896 (br, m, 32H, CH_2 -cyclen), 8.015-8.216 (m, 7H), 8.571(br, d, 1H), 9.109 (br, s, 1H); $^{13}\text{C NMR}$ (75MHz, CDCl_3) δ [ppm]: 50.3, 51.0, 80.1, 124.3, 124.7, 125.2, 125.4, 125.9, 127.3, 127.5, 128.3, 130.71, 131.2; **MS** (ES-MS) ($\text{DCM}/\text{MeOH} + 10\text{mM NH}_4\text{OAc}$) m/z (%) = 1223 (100) (MH^+), 1022.9 (20) ($\text{MH}^+ - 2\text{BOC}$)

4e: $^1\text{H NMR}$ (300MHz, CDCl_3) δ [ppm]: 2.730-2.941 (br, m, 28H), 3.472 (br, s, 2H), 4.391(br, s, 4H), 4.935 (br, d, 4H), 8.150 (t, 1H), 8.290-8.421 (m, 6H), 8.593 (d, 1H), 9.042 (d, 1H); $^{13}\text{C NMR}$ (75MHz, CDCl_3) δ [ppm]: 43.9, 45.0, 46.3, 47.3, 123.6, 123.9, 124.5, 125.4, 125.6, 126.0, 126.6, 127.3, 128.2, 128.7, 128.8, 130.1, 130.7, 132.2, 132.2, 169.3, 172.7; **MS** (ES-MS) ($\text{H}_2\text{O}/\text{MeOH} + 10\text{mM NH}_4\text{OAc}$) m/z (%) = 434.8 (100) ($\text{M}^{4+} + 2\text{CH}_3\text{COO}^-$) $^{2+}$. **M.P.:** 285-287 °C; **IR** (ATR) [cm^{-1}]: $\nu \sim$ 3125, 2890, 1650, 1545, 1175, 980, 880, 715; **UV** (HEPES pH 7.4, 25mM): λ_{max} ($\log \epsilon$) = 350 nm (4.16) **MF:** $[\text{C}_{35}\text{H}_{47}\text{N}_{11}\text{Zn}_2]^{4+}\text{Cl}_4^-$. **FW:** 894.39 g/mol.

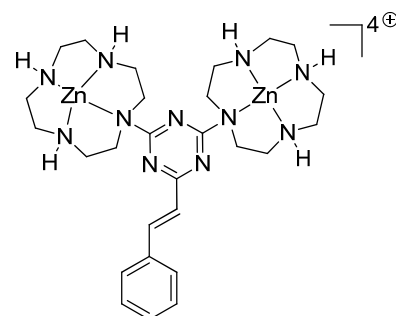


Compound 4f: The Boc-protected compound was obtained as a colorless solid (83mg, 78%) (R_f = 0.58, EE/PE 50:50). It was then Boc deprotected using TFA. (37mg, 97%) followed by Zn-complexation (72mg, 100%)

3f: $^1\text{H NMR}$ (300MHz, CDCl_3) δ [ppm]: 1.478 (s, 54H, CH_3 -BOC), 2.84 (t, 2H, CH_2), 3.12 (t, 2H, CH_2), 3.31-3.87 (br, m, 32H, CH_2 -cyclen), 7.22-7.26 (m, 5H, aromatic protons); $^{13}\text{C NMR}$ (75MHz, CDCl_3) δ [ppm]: 21.1 (CH_2), 28.4, 28.5 2 (CH_3 -Boc), 41.1 (CH_2), 50.1 (CH_2 - cyclen), 79.86 (C_{quart} , C-

Boc), 125.5, 128.2 (aromatic C), 144.2 (C_{quart} , aromatic C), 176.7 (C_{quart} , triazine); **MS** (ES-MS) (DCM/MeOH +10mM NH_4OAc) m/z (%) = 1126.7 (100) (MH^+), 1164.6 (40) (MK^+).

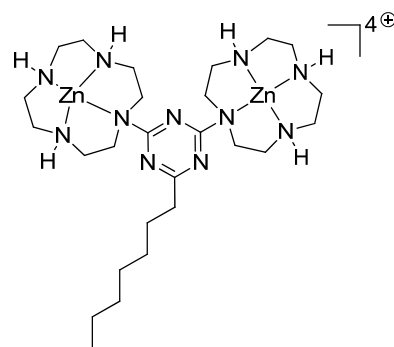
4f: **$^1\text{H NMR}$** (300MHz, CDCl_3) δ [ppm] = 2.84 (t, 2H, CH_2), 3.12 (t, 2H, CH_2), 3.29-3.55 (br, m, 32H, CH_2 -cyclen), 7.22-7.26 (m, 5H, aromatic protons); **$^{13}\text{C NMR}$** (75MHz, CDCl_3) δ [ppm]: 21.3 (CH_2), 41.1 (CH_2), 50.1 (CH_2 - cyclen), 79.8 (C_{quart} , C-Boc), 125.5, 128.2 (aromatic C), 144.2 (C_{quart} , aromatic C), 176.7 (C_{quart} , triazine); **MS** (ES-MS) ($\text{H}_2\text{O}/\text{MeOH}$ +10mM NH_4OAc) m/z (%) = 386.5 (100) ($\text{M}^{4+}+2\text{CH}_3\text{COO}^-$)²⁺. M.P.:290-293°C; **IR** (ATR) [cm^{-1}]: $\tilde{\nu}$ = 3290, 2942, 2971, 2863, 1645, 1470, 1385, 980, 824, 728; **MF**: $[\text{C}_{27}\text{H}_{47}\text{N}_{11}\text{Zn}_2]^{4+}\text{Cl}_4^-$. **FW**: 798.3 g/mol.



Compound 4g: The Boc-protected compound was obtained as a colorless solid (50mg, 47%) (R_f =0.71, EE/PE 50:50). It was then Boc deprotected using TFA. (23mg, 96%) followed by Zn-complexation (40mg, 100%)

3g: **$^1\text{H NMR}$** (300MHz, CDCl_3) δ [ppm]: 1.445(s, 54H, CH_3 -BOC), 3.428-4.085 (br, m, 32H, CH_2 -cyclen), 6.839(d, CH-ethylene, $J=15.9$), 7.338-7.358 (m, 3H, aromatic protons), 7.568 (d, 2H, aromatic protons, $J=7.2$), 7.959(d, 1H, CH-ethylene, $J=15.9$); **$^{13}\text{C NMR}$** (75MHz, CDCl_3) δ [ppm]: 28.3, 28.6 (CH_3 -Boc), 49.1, (CH_2 - cyclen), 78.8 (C_{quart} , C-Boc), 126.6, (C=C), 127.6, 127.9 (aromatic C), 135.0(C=C), 168.9 (C_{quart} , triazine); **MS** (ES-MS) (DCM/MeOH +10mM NH_4OAc) m/z (%) = 1124.5 (100) (MH^+).

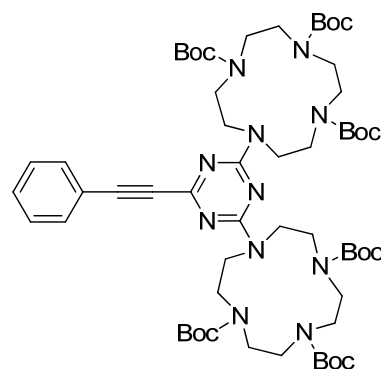
4g: **$^1\text{H NMR}$** (300MHz, CDCl_3) δ [ppm] = 2.67-3.76 (br, m, 38 H), 6.35(d, CH-ethylene), 7.18-7.55(m, aromatic protons), 7.79(d, CH-ethylene); **$^{13}\text{C NMR}$** (75MHz, CDCl_3) δ [ppm]: 43.9, 45.0, 46.3, 47.3, 123.6, 123.9, 124.4, 125.4, 125.6, 125.9, 126.6, 127.3, 128.2, 128.7, 128.8, 130.1, 130.7, 132.2, 132.2, 169.2, 172.7; **MS** (ES-MS) ($\text{H}_2\text{O}/\text{MeOH}$ +10mM NH_4OAc) m/z (%) = 385.5 (100) ($\text{M}^{4+}+2\text{CH}_3\text{COO}^-$)²⁺. **IR** (ATR) [cm^{-1}]: $\tilde{\nu}$ = 3385, 3083, 2966, 2896, 1680, 1644, 1525, 1465, 1182, 965, 812, 720; **UV** (HEPES pH 7.4, 25mM): λ_{max} (log ϵ) = 220nm (4.10) **MF**: $[\text{C}_{27}\text{H}_{45}\text{N}_{11}\text{Zn}_2]^{4+}\text{Cl}_4^-$. **FW**: 796.29 g/mol.



Compound 4h: The Boc-protected compound was obtained as a colorless solid (56mg, 52%) ($R_f = 0.68$, EE/PE 50:50). It was then Boc deprotected using TFA. (24mg, 92%) followed by Zn-complexation (48mg, 100%)

3h: $^1\text{H NMR}$ (300MHz, CDCl_3) δ [ppm]: 0.87 (t, 3H, CH_3), 1.455 (s, 54H, $\text{CH}_3\text{-Boc}$), 1.576-1.711 (m, 10H, CH_2), 2.458 (t, 2H, CH_2), 3.22-3.76 (br, m, 32H, $\text{CH}_2\text{-cyclen}$); $^{13}\text{C NMR}$ (75MHz, CDCl_3) δ [ppm]: 28.5, 28.7 ($\text{CH}_3\text{-Boc}$), 49.5 ($\text{CH}_2\text{-cyclen}$), 78.8 (C_{quart} , C-Boc), MS (**ES-MS**) (DCM/MeOH +10mM NH_4OAc) m/z (%) = 1120.9 (100) (MH^+).

4h: $^1\text{H NMR}$ (300MHz, $\text{dms}\text{-}d_6$) δ [ppm]: 0.86 (t, 3H, $\text{CH}_3\text{-alkyl chain}$) 1.26 (br, s, 8H), 1.75 (s, 7H), 2.1 (s, 6H), 2.89 (br, m, 16H), 3.4 (s, 13H); $^{13}\text{C NMR}$ (75MHz, $\text{dms}\text{-}d_6$) δ [ppm]: 13.7 ($\text{CH}_3\text{-alkyl chain}$), 17.8, 21.8, 22.1, 22.2, 26.2, 28.3 ($\text{CH}_2\text{-alkyl chain}$), 30.9, 39.1, **MS** (ES-MS) ($\text{H}_2\text{O}/\text{MeOH}$ +10mM NH_4OAc) m/z (%) = 383.6 (100) ($\text{M}^{4+} + 2\text{CH}_3\text{COO}^-$) $^{2+}$. **IR** (ATR) [cm^{-1}]: $\tilde{\nu} = 2921, 2852, 1693, 1561, 1525, 1465, 1420, 1346, 1282, 1085, 812$; **MF**: $[\text{C}_{26}\text{H}_{53}\text{N}_{11}\text{Zn}_2]^{4+}\text{Cl}_4^-$. **FW**: 792.35 g/mol



Synthesis of Compound 5: In a two necked flask, Boc-protected bis-cyclen chloro-triazene **1** (0.2 g, 0.19 mmol), Pd/C (10%, Fluka), PPh_3 , CuI in 1/0.04/0.16/0.04 molar ratio, were placed under nitrogen atmosphere along with DIPEA (1.5 ml) as the suitable base. After accurately purging with nitrogen, a solution of phenyl acetylene (0.05 ml, 0.48 mmol) in CH_3CN was added, the temperature was raised and the mixture was kept under vigorous stirring for overnight. After cooling and filtering the mixture on a short package of celite, the solution was evaporated under reduced pressure. The

crude reaction mixture was purified by column chromatography using 40% ethyl acetate in petrol ether as the eluent to get the pure product **5** (51%).

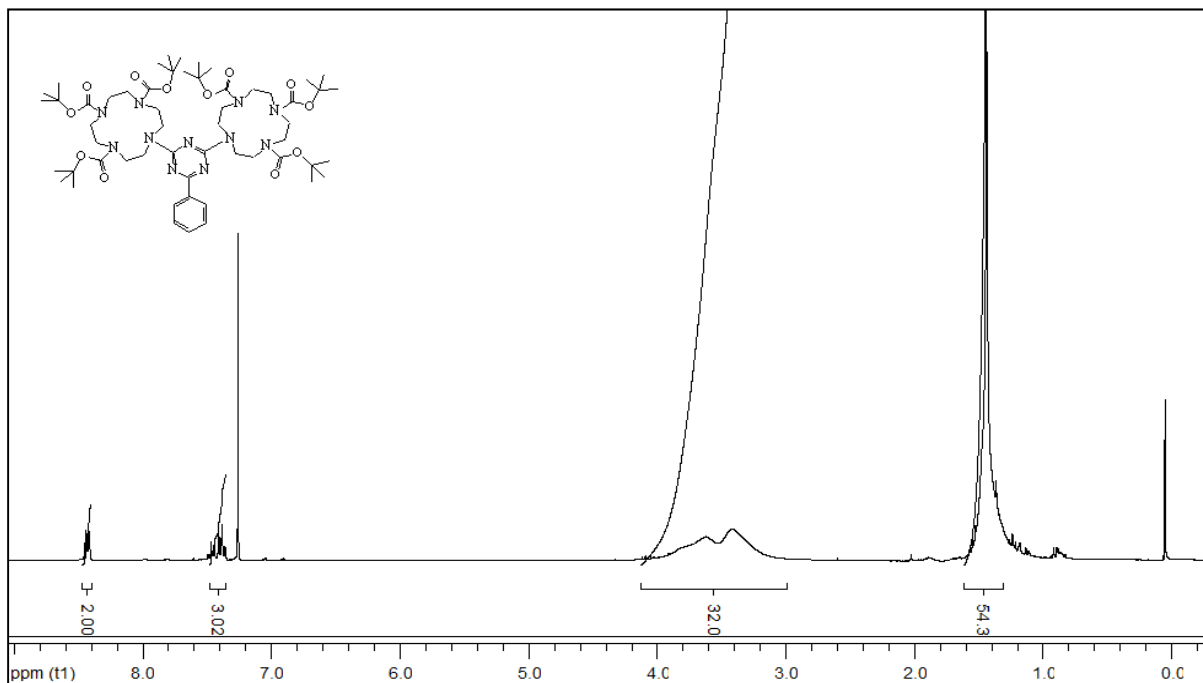
¹H NMR (300MHz, CDCl₃) δ [ppm]: 1.45 (s, 54H, CH₃-BOC), 3.24-4.00 (br, m, 32H, CH₂-cyclen, 7.5-7.57 (dd, 2H, benzene ring), 7.29-7.43 (m, br, 3H, benzene ring); **¹³C NMR** (75MHz, CDCl₃) δ [ppm]: 27.5, 48.9, 87.6, 120.8, 127.2, 128.3, 131.4, 158.0; **MS** (ES-MS) (DCM/MeOH +10mM NH₄OAc) *m/z* (%) = 1122.8 (100) (MH⁺); **IR** (ATR) [cm⁻¹]: $\tilde{\nu}$ = 3385, 3083, 2966, 2896, 2250, 1680, 1512, 1465, 1182, 965, 812, **MF**: C₅₇H₉₁N₁₁O₁₂, **FW**: 1122.4 g/mol

X-ray structure determination

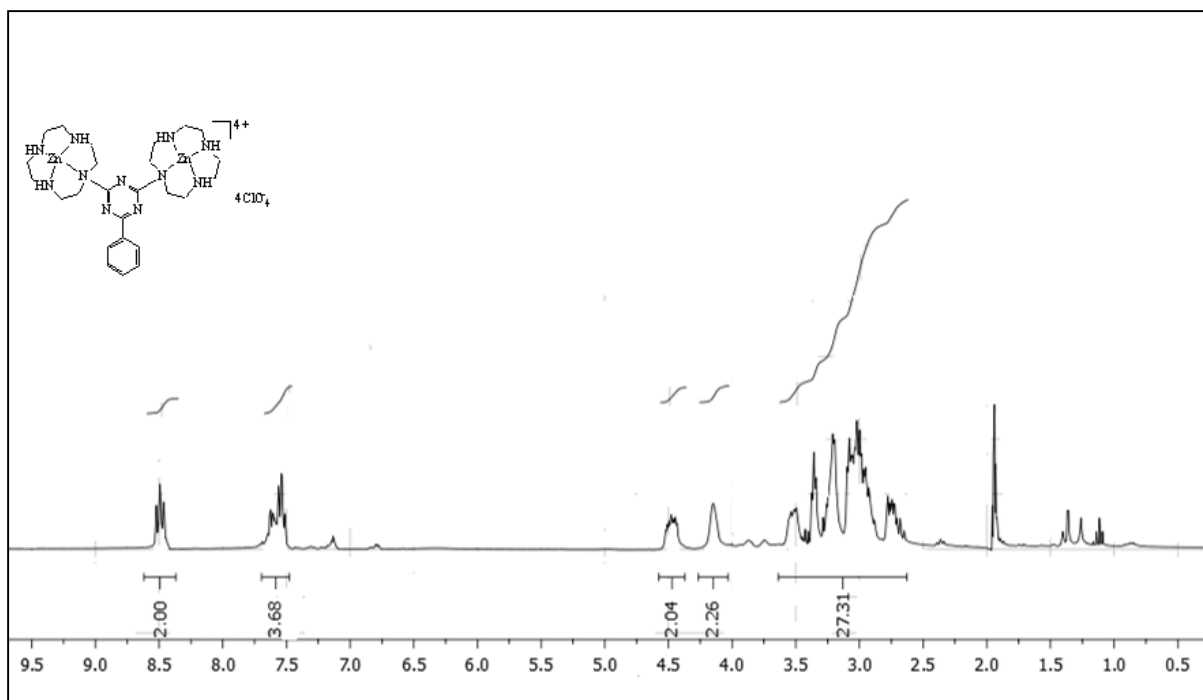
Crystal data for C₃₃H₄₇C₁₂N₁₁Zn₂·CH₃OH·ZnCl₄, CCDC 808617 M= 1038.73 g/mol, monoclinic, P 21/c, a= 13.33784(16) Å, b= 29.7188(4) Å, c= 10.88517(13) Å, α = 90°, β = 94.0245(11)°, γ = 90°, V= 4304.07(9) Å³, Z=4, 18752 reflections measured, 8828 independent (R_{int} = 0.0208), which were used in all calculations. The final wR2 was 0.0972 (all data). Intensity data were collected with a graphite-monochromated Mo-Kα radiation (λ = 1.54184Å) at 123K on a Goniometer Xcalibur, detector: Ruby (Gemini ultra Mo). Data collection, structure solution and refinement used programs: SHELXL,^[27] R1 is calculated for observed data and wR2 for all data.

1.6 Supporting data

^1H and ^{13}C spectra of synthesized compounds

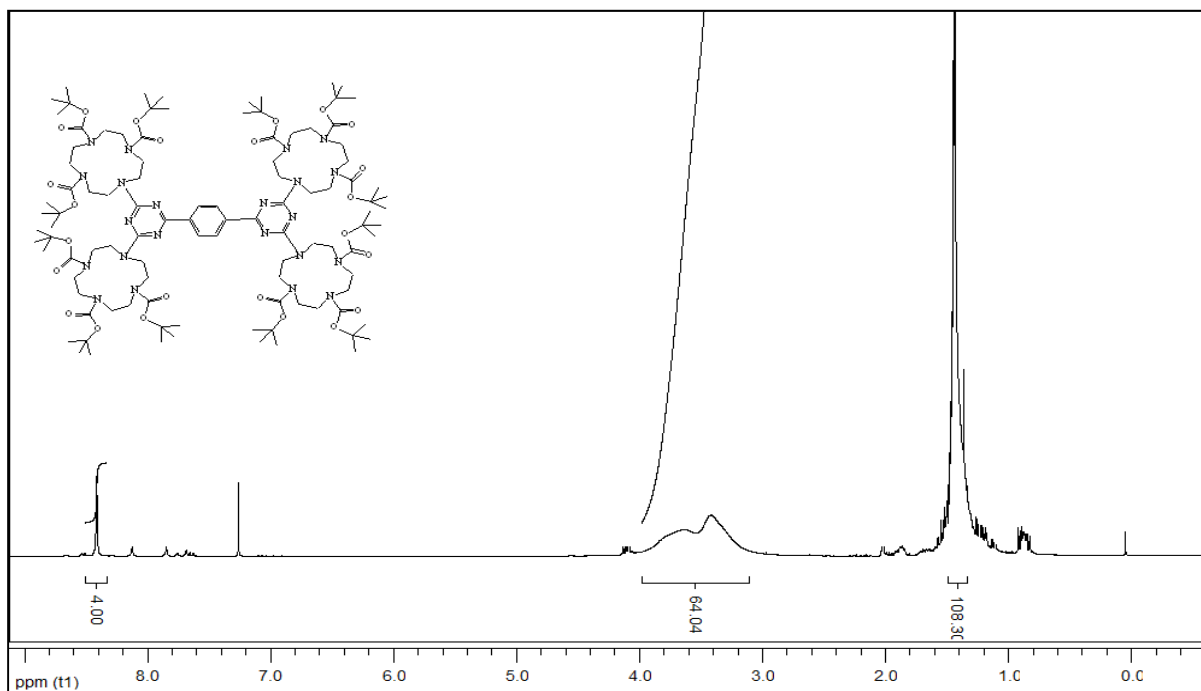


^1H -NMR spectrum of compound **3a** (300 MHz, CDCl_3)

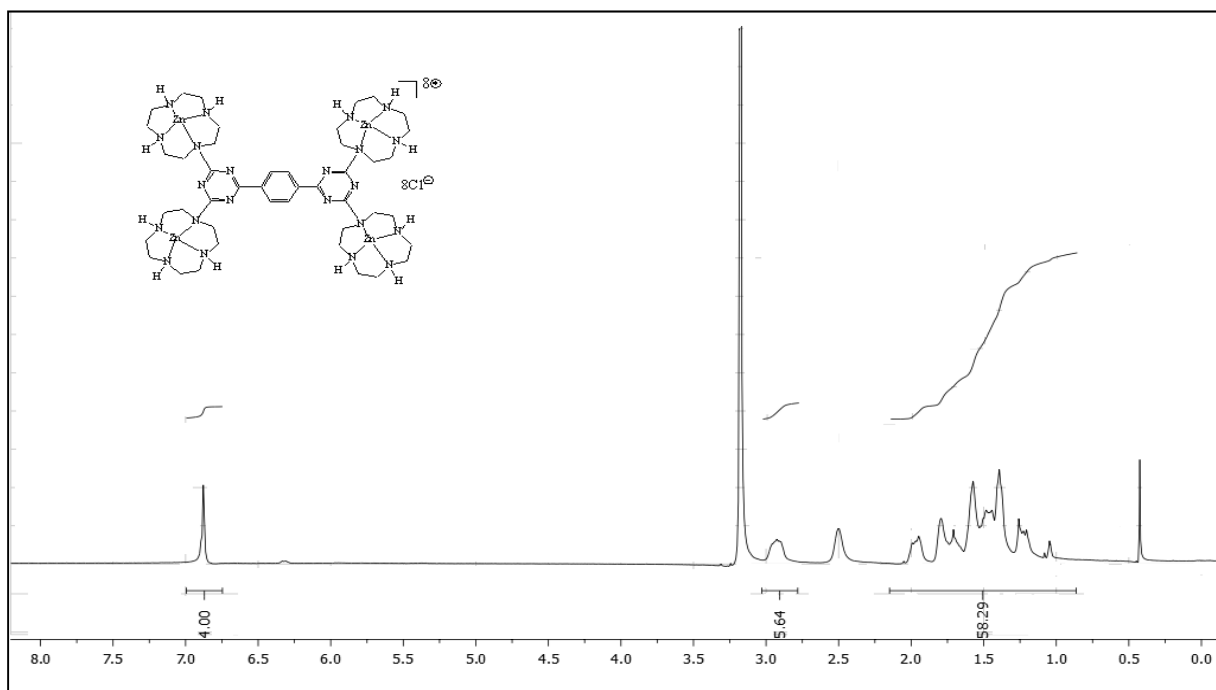


^1H -NMR spectrum of compound **4a** (300 MHz, CD_3CN)

1. Rigid Luminescent bis-Zinc(II)-bis-Cyclen Complexes for the Detection of Phosphate Anions and non-covalent Protein Labeling in Aqueous Solution

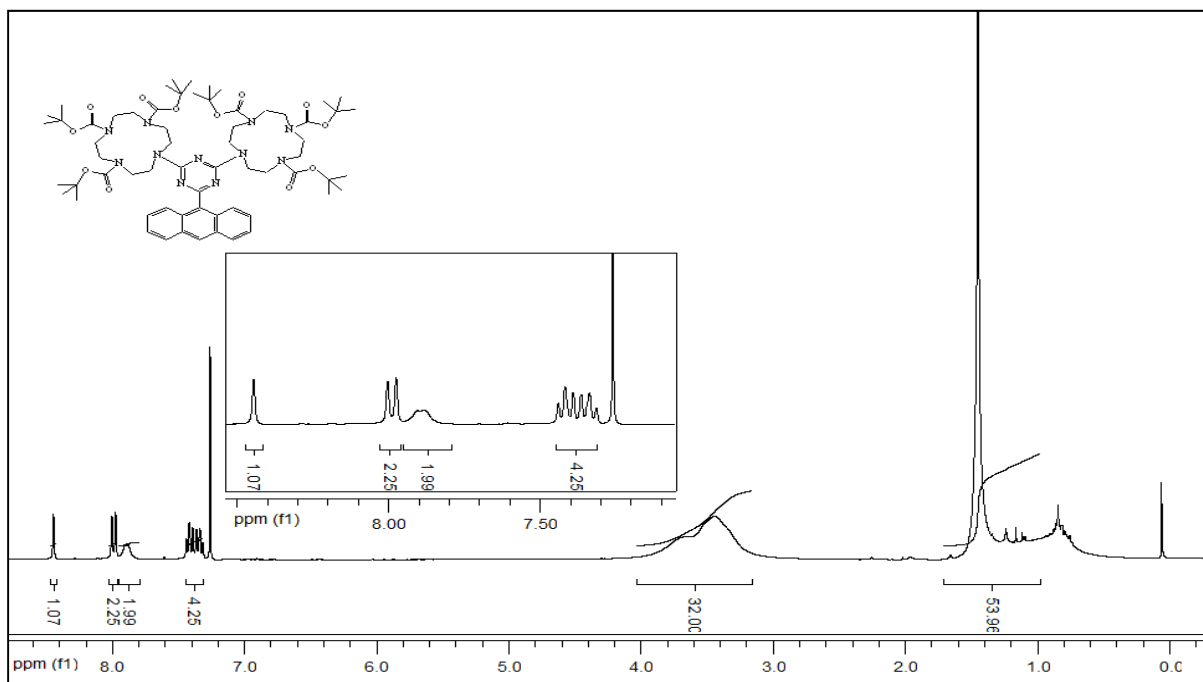


$^1\text{H-NMR}$ spectrum of compound **3b** (300 MHz, CDCl_3)

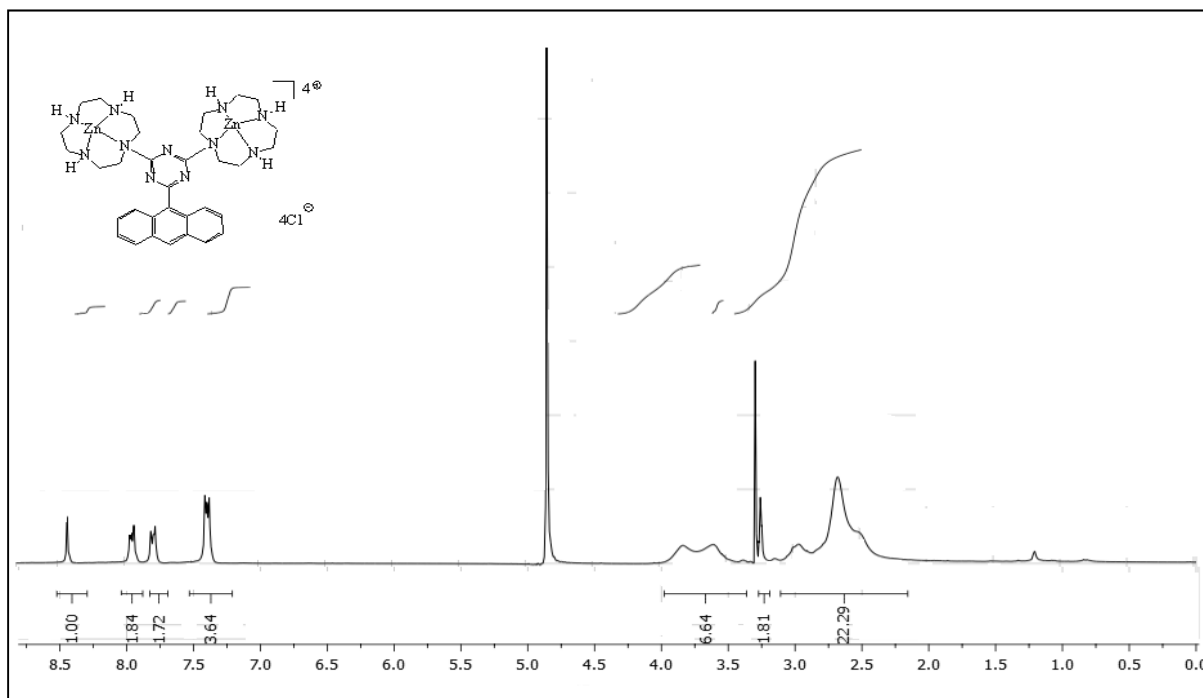


$^1\text{H-NMR}$ spectrum of compound **4b** (300 MHz, CD_3CN)

1. Rigid Luminescent bis-Zinc(II)-bis-Cyclen Complexes for the Detection of Phosphate Anions and non-covalent Protein Labeling in Aqueous Solution

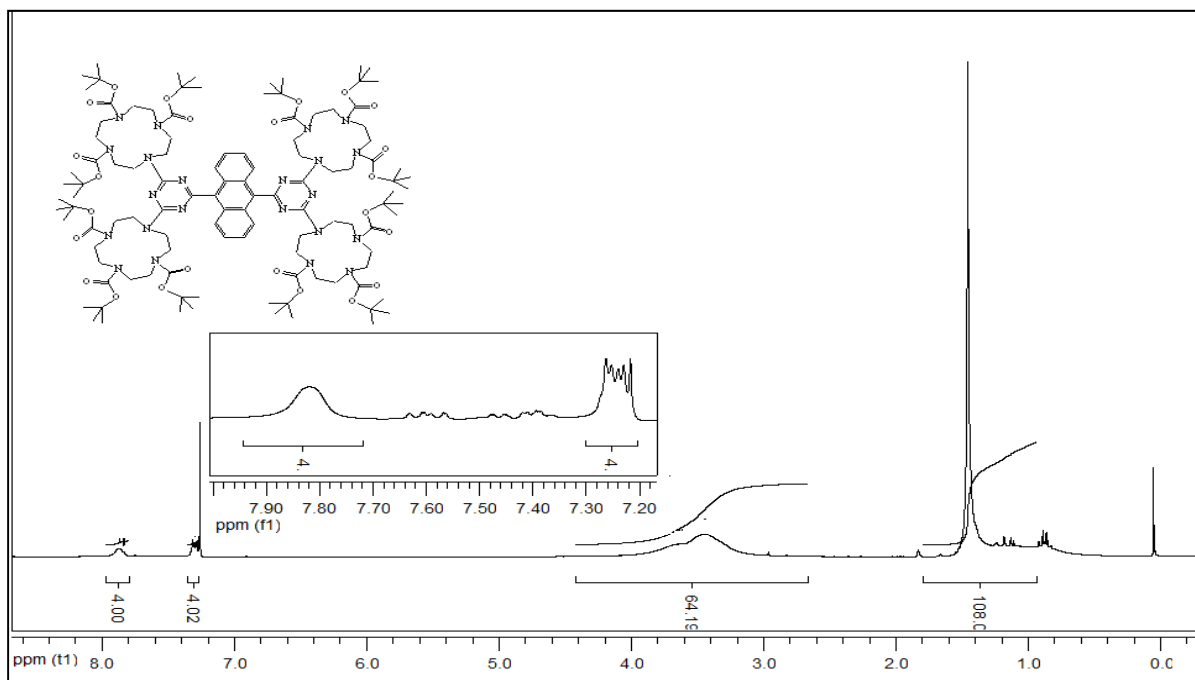


$^1\text{H-NMR}$ spectrum of compound **3c** (300 MHz, CDCl_3)

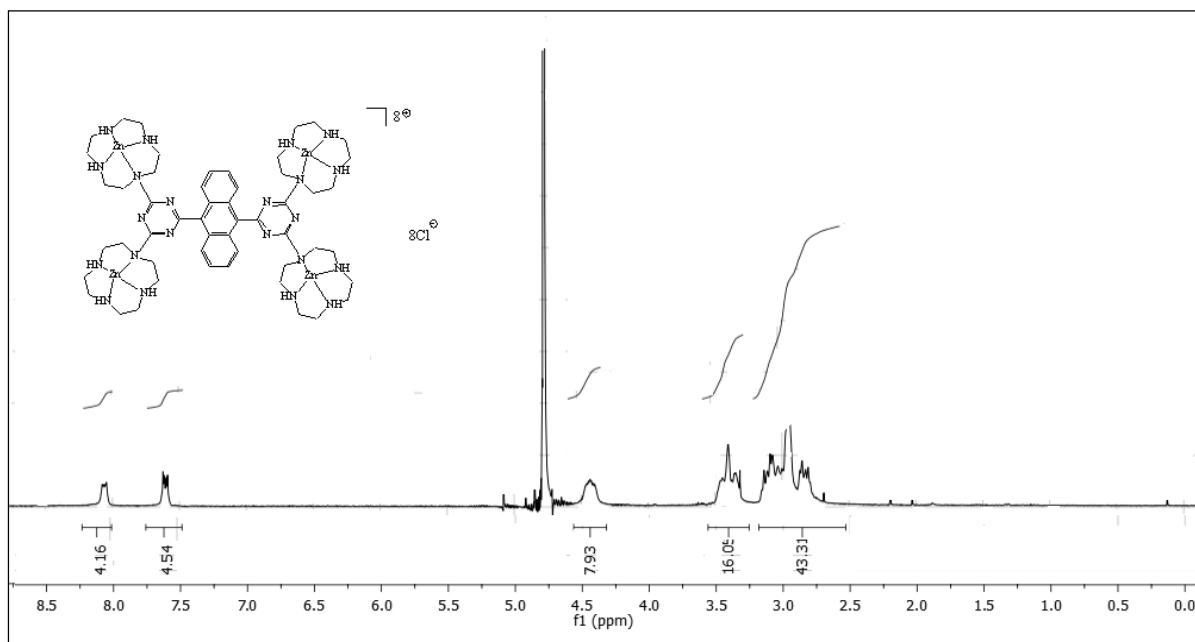


$^1\text{H-NMR}$ spectrum of compound **4c** (300 MHz, D_2O)

1. Rigid Luminescent bis-Zinc(II)-bis-Cyclen Complexes for the Detection of Phosphate Anions and non-covalent Protein Labeling in Aqueous Solution

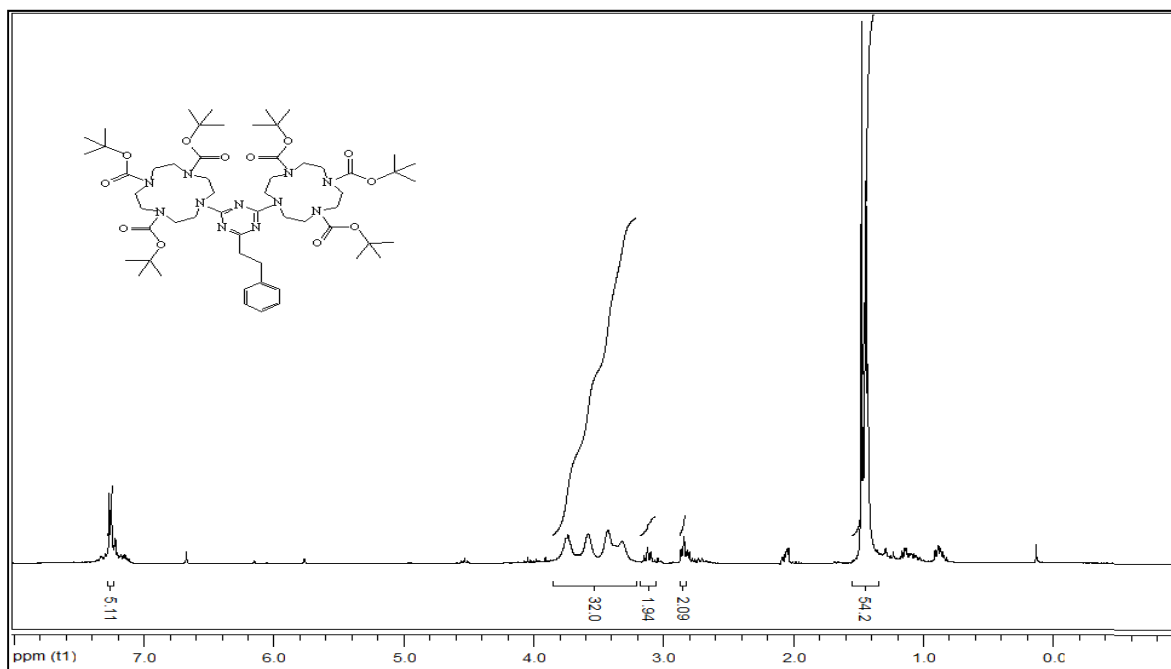


$^1\text{H-NMR}$ spectrum of compound **3d** (300 MHz, CDCl_3)

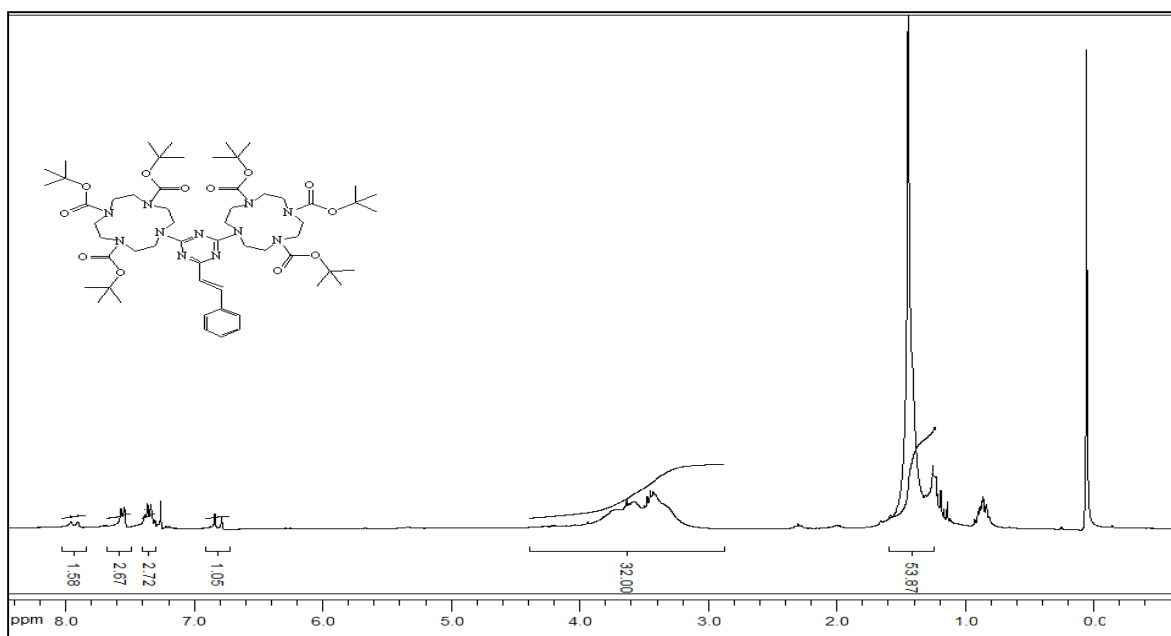


$^1\text{H-NMR}$ spectrum of compound **4d** (300 MHz, CD_3OD)

1. Rigid Luminescent bis-Zinc(II)-bis-Cyclen Complexes for the Detection of Phosphate Anions and non-covalent Protein Labeling in Aqueous Solution

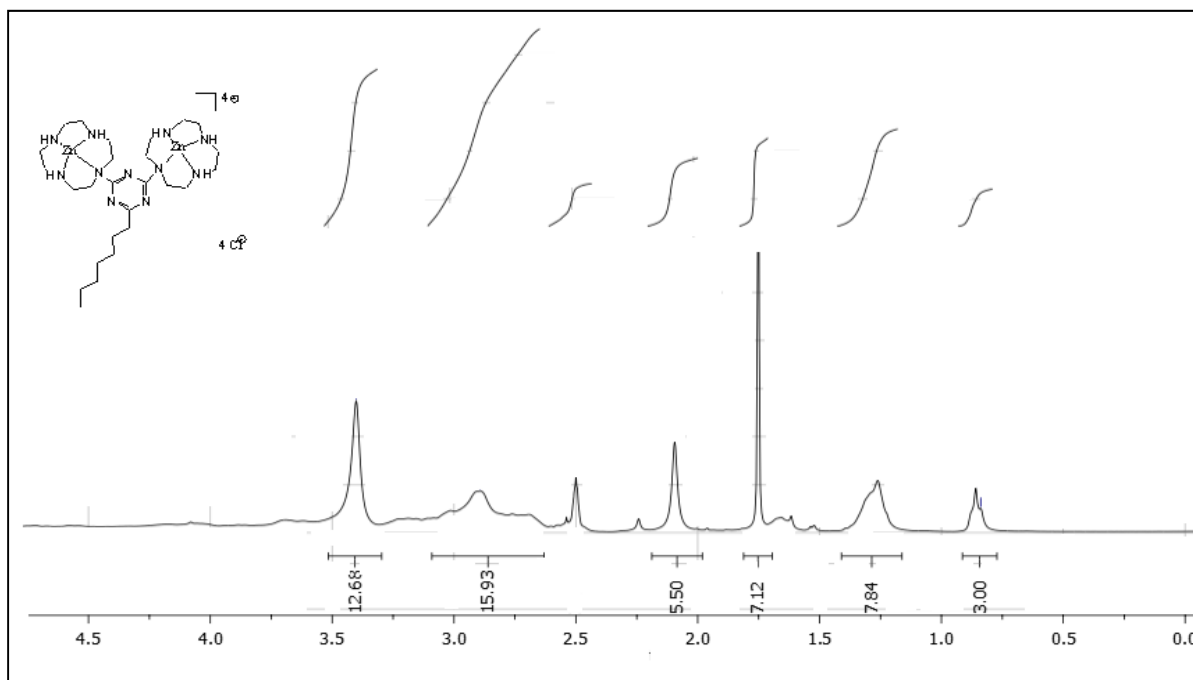


¹H-NMR spectrum of compound **3f** (300 MHz, CDCl₃)

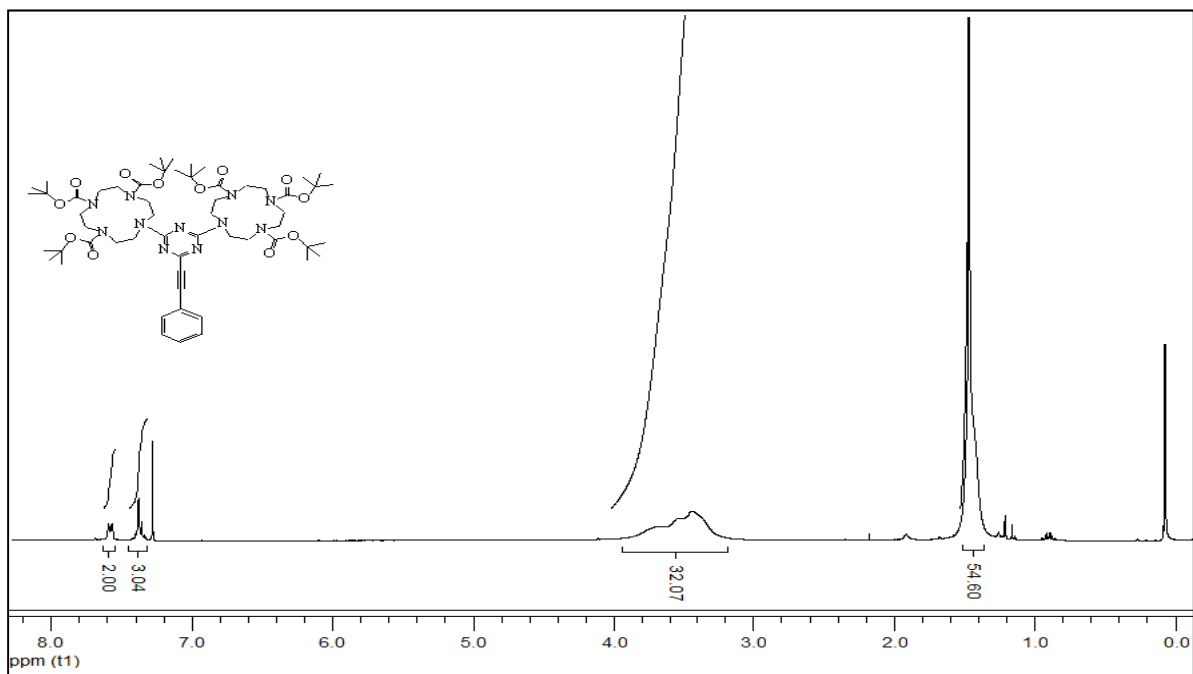


¹H-NMR spectrum of compound **3g** (300 MHz, CDCl₃)

1. Rigid Luminescent bis-Zinc(II)-bis-Cyclen Complexes for the Detection of Phosphate Anions and non-covalent Protein Labeling in Aqueous Solution

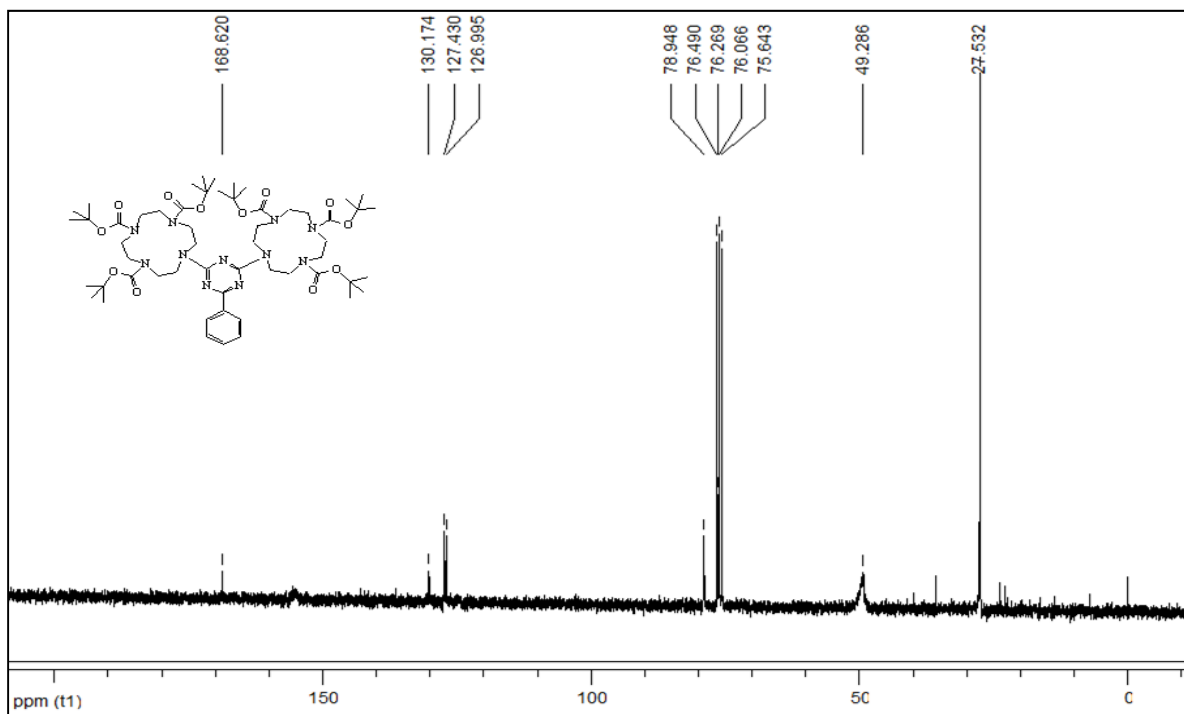


¹H-NMR spectrum of compound **4h** (300 MHz, (CD₃)₂SO)

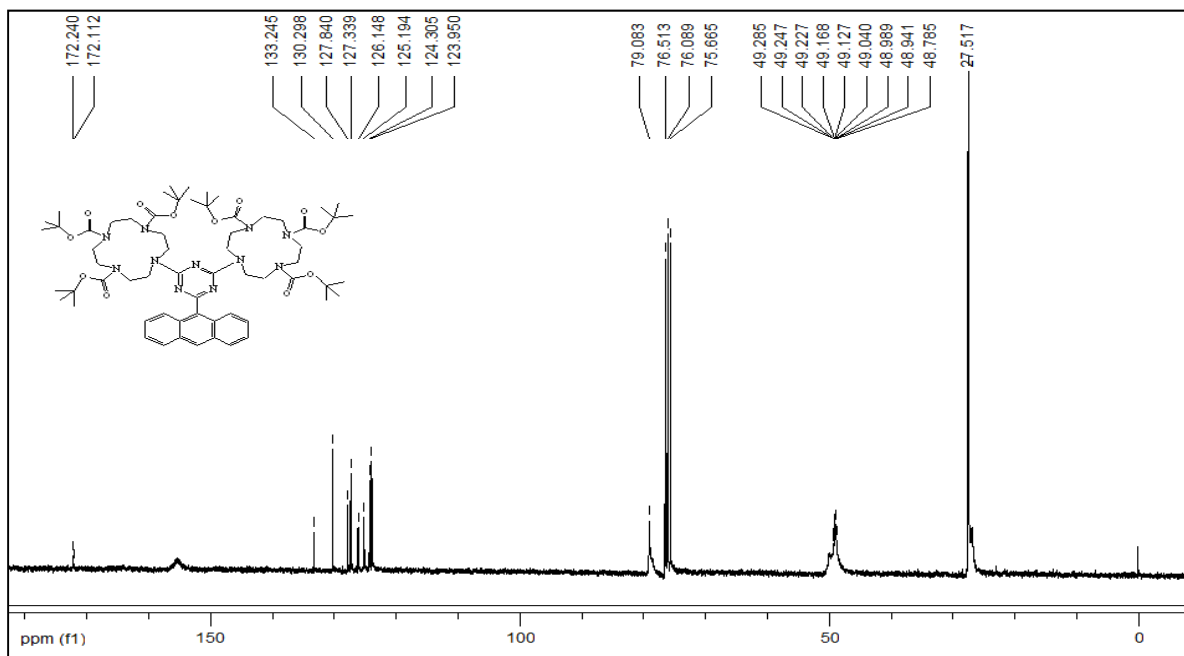


¹H-NMR spectrum of compound **5** (300 MHz, (CDCl₃))

1. Rigid Luminescent bis-Zinc(II)-bis-Cyclen Complexes for the Detection of Phosphate Anions and non-covalent Protein Labeling in Aqueous Solution

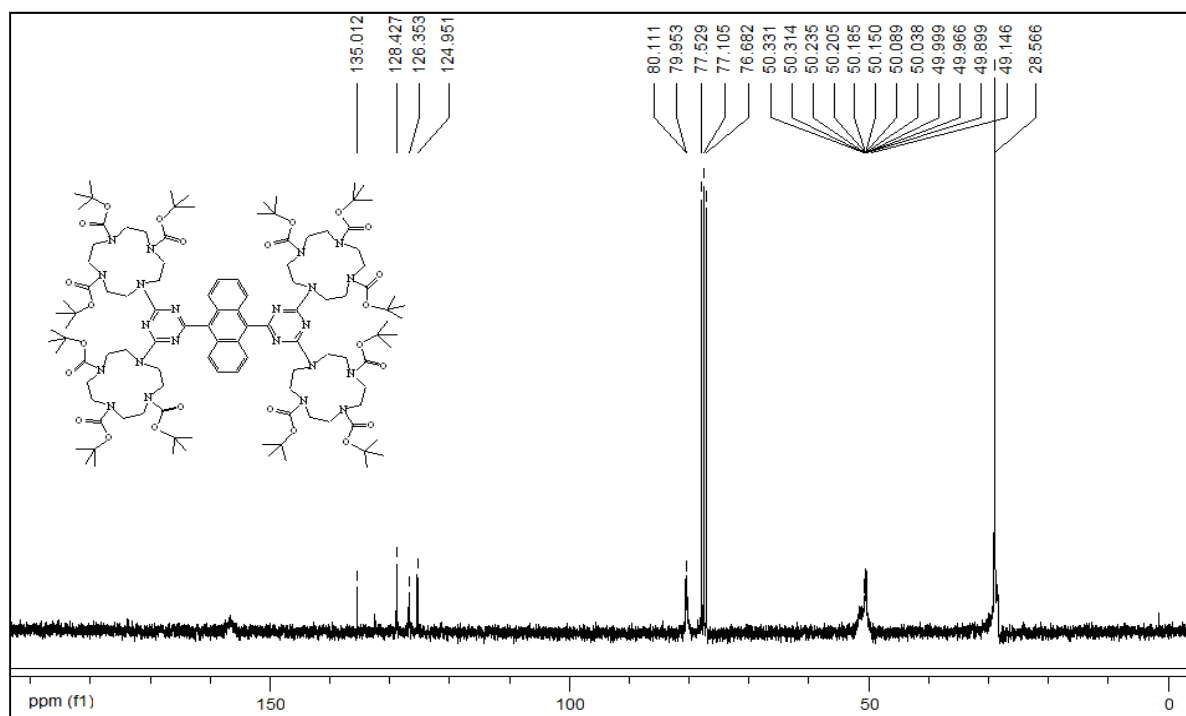


¹³C-NMR spectrum of compound **3a** (75 MHz, CDCl₃)

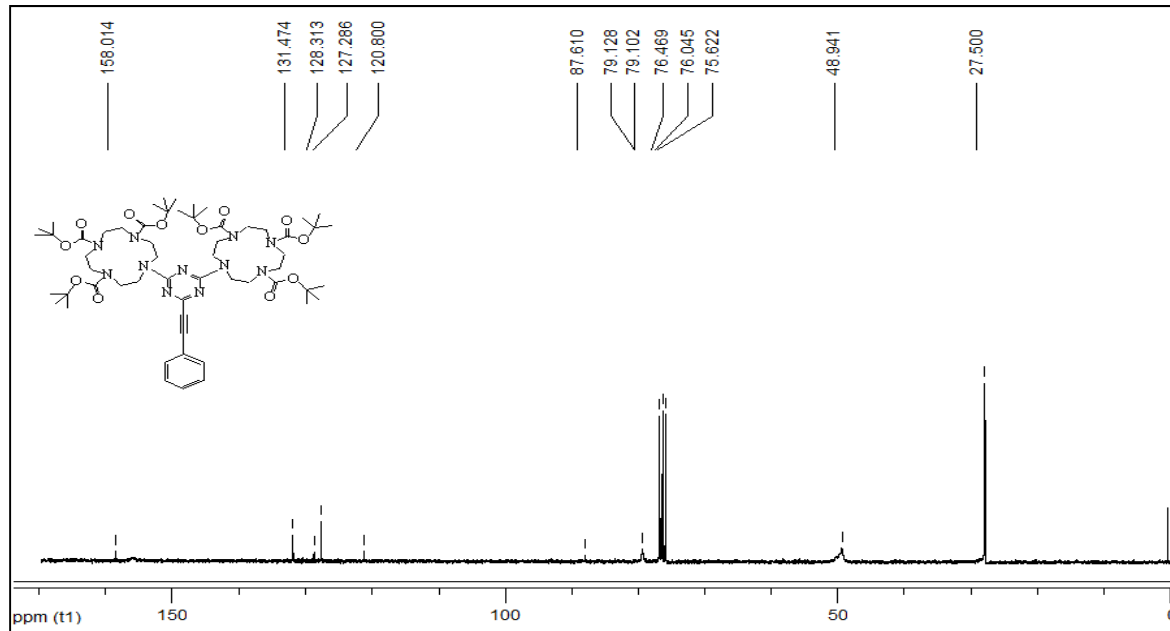


¹³C-NMR spectrum of compound **3c** (75 MHz, CDCl₃)

1. Rigid Luminescent bis-Zinc(II)-bis-Cyclen Complexes for the Detection of Phosphate Anions and non-covalent Protein Labeling in Aqueous Solution



¹³C-NMR spectrum of compound **3d** (75 MHz, CDCl₃)



¹³C-NMR spectrum of compound **5** (75 MHz, CDCl₃)

The emission titration data analysis and molecular modeling studies

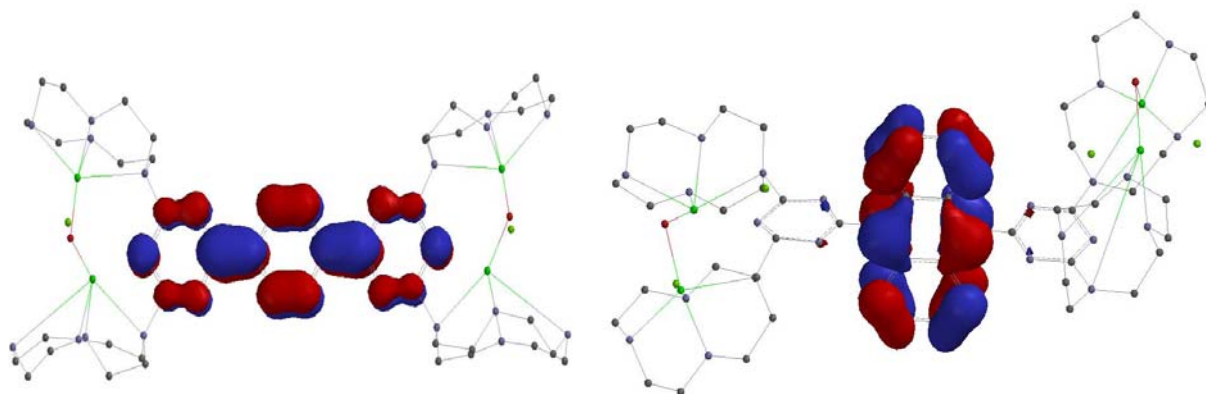


Figure11: HOMO of complex **4b** (left) and **4d** (right). In case of **4b** benzene and triazine moieties are in plane, while in case of **4d** plane of anthracene is found to be orthogonal to the plane of triazine units. All models were obtained by molecular modeling using the program package Spartan `06 (Wavefunction Inc.) by energy minimization (DFT, B3LYP, 6-31G*)

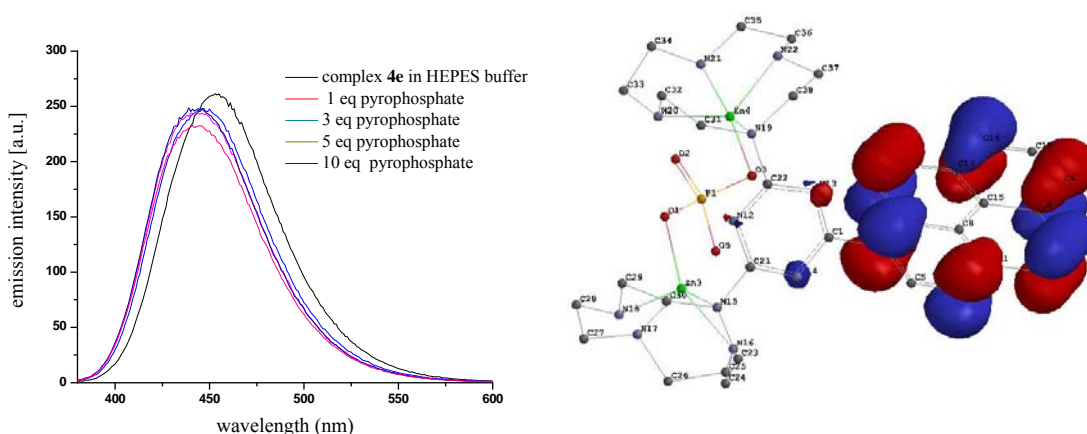


Figure12: left: Emission titration of **4e** with pyrophosphate in HEPES buffer solution. [**4e**] = 50 μ M, [PPI] = 2.5 mM, right: HOMO of complex **4e** in presence of pyrophosphate. The model was obtained by molecular modeling using the program package Spartan `06 (Wavefunction Inc.) by energy minimization (DFT, B3LYP, 6-31G*)

Mass Spectroscopic studies

ESI mass spectroscopic studies of the complexes were measured on a Thermo Quest Finnigan TSQ 7000 mass spectrometer. The solutions of interest were prepared as 10^{-4} M solution of a complex with a guest in 1:2 stoichiometry in water-acetonitrile mixture and one drop of triethylamine.

1. Rigid Luminescent bis-Zinc(II)-bis-Cyclen Complexes for the Detection of Phosphate Anions and non-covalent Protein Labeling in Aqueous Solution

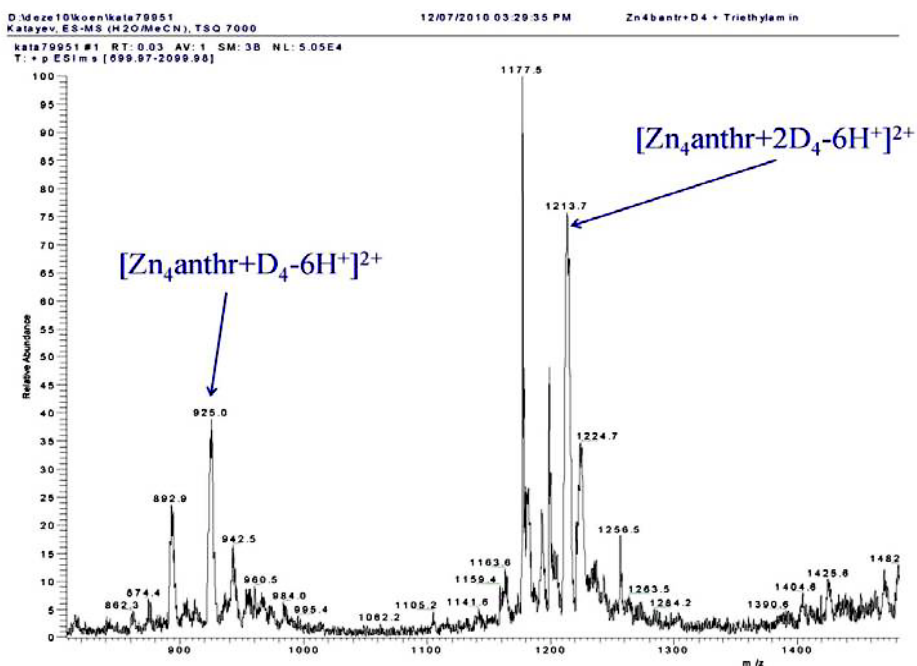


Figure 13: ESI of a mixture of **4d** (Zn4anthr) and D4 tag.

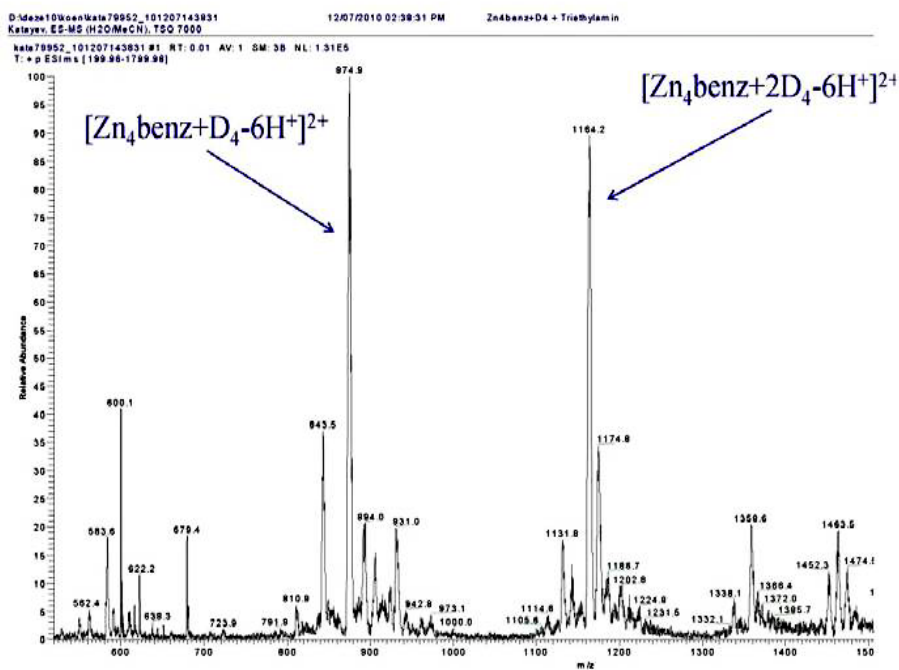


Figure 14: ESI of a mixture of **4b** (Zn4benz) and D4 tag.

1. Rigid Luminescent bis-Zinc(II)-bis-Cyclen Complexes for the Detection of Phosphate Anions and non-covalent Protein Labeling in Aqueous Solution

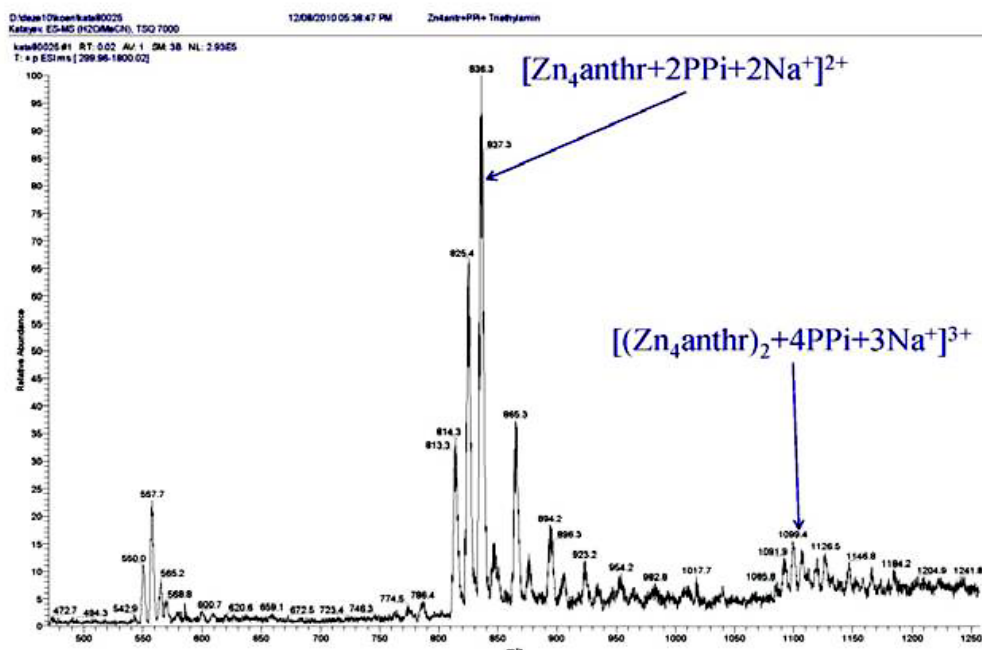


Figure 15: ESI of a mixture of **4d** (Zn₄anthr) and sodium pyrophosphate (PPi).

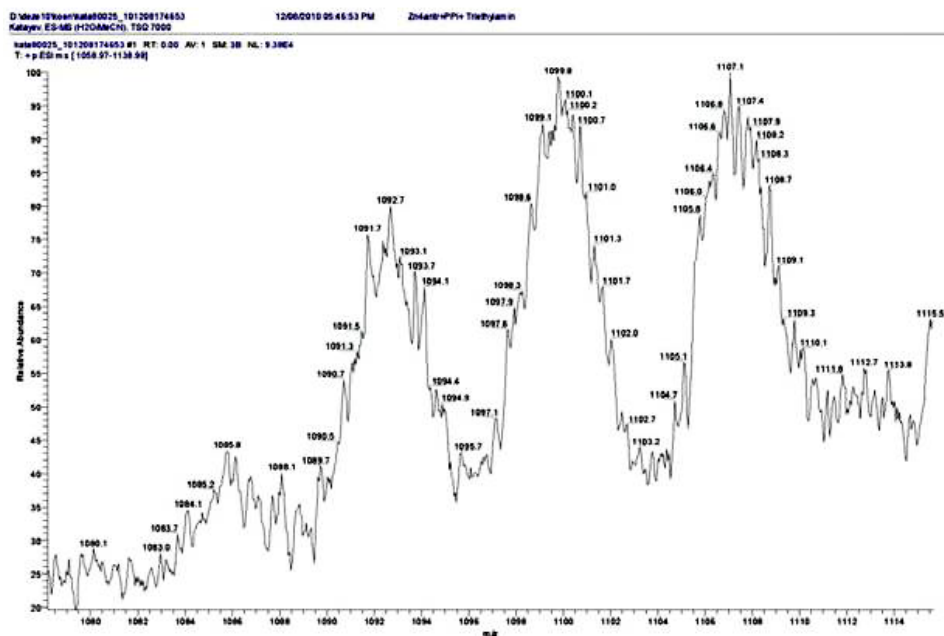


Figure 16: ESI in the area $m/z=1080-1114$ of a mixture of **4d** (Zn₄anthr) and sodium pyrophosphate (PPi) showing the peaks which correspond to the [2+4] complex. The difference between peaks $m/z=M(Na^+)/3$.

1. Rigid Luminescent bis-Zinc(II)-bis-Cyclen Complexes for the Detection of Phosphate Anions and non-covalent Protein Labeling in Aqueous Solution

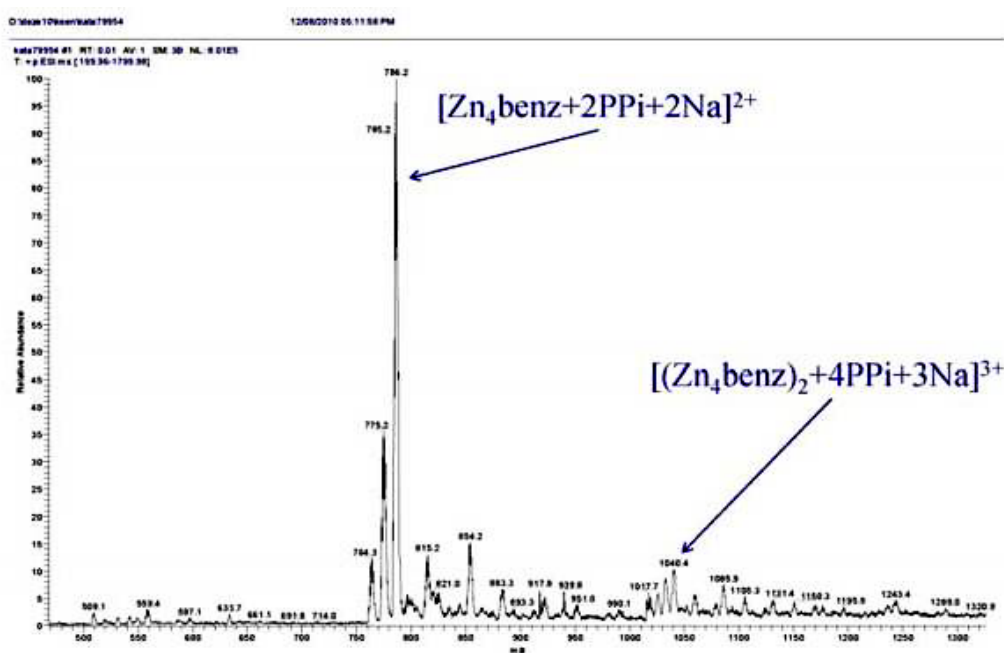


Figure 17: ESI of a mixture of **4b** (Zn₄benz) and sodium pyrophosphate (PPi).

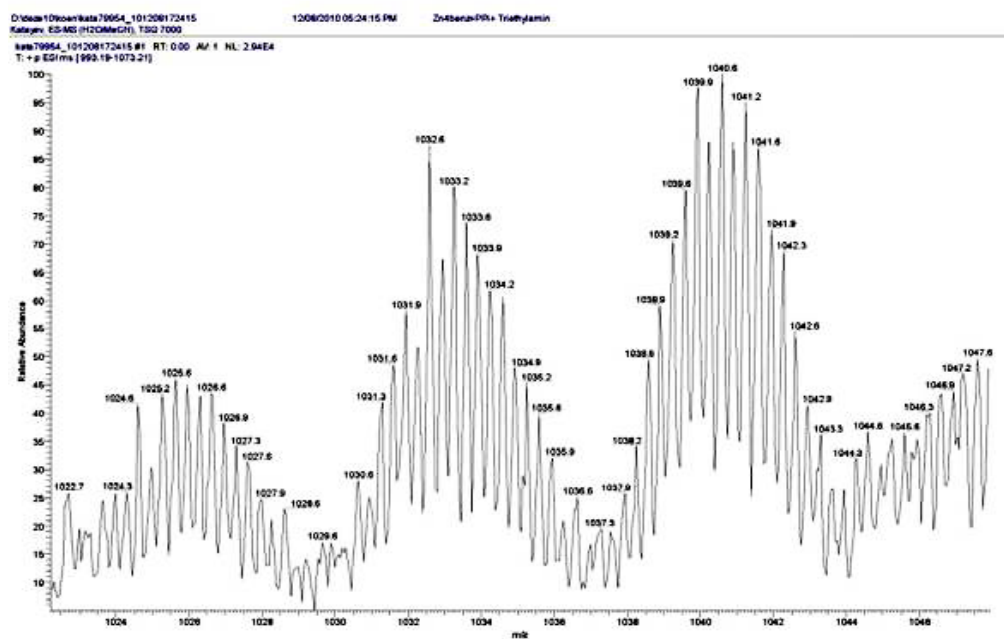


Figure 18: ESI in the area $m/z=1024-1048$ of a mixture of **4b** (Zn₄benz) and sodium pyrophosphate (PPi) showing the peaks which corresponds the [2+4] complex. The difference between peaks is $m/z=M(\text{Na}+)/3$

1. Rigid Luminescent bis-Zinc(II)-bis-Cyclen Complexes for the Detection of Phosphate Anions and non-covalent Protein Labeling in Aqueous Solution

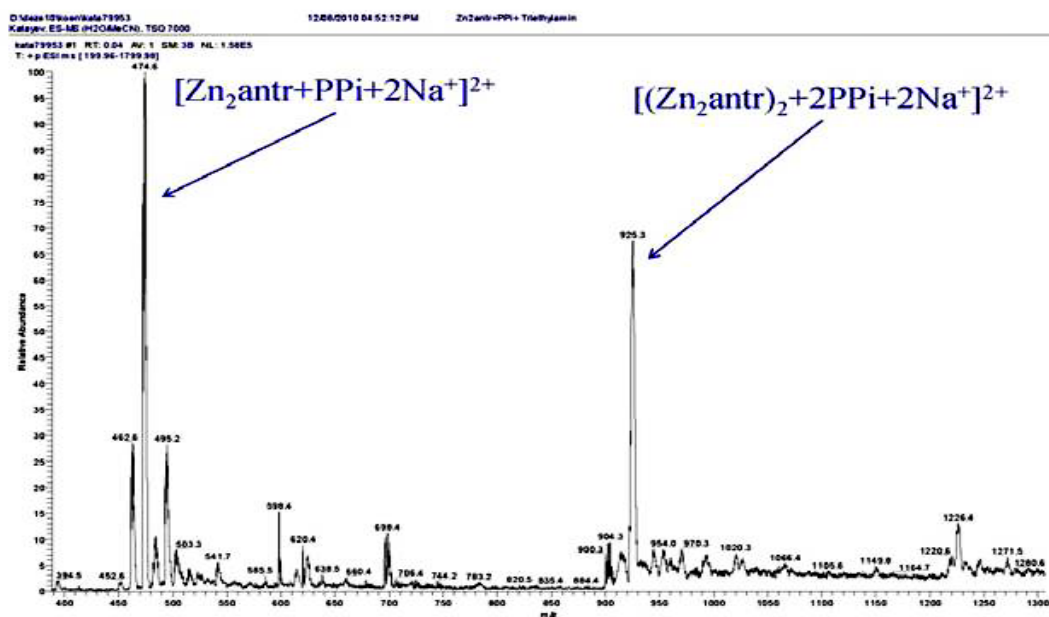


Figure 19: ESI spectra of a mixture of **4c** (Zn₂antr) and sodium pyrophosphate (PPi)

1.7 References

- [1] N. Soh *Sensors* **2008**, *8*, 1004.
- [2] K. M. Marks, G. P. Nolan *Nat Meth* **2006**, *3*, 591.
- [3] Y. X. Wang, J. Y. J. Shyy, S. Chien *Annu. Rev. Biomed. Eng.* **2008**, *10*, 1.
- [4] R. Y. Tsien *Annu. Rev. Biochem.* **1998**, *67*, 509.
- [5] N. George, H. Pick, H. Vogel, N. Johnsson, K. Johnsson *J. Am. Chem. Soc.* **2004**, *126*, 8896.
- [6] I. S. Carrico, B. L. Carlson, C. R. Bertozzi *Nat Chem Biol* **2007**, *3*, 321.
- [7] A. Keppler, H. Pick, C. Arrivoli, H. Vogel, K. Johnsson *Proc. Natl. Acad. Sci. USA* **2004**, *101*, 9955.
- [8] B. P. Duckworth, Z. Zhang, A. Hosokawa, M. D. Distefano *ChemBioChem* **2007**, *8*, 98.
- [9] H. Nonaka, S. Tsukiji, A. Ojida, I. Hamachi *J. Am. Chem. Soc.* **2007**, *129*, 15777.
- [10] a)L. W. Miller, J. Sable, P. Goelet, M. P. Sheetz, V. W. Cornish *Angew. Chem. Int. Ed.* **2004**, *43*, 1672; b)L. W. Miller, Y. Cai, M. P. Sheetz, V. W. Cornish *Nat Meth* **2005**, *2*, 255; c)K. M. Marks, P. D. Braun, G. P. Nolan *Proc. Natl. Acad. Sci. USA* **2004**, *101*, 9982.
- [11] a)T. Hunter *Cell* **2000**, *100*, 113; b)W. Saenger *Principles of Nucleic Acid Structure*, Springer, New York, **1998**; c)S. Aoki, E. Kimura *Rev. Mol. Biotechnol.* **2002**, *90*, 129; d)R. L. P. J. T. Adams Knowler, D. P. Leader, in *The Biochemistry of Nucleic Acids*, 10 ed., Chapman and Hall, New York, **1986**; e)L. N. Johnson, R. J. Lewis *Chem. Rev.* **2001**, *101*, 2209; f)M. B. Yaffe *Nat. Rev. Mol. Cell Biol.* **2002**, *3*, 117.
- [12] W. N. Lipscomb, N. Straeter *Chem. Rev.* **1996**, *96*, 2375.
- [13] E. G. Krebs, E. H. Fischer, in *Vitam. Horm.*, Vol. 22, Academic Press, **1964**, pp. 399.
- [14] a)S. Tamaru, I. Hamachi, in *Structure and Bonding (Recognition of Anions)*, Vol. 129 (Ed.: R. Villar), Springer, Berlin/Heidelberg, Germany, **2008**, p. 95; b)M. Kruppa, B. Koenig *Chem. Rev.* **2006**, *106*, 3520.
- [15] a)T. Sakamoto, A. Ojida, I. Hamachi *Chem. Commun.* **2009**, 141; b)A. Ojida, Y. Mito-oka, M. Inoue, I. Hamachi *J. Am. Chem. Soc.* **2002**, *124*, 6256; c)A. Ojida, S. K. Park, Y. Mito-oka, I. Hamachi *Tetrahedron Lett.*, **2002**, *43*, 6193; d)A. Ojida, I. Takashima, T. Kohira, H. Nonaka, I. Hamachi *J. Am. Chem. Soc.* **2008**, *130*, 12095; e)A. Ojida, H. Nonaka, Y. Miyahara, S.-I. Tamaru, K. Sada, I. Hamachi *Angew. Chem., Int. Ed.* **2006**, *45*, 5518.
- [16] a)D. H. Lee, J. H. Im, S. U. Son, Y. K. Chung, J. I. Hong *J. Am. Chem. Soc.* **2003**, *125*, 7752; b)D. H. Lee, S. Y. Kim, J. I. Hong *Angew. Chem. Int. Ed.* **2004**, *43*, 4777; c)H. K. Cho, D. H. Lee, J. I. Hong *Chem. Commun.* **2005**, 1690.
- [17] a)C. Lakshmi, R. G. Hanshaw, B. D. Smith *Tetrahedron* **2004**, *60*, 11307; b)W. M. Leevy, J. R. Johnson, C. Lakshmi, J. Morris, M. Marquez, B. D. Smith *Chem. Commun.* **2006**, 1595;

- c)W. M. Leevy, S. T. Gammon, H. Jiang, J. R. Johnson, D. J. Maxwell, E. N. Jackson, M. Marquez, D. Piwnica-Worms, B. D. Smith *J. Am. Chem. Soc.* **2006**, *128*, 16476.
- [18] S. Mizukami, T. Nagano, Y. Urano, A. Odani, K. Kikuchi *J. Am. Chem. Soc.* **2002**, *124*, 3920.
- [19] a)S. Aoki, M. Zulkefeli, M. Shiro, M. Kohsako, K. Takeda, E. Kimura *J. Am. Chem. Soc.* **2005**, *127*, 9129; b)E. Kimura, T. Shiota, T. Koike, M. Shiro *J. Am. Chem. Soc.* **1990**, *112*, 5805; c)T. Koike, S. Kajitani, I. Nakamura, E. Kimura, M. Shiro *J. Am. Chem. Soc.* **1995**, *117*, 1210; d)E. Kimura, S. Aoki, T. Koike, M. Shiro *J. Am. Chem. Soc.* **1997**, *119*, 3068.
- [20] D. S. Turygin, M. Subat, O. A. Raitman, S. L. Selector, V. V. Arslanov, B. König, M. A. Kalinina *Angew. Chem. Int. Ed.* **2006**, *45*, 5340.
- [21] E. Schneider, M. Keller, A. Brennauer, B. K. Hoefelschweiger, D. Gross, O. S. Wolfbeis, G. Bernhardt, A. Buschauer *ChemBioChem* **2007**, *8*, 1981.
- [22] A. Ojida, K. Honda, D. Shinmi, S. Kiyonaka, Y. Mori, I. Hamachi *J. Am. Chem. Soc.* **2006**, *128*, 10452.
- [23] B. Smith, E. J. O'Neil, B. D. Smith *Coord. Chem. Rev.* **2006**, *250*, 3068.
- [24] B. Gruber, S. Stadlbauer, K. Woinaroschy, B. König *Org. Biomol. Chem.* **2010**, *8*, 3704.
- [25] a)Y. H. Kim, H. C. Jeong, S.-H. Kim, K. Yang, S. K. Kwon *Adv. Funct. Mater.* **2005**, *15*, 1799 ; b)Q. Dai, D. Xu, K. Lim, R. G. Harvey *J. Org. Chem.* **2007**, *72*, 4856 ; c)P. A. Bonvallet, C. J. Breitkreuz, Y. S. Kim, E. M. Todd, K. Traynor, C. G. Fry, M. D. Ediger, R. J. McMahon *J. Org. Chem.* **2007**, *72*, 10051
- [26] a)K. V. B. Josyula, P. Gao, C. Hewitt *Tetrahedron Lett.* **2003**, *44*, 7789; b)G. V. Malkov, A. V. Shastin, Y. I. Estrin, E. R. Badamshina, Y. M. Mikhailov *Propellants Explos. Pyrotech.* **2008**, *33*, 431.
- [27] S. G. M. Sheldrick, v. 6.12, Structure Determination Software Suite, (2001) Bruker AXS, Madison, Wisconsin, USA.

Chapter 2

Rigid Amphiphilic Molecular receptors, Bioconjugates and Radiopharmaceuticals based on Metal-cyclen complexes via Click chemistry

“Click chemistry-the reinvigoration of an old style of organic synthesis”

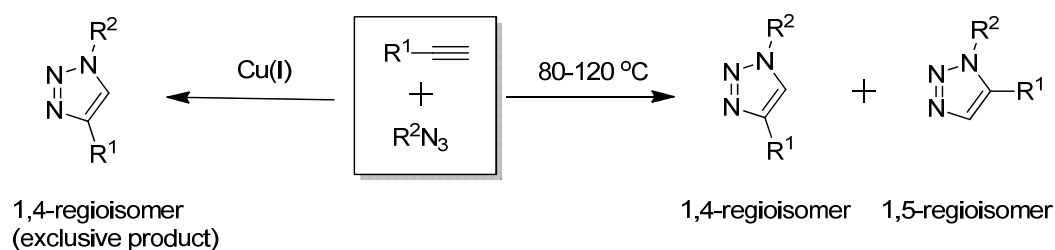
-Kolb, Finn and Sharpless in 2001^[1]

2.1 General Introduction

2.1.1 The “Click” Philosophy

Since their debut, click chemistry and related procedures have stimulated many different research fields. In 2001, Kolb, Finn and Sharpless published one important review coining the term “Click Chemistry” which addresses a set of powerful, highly reliable, and selective reactions for the rapid synthesis of useful new compounds and combinatorial libraries.^[2] The click reactions are governed by kinetic control and are highly reliable and selective processes. The set of stringent criteria that must be fulfilled in the context of click chemistry, as defined by Sharpless et al. are reactions that “are modular, wide in scope, high yielding, create only inoffensive by-products (that can be removed without chromatography), are stereospecific, simple to perform and that require benign or easily removed solvent”.^[3]

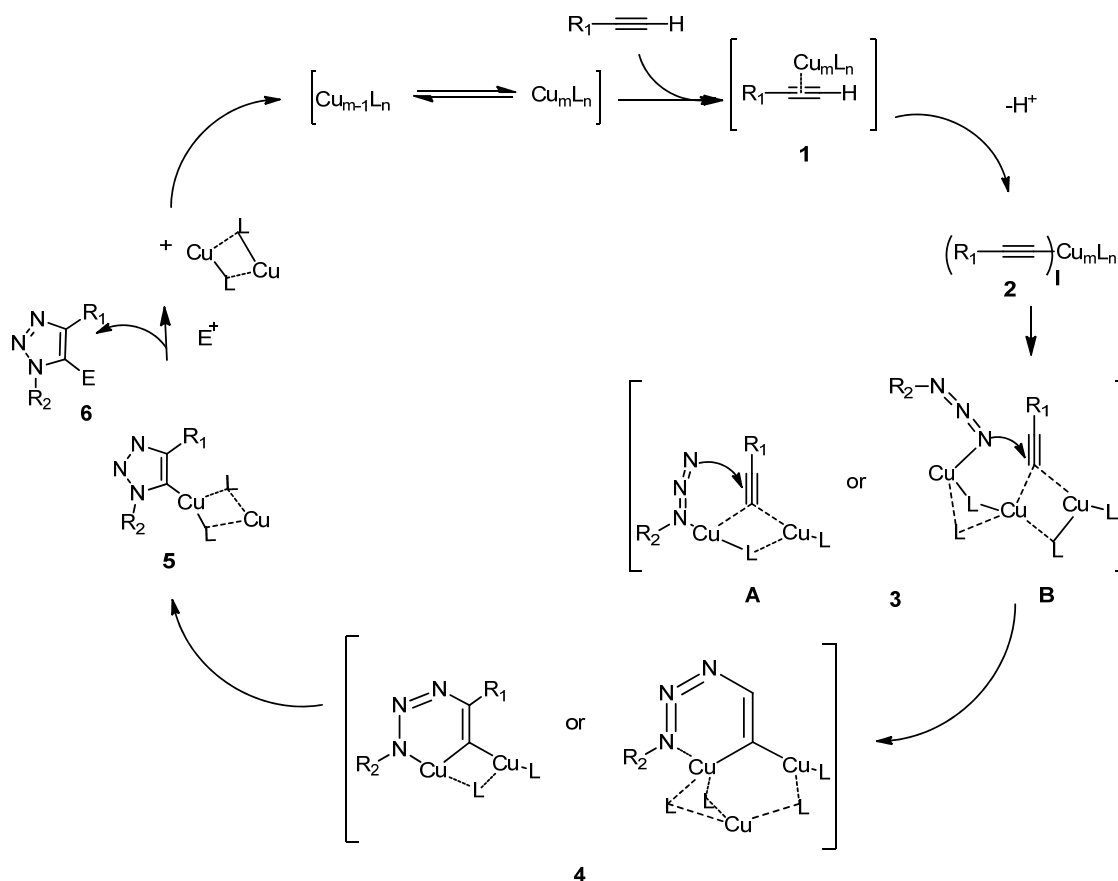
Although the criteria drawn for the “Click Chemistry” status are highly subjective, several processes or reactions have been identified which fit to the concept: Cycloaddition reactions (eg. Huisgen 1,3-dipolar cycloaddition reactions^[4], Diels-Alder reactions and inverse electron demand Diels-Alder reactions);^[1] carbonyl chemistry of the non-Aldol type (eg. formations of ureas, thioureas, hydrazones, oxime ethers, amides, aromatic heterocycles etc);^[3] nucleophilic ring opening reactions (eg. the openings of strained heterocyclic electrophiles, such as aziridines, epoxides, cyclic sulfates, aziridinium ions, episulfonium ions, etc);^[1] addition reactions to carbon-carbon multiple bonds (eg. epoxidations, aziridinations, dihydroxylations, sulfenyl halide additions, nitrosyl halide additions, and certain Michael additions)^[1, 3] are some of the major processes that can be mentioned.



Scheme 1: The CuAAC results in 1,4- regioisomer as exclusive product while thermal Huisgen 1,3-Cycloaddition results in a mixture of both 1,4 and 1,5- regioisomers often in 1:1 ratio.

Among all these processes, Huisgen 1,3-dipolar cycloaddition reaction has gained a special place. The ease of synthesis of the alkyne and azide functionalities, coupled with their kinetic stability and tolerance to a wide variety of functional groups and reaction conditions, make these complementary coupling partners particularly attractive.^[5] Above this, the dramatic rate acceleration

of the azide–alkyne coupling event under copper (I) catalysis^[6] and the selectivity for the 1,4-disubstituted 1,2,3-triazole (anti-1,2,3-triazole)^[7], the copper catalyzed version (CuAAC) has been the most popular and widely used and often referred simply as ‘The Click reaction’.



Scheme 2: Outline of a plausible mechanisms for the Cu(I) catalyzed reaction between organic azides and terminal alkynes [adapted from the quoted reference]^[8]

2.1.2 The Click reaction: An efficient strategy for bioconjugations

The term ‘bioconjugation’ comprehend a broad interdisciplinary area developed at the interface between molecular biology and chemistry.^[9] Bioconjugation techniques mainly involve the covalent attachment of biological molecules to non-biological molecules to form a novel complex having the combined properties of all the individual components and its integration in functional devices.^[10]

Bioorthogonal conjugations via the click reaction

Bioconjugation techniques are of general interest for both biologists and chemists. Over the

years several efficient bioconjugation techniques have been developed to attach fluorescent probes, affinity tags, or isotope labels to different biomolecules. Many different coupling strategies such as thiol-maleimide, amine-activated ester coupling, have been used repeatedly to decorate biomolecules or cell surface labeling *in vitro*.^[11] However for *in vivo* labeling of biomolecules, the couplings partners have to react efficiently and selectively even in presence of a vast variety of accessible reactive moieties, which are present in complex biological medium. To handle the problems of *in vivo* labeling, concept of bioorthogonal chemistry has been developed that deals with bioorthogonal chemical reporters, which are defined as “non-native, non-perturbing chemical handles that can be modified in living systems through highly selective reactions with exogenously delivered probes.”^[12] Several site-specific, bioorthogonal, conjugation techniques have been developed to overcome the problems encountered with *in vivo* labeling and one of the most frequently used techniques is the click reaction.^[1, 13] The reactant partners of the click reaction, azide and alkyne, both are highly energetic functional groups with relatively narrow distributions of reactivity^[13c] and the reaction can proceed irreversibly in water at neutral pH and biocompatible temperatures (25–37°C) without any cytotoxic reagents or byproducts. Azide functionality is particularly interesting in this case, as it is absent in almost all the known natural compounds and despite a high intrinsic reactivity, azides allow selective ligation with a limited number of reactive partners.^[5] This property of bioorthogonality provides extreme selectivity for bringing together azide and alkyne derivatives to form triazoles even in complex biological samples.^[9] Also it is noteworthy that azide and alkyne groups are easy to introduce into organic compounds by both nucleophilic and electrophilic processes. Hence these can be incorporated into biological molecules by organic synthesis and chemical conjugation (or via biosynthetic pathways using predesigned precursors^[14]).

The possibility of using CuAAC for bioconjugation was first demonstrated by Meldal *et al* in their publication in 2002, where they have reported synthesis of peptidotriazoles by solid phase synthesis.^[15] Following this landmark report, numerous functional and reporter groups are introduced into biomolecules such as peptide and proteins for DNA labeling and cell surface labeling.^[16] Sharpless *et al* could successfully demonstrate bioorthogonality of CuAAC by labeling of Cowpea mosaic virus (CPMV) (a biomolecular scaffold with a structurally rigid assembly of 60 identical copies of a two-protein asymmetric unit around a single-stranded RNA genome) with fluorescein in quantitative yield.^[13c]

Similarly some other notable bioorthogonal conjugations via click chemistry are: cell surface labeling of *Escherichia coli* via copper catalyzed click reaction [Link and Tirrell, 2003]^[16], total solid-phase synthesis of marine cyclodepsipeptide IB-01212 [Cruz *et al*, 2006]^[17], functionalization of modified DNA [Carell *et al*, 2006]^[18].

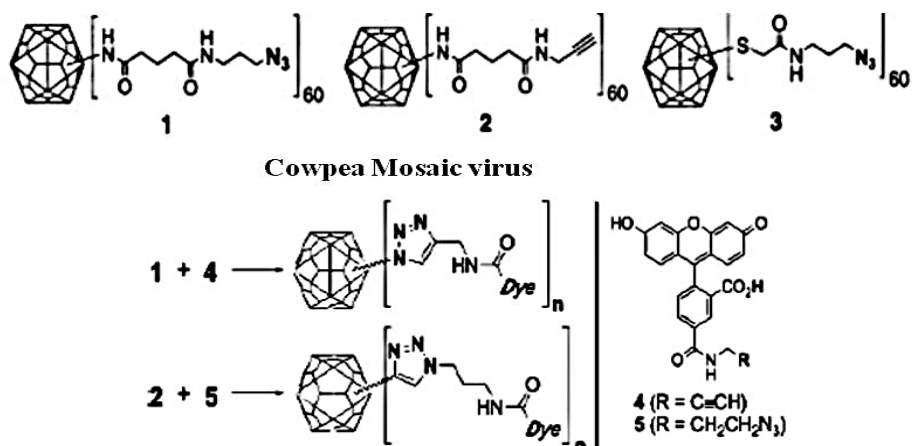


Figure 1: Labeling of Cowpea mosaic virus (CPMV) with fluorescein via click reaction [adapted from the quoted reference]^[13c]

The Click Reaction in Radiopharmaceutical Chemistry

Currently application of click chemistry receives growing interest in the field in radiopharmacy. The 1,2,3-triazole moiety was found to improve the pharmacokinetic properties of certain radiopharmaceuticals^[19] and there are several reports based on application of click chemistry for radiolabeling of peptidic compounds or new radiotracers. Since several noninvasive molecular imaging techniques such as positron emission tomography (PET), single-photon emission computed tomography (SPECT) emerge as highly sensitive imaging method for *in vivo* studies, radiolabeling of biologically active molecules has become an important tool to assess novel drug candidates. There are several reports where the click reaction was used as an efficient strategy to synthesize radiolabeled (¹⁸F, ¹¹C) peptides as imaging agents for PET.^[20]

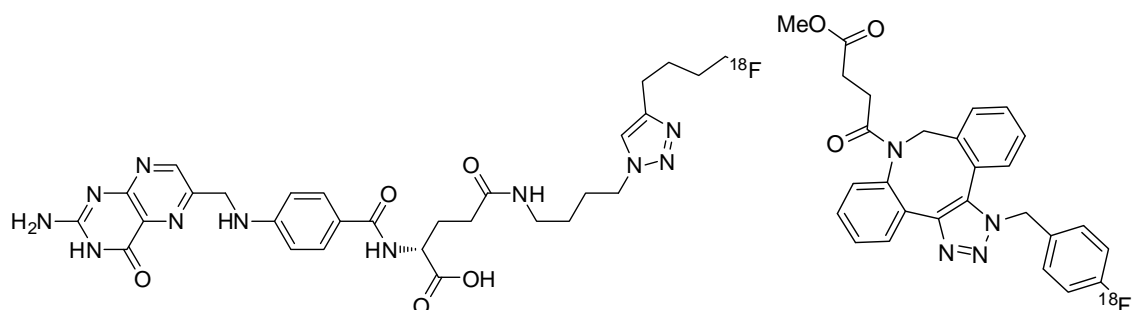


Figure 2: Some of the radiopharmaceuticals synthesized via click chemistry^[21]

2.2 Outline of the Chapter

In this chapter the use of click chemistry for the design and the synthesis of bioconjugates and radiopharmaceuticals and also of modified rigid amphiphilic molecular receptors based on metal-cyclen complexes are summarized. We have synthesized alkynes of different biologically important molecules such as cholesterol, biotin and used Cu(I) mediated click reaction to attach these alkynes to the azide of bis-cyclen by forming a 1,2,3-triazole. The applications or the potential applications of the synthesized bioconjugate and radiopharmaceuticals are discussed.

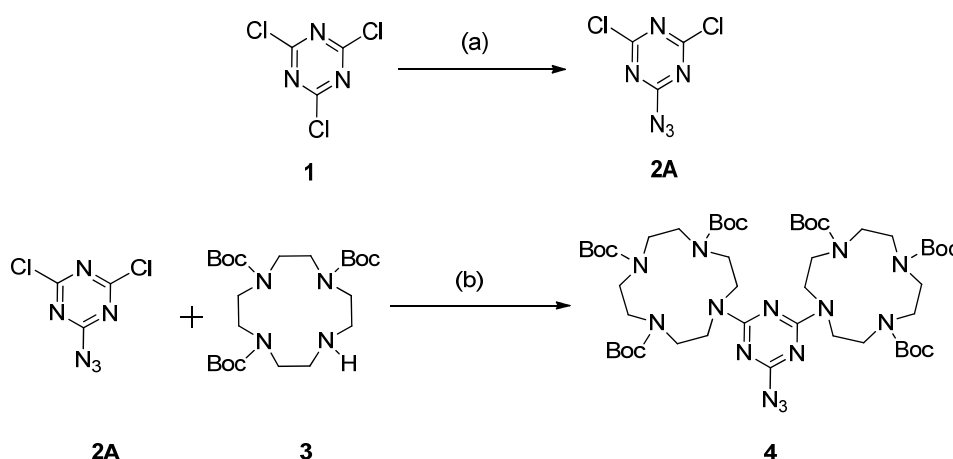
We also report the design and the synthesis of a modified rigid amphiphilic molecular receptor based on metal-cyclen complexes via click reaction for potential application in a template guided cooperative self-assembly of nucleotides at fabricated interfaces.

2.3 Design and synthesis of bioconjugates based on a Zn(II)-bis-cyclen complex:

Introduction to potential applications, results and discussions

2.3.1 Synthesis of bis-cyclen azide

The azide functionality used for the click reaction is a modification of bis-cyclen and it was synthesized as shown in Scheme 3



Scheme 3: Synthesis of bis-cyclen-azide (a) NaN₃ (1eq), acetone/water (1:1), 5 min, rt [yield: 15%], (b) K₂CO₃, acetone, 56°C, 12h [yield: 20%]

2.3.2 Biotin bioconjugate of a Zn(II)-bis-cyclen complex for potential applications in activity based proteomics¹

2.3.2.1 Introduction and aim of the project

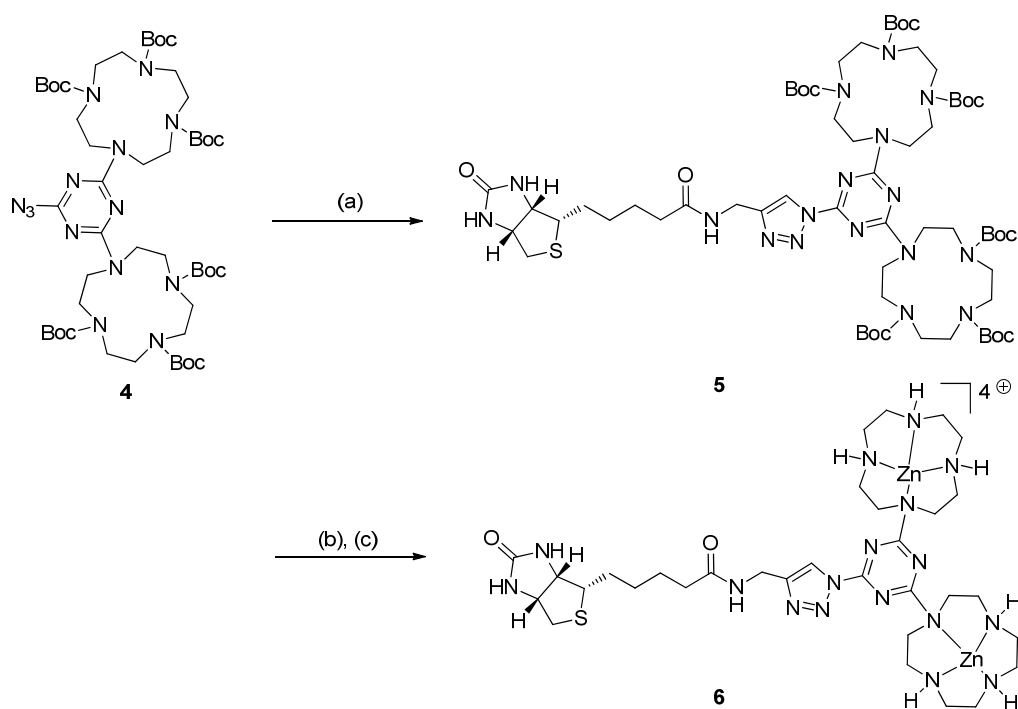
Over last two decades, activity based protein profiling (ABPP); originally invented by James C. Powers (Georgia Tech, Atlanta) in 1990;^[22] has proven to be an attractive toolkit for functional proteomic techniques. This technique uses chemically designed small activity probes (ABP) to tag, enrich, and isolate, distinct sets of proteins based on their enzymatic activity. The probes can be modified chemically to interact with a defined protein site and a complex mixture of proteins can be selectively enriched via a reactive activity probe. ABPs function as highly specific, mechanism-based reagents that provide a direct readout of enzymatic activity within complex proteomes. Modification of protein targets by an ABP facilitates their purification and isolation.^[23] The activity probes typically consist of two elements: a reactive group (RG) and a tag. Additionally, some probes may contain a binding group which enhances selectivity. The reactive group is designed to interact with a specific class of protein and the reporter tag to signal the interaction or binding (eg. fluorescence, affinity, isotope labeled tags).

Here, we report the design and synthesis of a biotin labeled Zn(II)-bis-cyclen complex as an activity probe (ABP) for profiling of phosphorylated proteins. These can also be considered as a chemically modified potential phosphospecific artificial antibody. Protein phosphorylation is recognized to play a crucial role in the regulation of cell growth and development.^[24] Also phosphorylation plays an important role in signaling pathways.^[25] Therefore it is important to detect the changes in the phosphorylation state of proteins. Zn(II)-bis-cyclen complex is known for its affinity towards phospho anions. Hence we have considered coupling of Zn(II)-bis-cyclen with a reporter tag to design an activity probe for phosphorylated proteins. Biotin is used as the reporter tag for the synthesized probe.

2.3.2.2 Design and synthesis of biotin bioconjugate of Zn(II)-bis-cyclen complex

The biotinylated Zn(II) bis-cyclen complex was synthesized by click reaction between biotinylated acetylene and bis cyclene azide as shown in Scheme 4.

¹ The biotin bioconjugate of Zn(II)-bis-cyclen was synthesized by Mouchumi Bhuyan. The gel phase studies were done by Thomas Zanni and Mouchumi Bhuyan. We are thankful to Dr. Sabine Amslinger for helpful discussions and collaboration.



Scheme 4: Synthesis of Biotin bioconjugate of Zn(II)-bis-cyclen complex (a) Biotin acetylene, CuSO₄, sodium ascorbate, TBTA, DMF, rt, 12h [yield: 90%]; (b) TFA, DCM, 4h, basic ion exchanger resin [yield: quantitative]; (c) Zn(ClO₄)₂, MeOH/MeCN, reflux, o/n [yield: 99%]. Counter ions of the complexes to yield a neutral complex are not shown for clarity.

The acetylene of biotin was synthesized following a reported procedure. Detailed experimental procedures and characterization are reported in the experimental and supporting data section.

2.3.2.3 Selective recognition of phosphorylated protein in gel phase

To evaluate the selectivity of our probe towards phosphorylated proteins, western blot technique has been carried out using a nitrocellulose membrane. Phosphorylated bovine α -casein, dephosphorylated α -casein, ovalbumin and bovine serum albumin were used as protein samples. We have used horseradish peroxidase conjugated streptavidin to detect the biotinylated Zn(II) complex bound to the protein in the membrane and commercially available “Thermo Scientific SuperSignal West Pico chemiluminescent substrate” as an enhanced chemiluminescent (ECL) substrate for horseradish peroxidase (HRP) enzyme. To minimise the nonspecific interaction of the horseradish peroxidase conjugated streptavidin with the membrane, we have used BSA as a blocking buffer.

Western blot technique showed that our probe detects phosphorylated casein and also 70% dephosphorylated casein while there was no signal for ovalbumin (Figure 2). Although ovalbumin has two phosphorylated sites, these may be not accessible by our probe due to steric reasons. These

preliminary studies encourage further investigations using a wider range of phosphorylated and non-phosphorylated proteins.

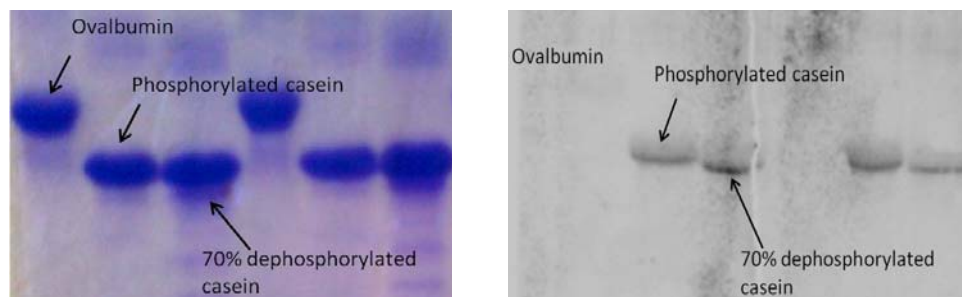


Figure 2: Gel phase studies with probe **6** using ovalbumin and α -casein. [Left] Coomassie blue stained electrophoretic gel for ovalbumin, phosphorylated α -casein and 70% dephosphorylated α -casein; [Right] Western blot studies for ovalbumin, phosphorylated α -casein and 70% dephosphorylated α -casein [each lane contains 11 μ g of protein, concentration of the biotinylated Zn(II) complex is 10^{-6} M, concentration of horseradish peroxidase conjugated streptavidin is 0.2 μ g/ml]

2.3.2.4 Concluding remarks

In conclusions we have reported the synthesis of a biotin bioconjugate of Zn(II)-bis-cyclen . The presence of the biotin moiety on the probe can be exploited for the enrichment and profiling of phosphorylated proteins. Preliminary western blot studies using phosphorylated casein and ovalbumin show the feasibility of the concept using biotinylated Zn(II) complex as a probe for activity based profiling of phosphorylated proteins. Further investigations on a wider range on proteins are under progress.

2.3.3 Modified cyclen based precursor for potential radiopharmaceuticals for Positron Emission Tomography (PET)²

2.3.3.1 Introduction and aim of the project

Positron emission tomography (PET) is a nuclear medicine imaging technique that produces a three-dimensional image or picture of functional processes in the body. It deals with detection of pairs of gamma rays emitted indirectly by a positron-emitting radionuclide (tracer), which is introduced into the body on a biologically active molecule. A majority of PET radiopharmaceuticals for clinical and research applications are labeled commonly with four radionuclides: ^{15}O , ^{13}N , ^{11}C and ^{18}F .

² This project is in progress in collaboration with Department of Chemistry and Pharmacy, Friedrich-Alexander University Erlangen, Germany. The synthetic part reported here is done at university of Regensburg by Mouchumi Bhuyan.

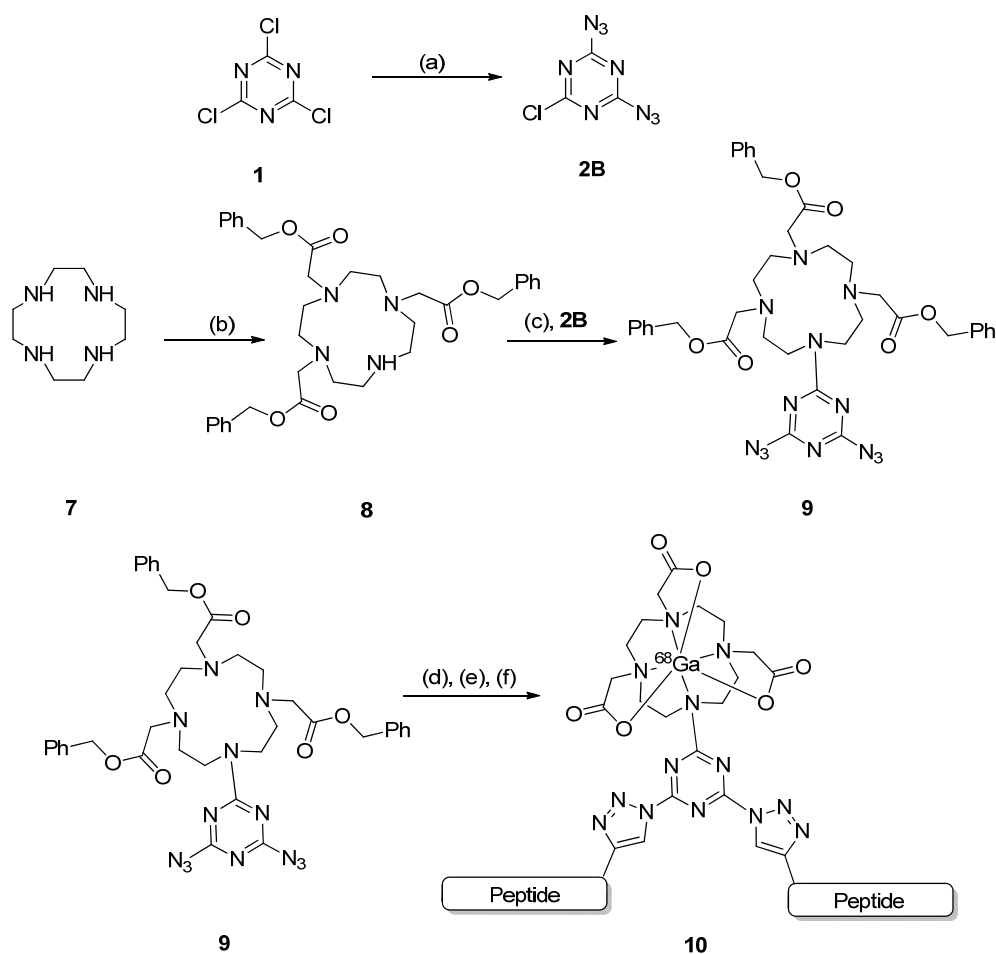
However, a number of metal radionuclides such as ^{55}Co , ^{44}Sc , ^{62}Cu , ^{68}Ga , ^{66}Ga have also been studied. Among these, the use of gallium radionuclides in nuclear medicine dates back to the late 1940s^[26] and it has three radioisotopes of interest for medical imaging, ^{67}Ga ($t_{1/2} = 3.25$ days), ^{66}Ga ($t_{1/2} = 9.5$ h) and ^{68}Ga ($t_{1/2} = 68$ min). ^{68}Ga is one very attractive radionuclide as it can be generated in situ easily, fast and cost effective way by using $^{68}\text{Ga}/^{68}\text{Ge}$ generator and leading to a minimum loss of activity.^[27]

There are two primary requirements for using gallium complexes as radiopharmaceuticals: first, the gallium complexes must resist hydrolysis at physiological pH [$\text{Ga}(\text{OH})_3$, the primary product of hydrolysis of a gallium complex is insoluble at physiological pH until $[\text{Ga}(\text{OH})_4]^-$ is formed at a higher pH (pH 9)]; second, the used gallium complexes should be more stable than the Ga(III)-transferrin complex.^[28] The ionic radii, ionization potential and coordination environment of Ga^{3+} is similar to that of Fe^{3+} . Hence gallium complexes used as radiopharmaceuticals must be stable enough to avoid trans-chelation of Ga^{3+} to various iron binding proteins, particularly transferrin, which has two binding sites. These special requirements made it crucial to design polydentate ligands for Ga^{3+} and typically these are hexadentate.

For *in vivo* cancer detection or for tracing tumour or neoplastic cells, peptides are gaining much attention as excellent tissue specific uptake can be achieved. Peptides can be modified and labeled chemically. Although among the radiolabeled peptides, ^{13}F and ^{11}C are commonly used radionuclides, there are some reports of radiolabeling of peptides with metallic radionuclides. Recently, Prante *et al* reported synthesis of ^{68}Ga -amino acid conjugate and could successfully show its potential application as tumour tracer for PET.^[29] As an extension to this idea, we (in collaboration with Department of Chemistry and Pharmacy, Friedrich-Alexander University Erlangen, Germany) developed a cyclen based ^{68}Ga -peptide conjugate for potential applications as radiopharmaceutical. The challenge in preparing (radio)metal containing amino acids or peptides with retained biological activity is to develop an appropriate synthetic strategy.^[29] We considered using the bioorthogonal and robust click reaction for the synthesis of the intended radiopharmaceuticals. We synthesised bis azide of cyclen based ^{68}Ga chelate, which can be attached to the target peptides by using the click reaction. The rationale behind the synthesis of a bis-azide is to increase the intramolecular peptide concentration of the compounds, while maintaining the overall molecular weight in a reasonable range.

2.3.3.2 Synthesis of precursor for potential Radiopharmaceuticals for Positron Emission Tomography (PET)

The cyclen based bis azide for ^{68}Ga -peptide conjugate was synthesized as shown in Scheme 5.



Scheme 5: Synthesis of precursor for potential Radiopharmaceuticals for positron emission tomography (PET) (a) $\text{NaN}_3(2\text{eq})$, acetone/water(1:1), 10 min, rt [yield: 30%]; (b) benzyl bromoacetate, NaHCO_3 , MeCN, reflux, 12h [yield: 45%]; (c) K_2CO_3 , acetone, reflux, 8h [yield: 30%]; (d) terminal acetylene of desired peptide, Cu(I), base; (e) H_2 , Pd/C, solvent; (f) metal complexation with ^{68}Ga salt [(d), (e) and (f) steps to be carried out in Department of Chemistry and Pharmacy, Friedrich-Alexander University Erlangen, Germany]

Detailed experimental procedures and characterization are reported in the experimental and supporting data section.

2.3.3.3 Concluding remarks

We have designed and synthesized precursor for ^{68}Ga based potential radiopharmaceuticals for Positron Emission Tomography (PET). Further synthetic development and investigations of the applicability of the synthesized complex as radiopharmaceutical are in progress.

2.3.4 Design and synthesis of rigid amphiphilic modified Zn(II)-cyclen based receptors for a template guided cooperative self-assembly of nucleotides at interfaces³

2.3.4.1 Introduction and aim of the project

Multivalent interactions based on non-covalent bonds, such as hydrogen bonding and metal-ligand coordination, as well as π - π stacking, hydrophobic, ionic, and van der Waals forces are essential ingredients in the mediation of biological processes, as well as in the construction of complex (super)structures for materials applications.^[30] Such weak interactions (bond energy 2-20 kcal mol⁻¹) play a key role in fundamental biological processes, such as protein folding or the expression and transfer of genetic information. Reversible formation of multiple hydrogen bonding is one of the most widely studied classes of non-covalent interactions in supramolecular chemistry, mainly because, the existence of H-bonds has long been regarded to play a crucial role in many biologically relevant processes, such as recognition between DNA base pairs, ligand-binding to receptor sites, enzyme catalysis, and α -helix or β -sheet formation.^[31]

Tailoring molecular organization is one of the final goals of supra molecular chemistry and is essential for the design of molecular devices.^[32] In 1991, Kurihara *et al* reported for the first time the formation of two-dimensional arrangement of molecules at the air-water interface on a Langmuir-Blodgett (LB) trough. They showed arrangement of nucleic acid bases at the air water interface, where the hydrogen bonding took place in the water phase and an amphiphilic diaminotriazine was able to selectively bind nucleosides and nucleic acid bases.^[33] Over the last two decades, several strategies were reported using nucleic acid base pairing as a basis for planar molecular-recognition systems. Most of these reports focused on self-assembled monolayers (SAMs) or Langmuir monolayers that are formed from compounds bearing nucleobases or their synthetic analogues. However, both techniques individually have some limitations. Although LB is a well developed method, its practical applicability is severely limited and due to steric hindrance and phase separation of monolayer constituents, SAM based methods are not suitable for lateral tailoring of molecular recognition and also it is difficult to precisely control the size and distribution of the SAMs because the structure is determined by the interplay of the kinetics and thermodynamics of the self-assembly process.^[32, 34] Langmuir-Blodgett (LB) monolayer technique in combination with the SAM-based approach can overcome the steric limitation of SAM. This combined approach was reported previously from our group. This technique showed fabrication of double layers modified by amphiphilic Zn(II)-cyclen complexes from self assembled monolayers and LB films and this double

³ The rigid amphiphilic Zn(II)-bis-cyclen receptors were synthesized at University of Regensburg by Mouchumi Bhuyan. The investigations at interfaces are in progress at the Institute of Physical Chemistry and Electrochemistry of the Russian Academy of Sciences in Moscow in the group of Prof. M. A. Kalinina.

layer could act as a 2D synthetic template for cooperative self-assembly of adenosine and uridine nucleotides.^[34a]

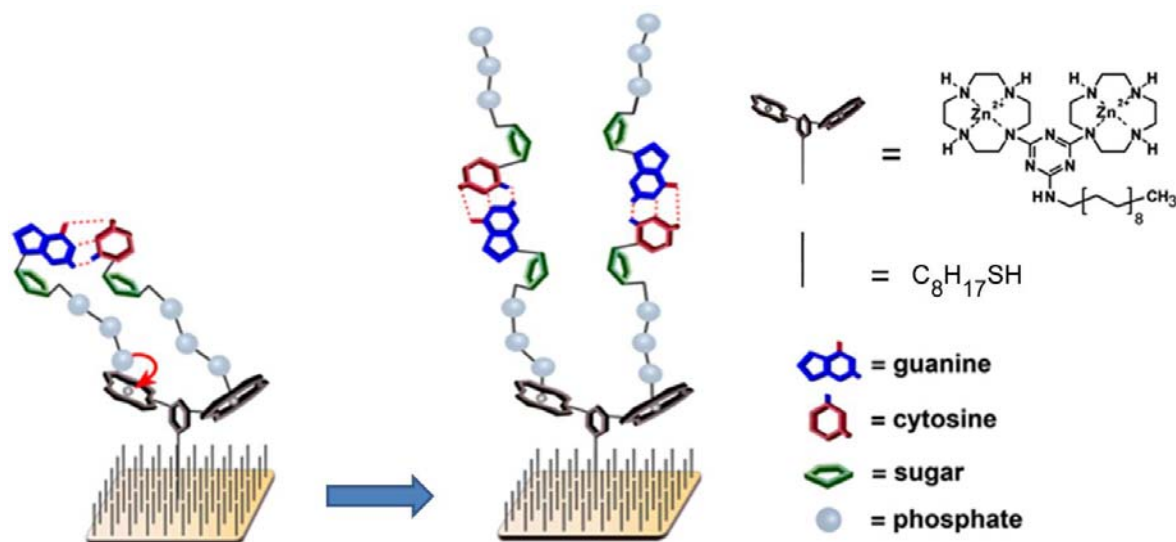


Figure 2: Schematic representation of the proposed mechanism of the stepwise self-assembly of complementary nucleotides on a SAM-Zn(II)-BC template [adapted from the quoted reference]^[34a]

To expand the scope of this methodology and to extend the cooperativity, we considered to synthesize a rigid modified Zn(II)-tetra-cyclen based amphiphilic receptor and a cholesterol bioconjugate of a Zn(II)-bis-cyclen complex for template guided cooperative self-assembly of nucleotides at interfaces.

2.3.4.2 Design and synthesis of rigid Zn(II)-bis-cyclen based amphiphilic receptors

The rigid modified amphiphilic Zn(II)-bis-cyclen systems that were designed and synthesized for self assembled monolayer formation are shown in Figure 3.

A monolayer based on **Amp-1** may lead to the formation of an arrangement of four different nucleosides by stepwise self-assembly of complementary nucleotides. Again, cholesterol has a long hydrophobic steroid chain, which makes it a suitable candidate to assemble on the hydrophobic surface. Also, cholesterol, a sterol, is an essential component of cell membranes and some of the hormones and is known to alter several properties of lipid bilayers as it influences the permeability and fluidity of membranes.^[35] Incorporation of cholesterol into Zn(II)-bis-cyclen (**Amp-2**) may lead to a modification of the response of the prepared layers to substrates or change their stability.

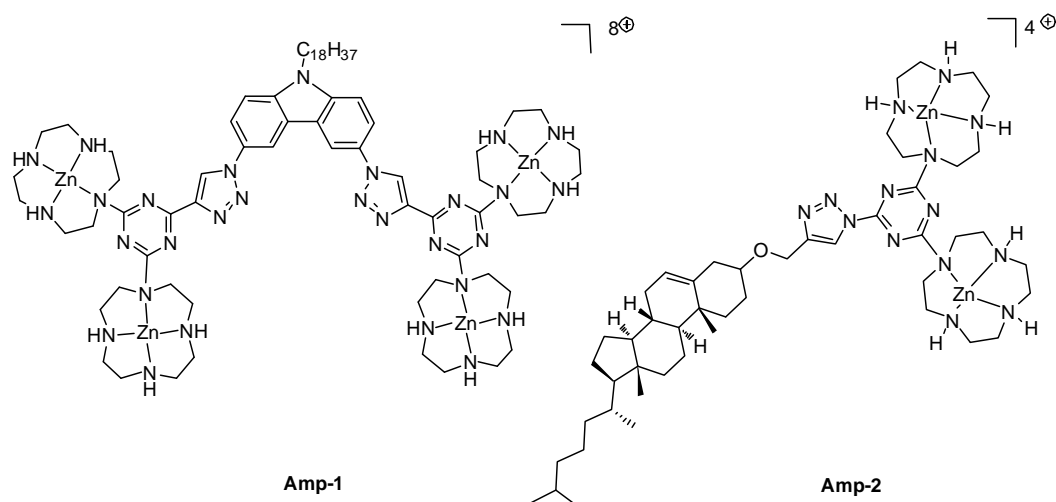
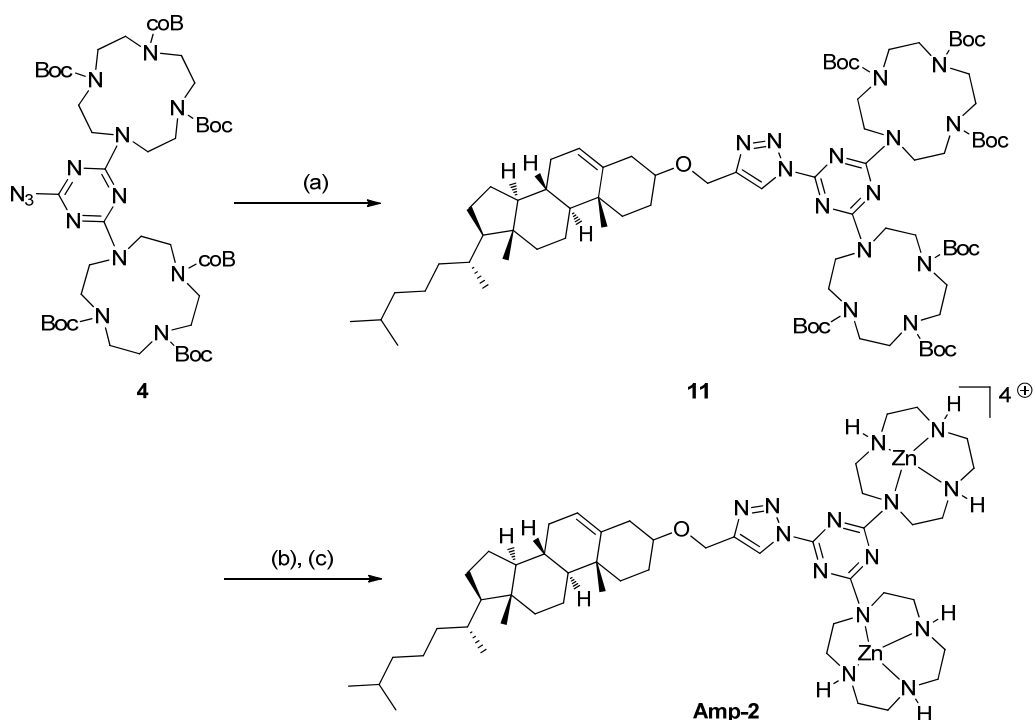


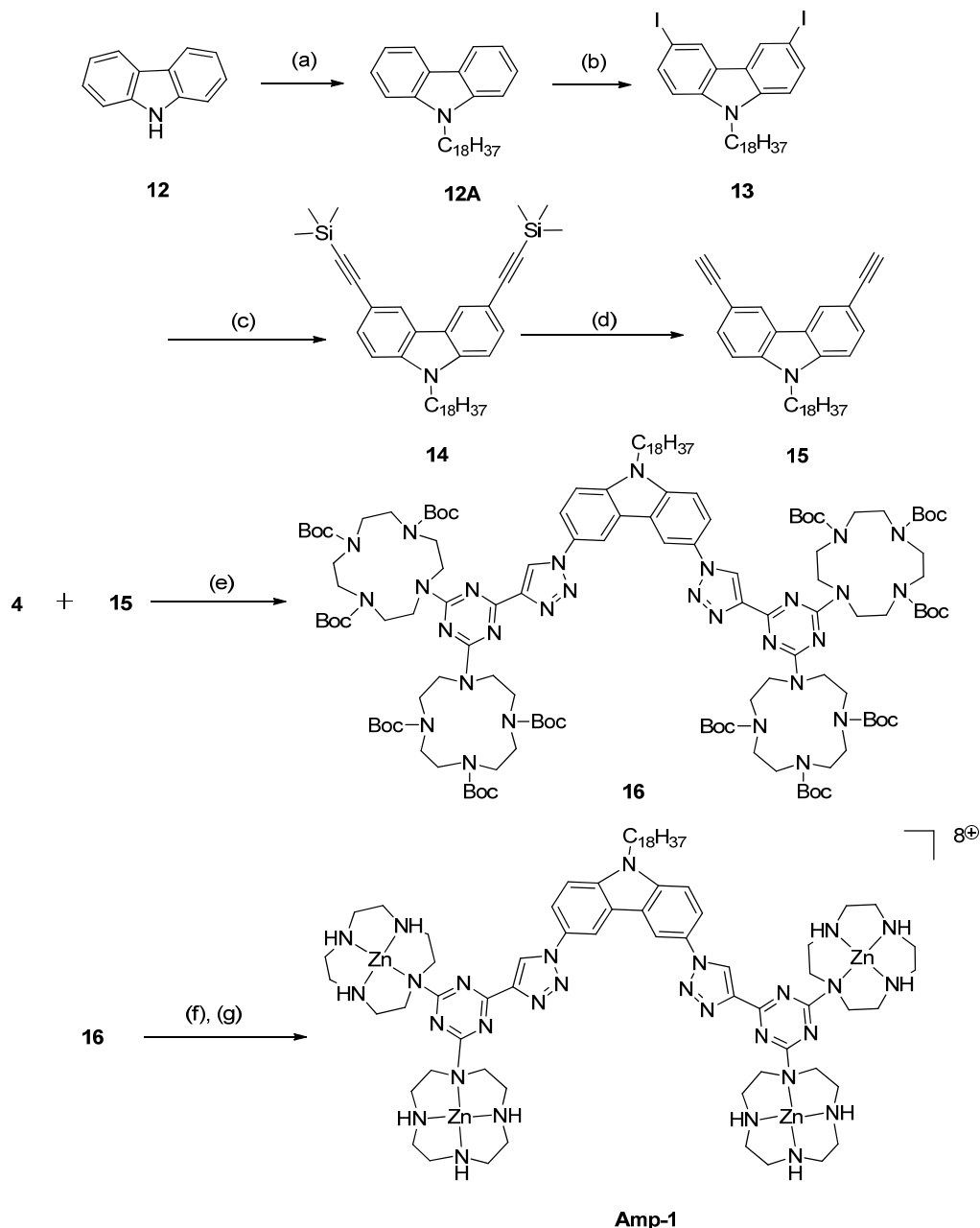
Figure 3: Rigid modified Zn(II)-Bis-cyclen based amphiphilic receptor for a template guided cooperative self-assembly of nucleotides [Counter ions of the complexes to yield a neutral complex are not shown for clarity]

The cholesterol bioconjugate of the Zn(II)-bis-cyclen complex was synthesized as shown in the Scheme 6.



Scheme 6: Synthesis of a cholesterol bioconjugate of a Zn(II)-bis-cyclen complex (a) Cholesterol acetylene, CuSO₄, sodium ascorbate, TBTA, DMF, rt, 12h [yield: 87%]; (b) TFA, DCM, 4h, basic ion exchanger resin [yield: quantitative]; (c) Zn(ClO₄)₂·6H₂O, MeOH / MeCN, reflux, o/n [yield: 99%]. Counter ions of the complexes to yield a neutral complex are not shown for clarity.

The amphiphilic Zn(II)-tetra-cyclen complex (**Amp-1**) and was synthesized as shown in the Scheme 7. To combine two bis-cyclen moieties we considered using the bis-acetylene of carbazole. The hydrophobic C₁₈ chain was incorporated into carbazole by nucleophilic substitution of the N-heterocycle. The detailed experimental procedures and characterization are reported in the experimental and supporting data section.



Scheme 7: Synthesis of amphiphilic modified Zn(II)-bis-cyclen based receptors (a) 1-bromo-octadecane, K₂CO₃, DMF (dry) [yield: 95%]; (b) KI, KIO₃, acetic acid, 85°C, 12h [yield: 80%]; (c) TMS acetylene, CuI, Pd(PPh₃)₂Cl₂, NEt₃, THF, rt, 8h [yield: 82%]; (d) K₂CO₃, MeOH [yield: quantitative] (e) CuI, NEt₃, THF, rt, 8h [yield: 85%]; (f) TFA, DCM, 8h, basic ion exchanger resin [yield: quantitative]; (g) Zn(ClO₄)₂·6H₂O,

MeOH/MeCN, reflux, o/n [yield: 99%]. Counter ions of the complexes to yield a neutral complex are not shown for clarity.

2.3.4.3 Concluding remarks

We have synthesized new rigid Zn(II)-cyclen based amphiphilic receptors for a template guided cooperative self-assembly of nucleotides at interfaces. Investigations of the binding properties of new amphiphilic complex embedded surfaces are in progress.

2.4 Experimental Section

General methods and materials

All reagent grade chemicals were used without purification unless otherwise specified. Cyanuric chloride, biotin, carbazole, propargyl amine, propargyl bromide were obtained from Aldrich and used as received.

Acetylene of biotin^[36] and cholesterol^[37] were synthesized following reported procedures. Mono and bis azide derivatives of cyanuric chloride were also synthesized adapting a reported procedure.^[38]

For gel phase studies, ovalbumin, phosphorylated bovine α -casein and 70% dephosphorylated bovine α -casein were obtained from Sigma Aldrich. BSA was received from Roth. Streptavidin-Horseradish Peroxidase (HRPO) was obtained from Biotrend Chemikalien GmbH.

NMR Spectra

NMR spectra were measured with Bruker Avance 600 (1H: 600.1 MHz, 13C: 150.1 MHz, T = 300 K), Bruker Avance 400 (1H: 400.1 MHz, 13C: 100.6 MHz, T = 300 K), Bruker Avance 300 (1H: 300.1 MHz, 13C: 75.5 MHz, T = 300 K). The chemical shifts are reported in δ [ppm] relative to external standards (solvent residual peak). The spectra were analysed by first order, the coupling **S-1** constants are given in Hertz [Hz]. Characterisation of the signals: s = singlet, d = doublet, t = triplet, q = quartet, m = multiplet, br = broad, dd = double doublet. Integration is determined as the relative number of atoms. The solvent used is reported for each spectrum.

Mass Spectra

Mass spectra were obtained with Varian CH-5 (EI), Finnigan MAT 95 (CI; FAB and FD), Finnigan MAT TSQ 7000 (ESI). Xenon serves as the ionisation gas for FAB.

IR Spectra

IR spectra were recorded with a Bio-Rad FTS 2000 MX FT-IR and Bio-Rad FT-IR FTS 155.

SDS-PAGE

Proteins were resolved on mini gels under denaturing and reducing Laemmli conditions on a PeqLab 45-1010-i apparatus. The gels consisted of a 5% acrylamide (w/v), 5mM Tris-HCl (pH 6.8), 0.1% SDS (w/v) stacking gel and a 12.5% acrylamide (w/v), 375 mM Tris-HCl (pH 8.8), 0.1% SDS (w/v) running gel. A 25 mM Tris, 192 mM glycine, 0.1% SDS (w/v) running buffer (pH 8.3) was used. Protein samples were heated to 95 °C for 10 min with reducing and denaturing RotiLoad 1 sample buffer (purchased from Carl Roth, Germany) before being loaded onto the gel. The gels were run at 150V. Water cooling was used during the entire run.

Staining

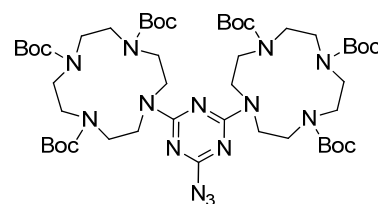
The protein samples in the SDS gel phase was accomplished with 0.1% Coomassie R-250, 50% MeOH, 10% AcOH for 1h. Destaining was accomplished in 7% AcOH, 10% MeOH overnight.

Western blot

Unstained proteins were transferred from gel to nitrocellulose membrane with BioRad Mini Trans Blot Electrophoretic Transfer Cell apparatus. 25 mM Tris, 192 mM glycine, 0.1% SDS (w/v) buffer was used for blotting. Blots were run at 125 V for 1h.

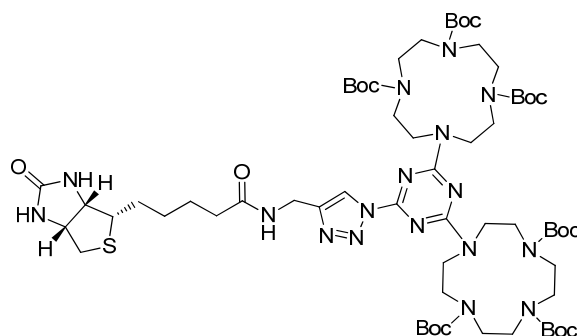
Chemiluminescent detection of proteins

after blotting, nitrocellulose membranes were washed with BSA buffer (1% BSA (as blocking buffer), 40 mM Tris HCl, 300 mM NaCl, 1% (v/v) Tween 20 (pH 7.4) for 30 min. Membranes were then incubated in a solution of the biotinylated probe (10^{-6} M in BSA buffer) for 1 h. The membranes were then washed with BSA buffer for 3x 5 minutes and subsequently incubated with 0.2 µg/ ml of streptavidin-horseradish peroxidase (HRPO) for 30minutes. Unbound streptavidin-HRPO was washed away by treating with washing buffer for 3x 15 minutes. Detection was performed with ECL substrate (Thermo Scientific SuperSignal West Pico chemiluminescent substrate). The chemiluminescence detections of the membranes were done by Fujifilm LAS 3000 luminescent image analyzer.



Synthesis of Compound 4: In a round bottom flask, mono azide derivative of trichlorotriazine (**2A**) (0.2 g, 1.08 mmol) and K_2CO_3 (0.6 g, 4.32 mmol) were suspended in 70 ml of acetone. To this suspension a solution of threefold Boc-protected cyclen (**3**) (1.02 g, 2.16 mmol) in 30 ml acetone was slowly added. The reaction mixture was then heated under reflux for 12h. The solvent was removed under reduced pressure and the crude mixture was purified by column chromatography using 30% ethyl acetate in petrol ether as the eluent to get pure product **4** (yield: 20%).

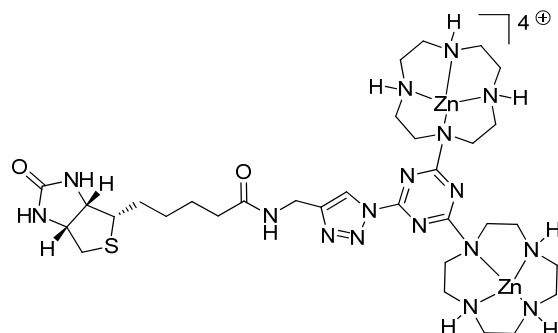
1H NMR (300MHz, $CDCl_3$) δ [ppm]: 1.39 (s, 54H, CH_3 -BOC), 3.04-3.75 (br, m, 32H, CH_2 -cyclen); **^{13}C NMR** (75MHz, $CDCl_3$) δ [ppm]: 28.4, 31.7, 50.0, 53.8, 69.4, 79.9, 156.1, 168.2, 210.7; **MS** (ESI-Q1MS) m/z (%) = 1063.8 (100) (MH^+); **M.P.:** 87-89 °C; **IR** (ATR) [cm^{-1}]: ν = 2974, 2928, 2865, 1694, 1540, 1361, 1169; **MF:** $C_{48}H_{84}N_{14}O_{12}$, **FW:** 1048.64 g/mol



Synthesis of Compound 5: To a stirred solution of **4** (0.28 g, 0.29 mmol) in degassed dry DMF (3 ml), acetylene of biotin (0.09 g, 0.35 mmol), $CuSO_4 \cdot 5H_2O$ (1 mg, 0.005 mmol, 0.02eq), sodium ascorbate (2 mg, 0.016 mmol 0.04 eq) and TBTA (4 mg, 0.02eq) were added and the reaction mixture was stirred at room temperature for 12 h. Then the solvent was evaporated. The residual solid was dissolved in DCM (50 mL) and successively washed by water (2 X 10 mL) and brine (10 mL). The organic layer was then dried on $NaSO_4$ and evaporated under reduce pressure. The crude product was purified by column chromatography using 6:1 chloroform/methanol mixture to get **5** (yield: 90%).

1H NMR (300MHz, $CDCl_3$) δ [ppm]: 1.33 (br, 2H), 1.40 (s, br, 54H) 1.62 (m, 4H), 2.18 (t, 2H), 2.70-2.89 (m, 2H), 3.07-4.01(m, br, 33H), 4.29-4.38 (m, 2H), 4.47-4.59 (m, 2H), 6.72 (s, 1H), 7.32 (s, 1H), 7.91 (br, 1H), 8.40 (s, 1H); **^{13}C NMR** (75MHz, $CDCl_3$) δ [ppm]: 25.4, 27.9, 28.3, 28.4, 34.1, 35.8, 40.6, 49.9, 50.3, 50.9, 55.7, 60.3, 61.6, 76.7, 80.1, 80.2, 121.1, 144.6, 156.3, 159.9, 164.8, 165.6,

173.2 ; **MS** (ES-MS) m/z (%) =1345.1(100) $[MH^+]$, 673.0 (65) $[(M+2H)^{2+}]$, 623.0 (65) $[(M+2H)^{2+}$ -Boc], 594.9 (30) $[(M+2H)^{2+}$ -Boc-C₄H₈]; **MF**: C₆₂H₁₀₅N₁₇O₁₄S, **FW**: 1344.67 g/mol



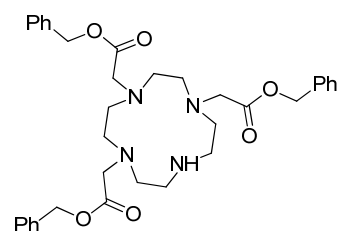
Synthesis of Compound 6:

Boc-deprotection of Compound 5: Compound **5** (0.25 g, 0.18 mmol) was dissolved in DCM. Trifluoroacetic acid (2 ml, 0.02 mol) was added to it and the reaction mixture was stirred for 4h. Subsequently DCM was evaporated and the obtained TFA salt was dissolved in water and passed through a basic ion exchanger column resin. The elution of the product was controlled by pH indicator paper (pH > 10) and was completed when pH again was neutral. The eluate was concentrated and lyophilised to yield the Boc-deprotected compound (yield: quantitative).

¹H NMR (300MHz, CDCl₃) δ [ppm]: 1.42 (br, 2H), 1.67 (m, 4H), 2.26 (t, 2H), 2.68-2.72 (dd, 16H), 2.81-3.00 (m, 10H), 3.09-3.17 (m, 2H), 3.87 (m, br, 8H), 4.23-4.27 (m, 1H), 4.45-4.51 (m, 3H), 8.71 (br, 1H), 8.63 (s, 1H) ; **¹³C NMR** (75MHz, CDCl₃) δ [ppm]: 26.8, 29.5, 29.7, 30.1, 35.5, 36.6, 41.1, 47.1, 49.9, 50.1, 57.1, 61.6, 63.3, 123.2, 146.6, 161.1, 166.1, 167.9, 176.1; **MS** (ESI-MS) m/z (%) =744.46 (50) $[MH^+]$, 372.7 (50) $[(M+2H)^{2+}]$, 358.73(100) $[(M+2H)^{2+}$ -N₂]; **MF**: C₃₂H₅₇N₁₇O₂S, **FW**: 743.97 g/mol

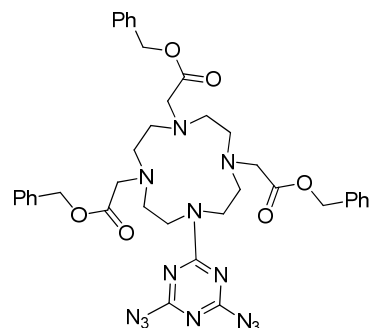
Metal complexation of Boc-deprotected compound 5: The Boc-deprotected compound (0.05g, 0.067 mmol), was dissolved in 3 mL acetonitrile and ZnClO₄.6H₂O (0.05g, 0.13 mmol) dissolved in methanol was added slowly. The reaction mixture refluxed overnight under vigorously stirring. The hot reaction mixture was filtered and the filtrate was evaporated under reduced pressure to get the complex **6** (yield: 99%).

¹H NMR (300MHz, CDCl₃) δ [ppm]: 1.39 (br, 2H), 1.61 (m, 4H), 2.21 (t, 2H), 2.51-2.70 (dd, 16H), 2.75-3.00 (m, 10H), 3.09-3.15 (m, 2H), 3.85 (m, br, 8H), 4.21-4.26 (m, 1H), 4.41-4.50 (m, 3H), 8.68 (br, 1H), 8.61 (s, 1H) ; **¹³C NMR** (75MHz, CDCl₃) δ [ppm]: 22.1, 24.9, 27.8, 29.3, 34.8, 33.5, 42.7, 44.7, 48.2, 51.2, 53.3, 130.3, 139.7, 167.3, 171.2; **MS** (ESI-MS) m/z (%) =744.46 (50) $[MH^+]$, 372.7 (50) $[(M+2H)^{2+}]$, 358.73(100) $[(M+2H)^{2+}$ -N₂]; **MF**: C₃₂H₅₇N₁₇O₂S, **FW**: 743.97 g/mol



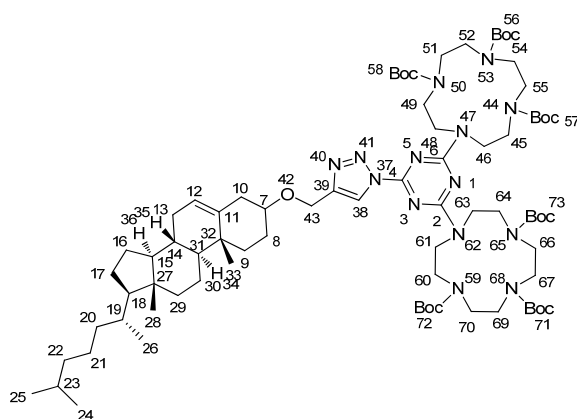
Synthesis of Compound 8: Sodium hydrogen carbonate (1.34 g, 15.96 mmol) was added to a suspension of tetraazacyclododecane **7** (0.83 g, 4.83 mmol) in CH₃CN (50 ml) and stirred for 15min. A solution of benzylbromoacetate (2.36 ml, 14.9 mmol) in CH₃CN (10 ml) was added dropwise over 30 min and the reaction mixture was refluxed for 12h. The reaction was monitored by TLC. After 12h the inorganic salt was filtered and filtrate was removed under reduced pressure. The crude residue was purified by column chromatography on silica gel (2% CH₃OH in CH₂Cl₂) to get **8** as oily substance (yield: 45%).

¹H NMR (300MHz, CDCl₃) δ [ppm]: 2.80-3.01 (br, m, 16H), 3.34 (s, 2H), 3.41 (s, 4H), 5.05 (s, 6H), 7.27 (m, 15H) 9.89 (s, br, 1H); ¹³C NMR (75MHz, CDCl₃) δ [ppm]: 47.3, 49.3, 51.4, 51.6, 57.1, 66.5, 128.4, 128.5, 128.6, 135.3, 170.1, 171.1; MS (ESI-MS) *m/z* (%) = 615 (100) [M⁺]; MF: C₃₅H₄₄N₄O₆, FW: 616.75g/mol



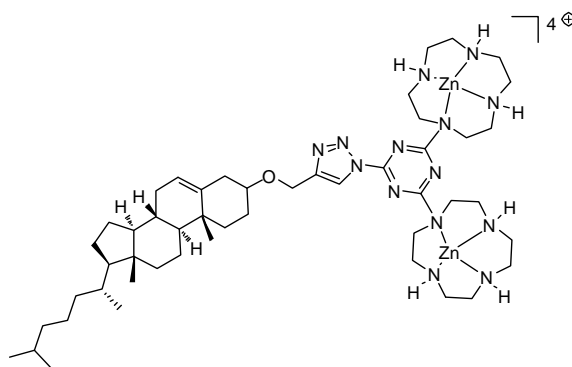
Synthesis of Compound 9: In a round bottom flask **2B** (0.07 g, 0.33 mmol) and K₂CO₃ (0.18 g, 1.32 mmol) were suspended in 10 ml of acetone. To this suspension **8** (0.19 g, 0.33 mmol) in 15 ml acetone were slowly added via a syringe. The reaction mixture was refluxed for 17h. The solvent was removed under reduced pressure. The crude product was purified by column chromatography on silica gel (30% ethyl acetate in petrol ether) to get pure compound **9** (yield: 30%).

¹H NMR (300MHz, CDCl₃) δ [ppm]: 2.74-3.44 (br, m, 16H), 3.41 (s, 4H), 5.10 (s, 6H), 7.33 (m, 15H); ¹³C NMR (75MHz, CDCl₃) δ [ppm]: 47.3, 48.6, 49.3, 51.4, 51.6, 57.1, 66.5, 128.4, 128.5, 128.6, 135.3, 170.1, 171.0 MS (ESI-MS) *m/z* (%) = 778.4 (100) [M⁺]; MF: C₃₈H₄₃N₁₃O₆, FW: 777.35 g/mol



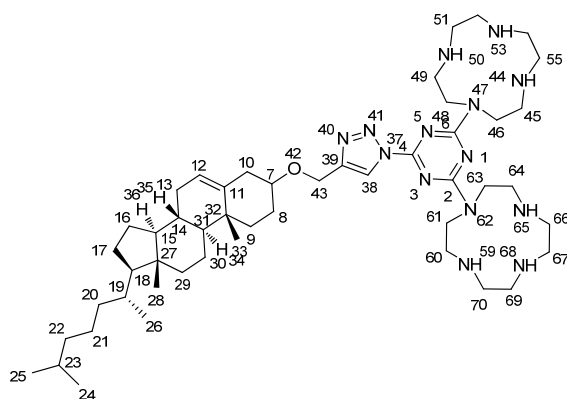
Synthesis of Compound 11: To a stirred solution of **4** (0.41 g, 0.39 mmol) in degassed dry DMF (3 ml), acetylene of cholesterol (0.2g, 0.47 mmol), CuSO₄·5H₂O (1.5 mg, 0.007 mmol, 0.02eq), sodium ascorbate (3 mg, 0.016 mmol 0.04eq) and TBTA (5 mg, 0.02eq) were added and the reaction mixture was stirred at room temperature for 12 h. Then the solvent was evaporated. The residual solid was dissolved in DCM (50 mL) and successively washed by water (2 X 10 mL) and brine (10 mL). The organic layer was then dried on NaSO₄ and evaporated under reduce pressure. The crude product was purified by column chromatography using 30% ethyl acetate in hexane to get **11** (yield: 87%).

¹H NMR (600MHz, CDCl₃, COSY, HSQC, HMBC) δ [ppm]: 0.65 (s, 3H, 28), 0.82 (d, 3H, 25), 0.83 (d, 3H, 24), 0.85-0.94 (m, 4H, 31+26), 0.93-1.01 (m, 5H, 15+20'+33), 1.01-1.03 (m, 1H, 9'), 1.03-1.12 (m, 2H, 16'+18), 1.09-1.16 (m, 2H, 30'+22'), 1.24-1.28 (m, 1H, 17), 1.33-1.38 (m, 57H, Boc-CH₃+23+30+20), 1.40-1.41 (m, 3H, 8'+35), 1.42-1.52 (m, 4H, 13+21+21'+23), 1.52-1.54 (m, 1H, 16), 1.75-1.89 (m, 2H, 9+17), 1.85-1.90 (m, 1H, 8), 1.88-2.01(m, 1H, 29), 2.31-2.35(m, 1H, 10), 3.09-3.11 (m, 1H, 7), 3.18-4.01 (m, br, cyclen-CH₂), 5.30-5.32 (m, 1H, 12); ¹³C NMR (150MHz, CDCl₃, HSQC, HMBC) δ [ppm]: 10.9 (+, 1C, 28), 18.5 (+, 1C, 26), 19.1 (+, 1C, 33), 20.9 (-, 1C, 21), 22.1 (+, 1C, 24), 22.3 (+, 1C, 25), 23.8 (-, 1C, 30), 23.9 (-, 1C, 16), 27.8 (+, 1C, 23), 28.1(-, 1C, 17), 28.2 (-, 1C, 8), 28.4, 28.5 (+, Boc-CH₃), 30.5 (-, 1C, 13), 31.5 (+, 1C, 14), 35.4 (+, 1C, 19), 35.9 (-, 1C, 20), 36.2 (C_{quat}, 1C, 32), 36.9 (-, 1C, 9), 39.1 (-, 1C, 10), 39.2 (-, 1C, 22), 39.5 (-, 1C, 29), 42.1 (C_{quat}, 1C, 27), 48.7, 48.9 (-, cyclen-CH₂) 49.8 (+, 1C, 31), 55.9 (+, 1C, 18), 56.2 (+, 1C, 15), 67.2 (-, 1C, 43), 80.1 (-, 1C, 7), 80.5, 80.7 (C_{quat}, C-Boc), 121.3 (+, 1C, 12), 140.8 (C_{quat}, 1C, 11), 153.2, 156.1 (C_{quat}, C=O Boc), 168.2 (C_{quat}, triazine-C_{Aryl}-N); **MS** (ES-MS) *m/z* (%) =1505.6 (100) [MNH₄⁺], 1488.5 (70) [MH⁺], 761.8 (90) [(M+2NH₄⁺)²⁺], 753.3 (20) [(MH⁺+NH₄⁺)²⁺]; **MF**: C₇₉H₁₃₄N₁₄O₁₃, **FW**: 1488.00g/mol.



Synthesis of Compound Amp-2:

Boc-deprotection of Compound 11: Compound **11** (0.3 g, 0.21 mmol) was dissolved in DCM. Trifluoroacetic acid (3 ml, 0.03 mol) was added to it and the reaction mixture was stirred for 3h. Subsequently DCM was evaporated and the obtained TFA salt was dissolved in water and passed through a basic ion exchanger column resin. The elution of the product was controlled by pH indicator paper (pH > 10) and was completed when pH again was neutral. The eluate was concentrated and lyophilised to yield the Boc-deprotected compound (yield: quantitative).

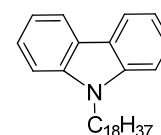


$^1\text{H NMR}$ (600MHz, CDCl_3 , COSY, HSQC, HMBC) δ [ppm]: 0.62 (s, 3H, 28), 0.80 (d, 3H, 25), 0.83 (d, 3H, 24), 0.78-0.82 (m, 4H, 31+26), 0.91-0.95 (m, 5H, 15+20'+33), 1.01-1.03 (m, 1H, 9'), 1.03-1.12 (m, 2H, 16'+18), 1.09-1.16 (m, 2H, 30'+22'), 1.21-1.23 (m, 1H, 17), 1.30-1.33 (m, 3H, 23+30+20), 1.38-1.40 (m, 3H, 8'+35), 1.42-1.52 (m, 4H, 13+21+21'+23), 1.52-1.54 (m, 1H, 16), 1.75-1.89 (m, 2H, 9+17), 1.85-1.90 (m, 1H, 8), 1.88-2.01(m, 1H, 29), 2.31-2.35(m, 1H, 10), 3.12-3.17 (m, 1H, 7), 3.19-3.97 (m, br, cyclen- CH_2), 5.29-5.30 (m, 1H, 12); $^{13}\text{C NMR}$ (150MHz, CDCl_3 , HSQC, HMBC) δ [ppm]: 10.6 (+, 1C, 28), 18.1 (+, 1C, 26), 19.5 (+, 1C, 33), 20.9 (-, 1C, 21), 22.1 (+, 1C, 24), 22.3 (+, 1C, 25), 23.8 (-, 1C, 30), 23.9 (-, 1C, 16), 27.8 (+, 1C, 23), 28.1(-, 1C, 17), 28.2 (-, 1C, 8), 31.4 (-, 1C, 13), 31.5 (+, 1C, 14), 31.4 (+, 1C, 19), 35.9 (-, 1C, 20), 36.9 (-, 1C, 9), 39.1 (-, 1C, 10), 39.2 (-, 1C, 22), 36.5 (-, 1C, 29), 42.1 (C_{quat} , 1C, 27), 48.2, 48.5 (-, cyclen- CH_2) 49.8 (+, 1C, 31), 57.1 (+, 1C, 18), 56.2 (+, 1C, 15), 67.2 (-, 1C, 43), 80.1 (-, 1C, 7), 80.5, 80.7 (C_{quat} , C-Boc),

121.3 (+, 1C, 12), 140.8 (C_{quat}, 1C, 11), 165.7 (C_{quat}, triazine-Caryl-N); **MS** (ES-MS) *m/z* (%) = 884 (100) [MH⁺]; **MF**: C₄₉H₈₆N₁₄O, **FW**: 887.30 g/mol.

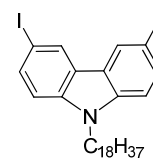
Metal complexation of Boc-protected compound 11: The Boc-protected compound (0.05g, 0.05 mmol), was dissolved in 3 mL acetonitrile and ZnClO₄·6H₂O (0.05g, 0.13 mmol) dissolved in methanol was added slowly. The reaction mixture refluxed overnight under vigorously stirring. The hot reaction mixture was filtered and the filtrate was evaporated under reduced pressure to get **amp-2** (yield: 99%).

¹H NMR (600MHz, CDCl₃, COSY, HSQC, HMBC) δ [ppm]: 0.60 (s, 3H, 28), 0.79 (d, 3H, 25), 0.81 (d, 3H, 24), 0.83-0.91 (m, 4H, 31+26), 0.91-0.98 (m, 5H, 15+20'+33), 1.01-1.03 (m, 1H, 9'), 1.01-1.09 (m, 2H, 16'+18), 1.05-1.11 (m, 2H, 30'+22'), 1.20-1.21 (m, 1H, 17), 1.33-1.38 (m, 3H, 23+30+20), 1.38-1.40 (m, 3H, 8'+35), 1.42-1.47 (m, 4H, 13+21+21'+23), 1.51-1.54 (m, 1H, 16), 1.75-1.89 (m, 2H, 9+17), 1.85-1.90 (m, 1H, 8), 1.88-2.01 (m, 1H, 29), 2.31-2.35 (m, 1H, 10), 3.09-3.11 (m, 1H, 7), 3.18-4.01 (m, br, cyclen-CH₂), 5.28-5.31 (m, 1H, 12); **¹³C NMR** (150MHz, CDCl₃, HSQC, HMBC) δ [ppm]: 9.9 (+, 1C, 28), 12.5 (+, 1C, 26), 14.1 (+, 1C, 33), 20.7 (-, 1C, 21), 22.1 (+, 1C, 24), 22.5 (+, 1C, 25), 23.7 (-, 1C, 30), 23.9 (-, 1C, 16), 26.5 (+, 1C, 23), 28.0 (-, 1C, 17), 27.9 (-, 1C, 8), 28.4, 30.5 (-, 1C, 13), 31.5 (+, 1C, 14), 35.4 (+, 1C, 19), 35.9 (-, 1C, 20), 36.0 (C_{quat}, 1C, 32), 36.9 (-, 1C, 9), 39.1 (-, 1C, 10), 39.2 (-, 1C, 22), 39.5 (-, 1C, 29), 40.1 (C_{quat}, 1C, 27), 47.7, 47.9 (-, cyclen-CH₂) 49.6 (+, 1C, 31), 55.1 (+, 1C, 18), 56.2 (+, 1C, 15), 67.2 (-, 1C, 43), 80.1 (-, 1C, 7), 80.5 (C_{quat}, C-Boc), 118.3 (+, 1C, 12), 142.8 (C_{quat}, 1C, 11), 161.3 (C_{quat}, triazine-Caryl-N); **MS** (ES-MS) *m/z* (%) = 1016.6 (100) [MH⁺]; **MF**: C₄₉H₈₆N₁₄OZn₂, **FW**: 1018.06g/mol.



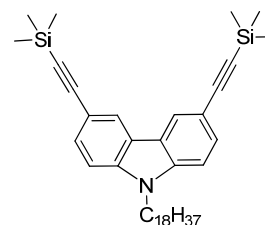
Synthesis of Compound 12A: The mixture of carbazole **12** (1.5 g, 8.97 mmol), 1-bromo-octadecane (1.8 g, 5.39 mmol) and potassium carbonate (2 g, 14.4 mmol) in anhydrous DMF (7 ml) was heated at 50° C for 24 h under nitrogen and then 50 ml water was added. DCM was used in three portions (20 ml each) to extract the product. The organic layer was washed with water and dried over MgSO₄. The solvent was removed under reduced pressure to get the crude product which was subsequently purified by column chromatography using hexane as eluent (yield: 95%)

¹H NMR (300MHz, CDCl₃) δ [ppm]: 8.11 (d, ³J = 7.7 Hz, 2H), 7.48-7.39 (m, 4H), 7.22 (t, ³J = 7.4 Hz, 2H), 4.30 (t, ³J = 7.2 Hz, 2H), 1.89-1.85 (m, 2H), 1.40-1.23 (m, 30H), 0.88 (t, ³J = 6.9 Hz, 3H); **¹³C NMR** (75MHz, CDCl₃) δ [ppm]: 140.5, 125.7, 122.9, 120.4, 118.8, 108.8, 43.2, 32.1, 29.9, 29.83, 29.80, 29.76, 29.73, 29.66, 29.60, 29.57, 29.5, 29.1, 27.5, 22.9, 14.3; **MS** (ESI-MS) *m/z* (%) = 418.9 (100) [M⁺]; **MF**: C₃₀H₄₅N, **FW**: 419.69 g/mol



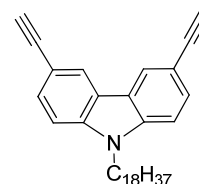
Synthesis of Compound 13: In a round bottom flask equipped with a condenser, 9-octadecylcarbazole **12A** (5.2 g, 12.4 mmol), potassium iodide (2.6 g, 16.3 mmol) and potassium iodate (3.5 g (28.1 mmol) were dissolved in 100 mL acetic acid under gentle stirring. The mixture was heated at 80 °C for 12 h. After the reaction mixture was cooled to room temperature, the crude iodinated product was obtained by filtration. The filter cake was washed consecutively with 100 mL of water, sodium bicarbonate (1 M), sodium thiosulfate solution (1 M), and water. Compound **13** was obtained a white solid after recrystallization from the ethanol/water mixture (2:1 by volume) (yield: 80%).

¹H NMR (300MHz, CDCl₃) δ [ppm]: 8.33 (s, 2H), 7.72 (d, ³J= 8.6 Hz, 2H), 7.18 (d, ³J = 8.6 Hz, 2H), 4.22 (t, ³J= 7.1 Hz, 2H), 1.81-1.79 (m, 2H), 1.29-1.22 (m, 30H), 0.88 (t, ³J = 7.0 Hz, 3H); **¹³C NMR** (75MHz, CDCl₃) δ [ppm]: 139.3, 129.0, 123.4, 111.9, 110.4, 43.3, 31.95, 29.7, 29.6, 29.6, 29.5, 29.5, 29.4, 29.3, 29.3, 28.8, 27.2, 22.7, 14.1 **MS** (ESI-MS) *m/z* (%) = 670.4 (100) [M⁺]; **MF**: C₃₀H₄₃I₂N, **FW**: 671.48 g/mol.



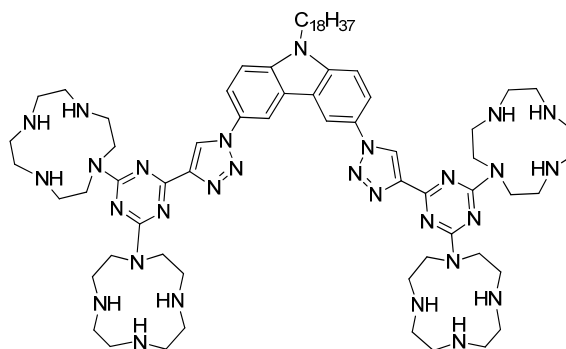
Synthesis of Compound 14: To a flask containing Pd(PPh₃)₂Cl₂ (0.15 g, 0.21 mmol), CuI (0.06 g, 0.33 mmol), and **13** (6.08 g, 9.0 mmol) were added (trimethylsilyl) acetylene (2.65 g, 38.4 mmol) in triethylamine (75 mL) and tetrahydrofuran (125 mL). The mixture was stirred at room temperature under nitrogen atmosphere for 48 h and then filtered. The filtrate was concentrated and the crude solid was purified by column chromatography on silica gel using petroleum ether as an eluent to get 3, 6-Bis[(trimethylsilyl)ethynyl]-9-octadecylcarbazole, **14** (yield: 82%).

¹H NMR (300MHz, CDCl₃) δ [ppm]: 8.20 (s, 2H), 7.59 (d, ³J=8.2 Hz, 2H), 7.30 (d, ³J = 8.5 Hz, 2H), 4.22 (t, ³J = 7.2 Hz, 2H), 1.84-1.75 (m, 2H), 1.41-1.27 (m, 29H), 0.87 (t, ³J = 7.3 Hz, 3H), 0.31 (s, 18H); **¹³C NMR** (75MHz, CDCl₃) δ [ppm]: 139.4, 129.0, 123.7, 121.2, 112.9, 107.7, 106.5, 88.3, 42.2, 30.9, 28.6, 28.6, 28.5, 28.5, 28.3, 27.8, 26.1, 21.6, 13.1; **MS** (EI-MS) *m/z* (%) = 611.3(100%) [M⁺]; **MF**: C₄₀H₆₁NSi₂, **FW**: 612.09 g/mol



Synthesis of Compound 15: K_2CO_3 aqueous solution (1.9 M, 4 ml) was added to a stirred solution of 3, 6-bis [(trimethylsilyl)ethynyl]-9-octadecylcarbazole **14** (1.55 g, 2.5 mmol) in methanol (148 ml). The mixture was stirred at room temperature under nitrogen atmosphere for 1h and then diluted with diethyl ether and water. The aqueous phase was washed with diethyl ether, and the combined organic phase was washed with saturated brine. The organic phase was dried over $MgSO_4$, and the solvent was evaporated under reduced pressure. The crude residual material was purified by column chromatography on silica gel using petroleum ether as an eluent to give **15** as a light yellow solid (yield: quantitative).

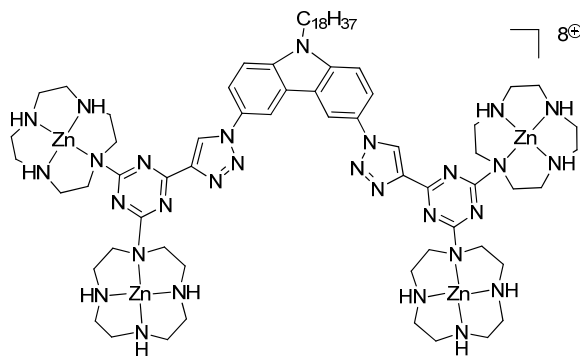
1H NMR (300MHz, $CDCl_3$) δ [ppm]: 0.88 (t, $^3J = 7.3$ Hz, 3H), 1.32-1.25 (m, 32H), 1.84-1.80 (m, 2H), 3.08 (s, 2H), 4.27 (t, $^3J = 7.2$ Hz, 2H), 7.35 (d, $^3J = 8.5$ Hz, 2H), 7.61 (d, $^3J = 8.5$ Hz, 2H), 8.22 (s, 2H); **^{13}C NMR** (75MHz, $CDCl_3$) δ [ppm]: 140.67, 130.13, 124.78, 122.26, 112.69, 108.96, 84.75, 43.34, 31.95, 29.72, 29.68, 29.64, 29.60, 29.54, 29.47, 29.38, 28.91, 27.23, 22.71, 14.14; **MS** (EI-MS) m/z (%) = 468.4 (100) [MH^+]; **MF:** $C_{34}H_{45}N$, FW: 467.36 g/mol .



Synthesis of Compound 16: To a stirred solution of **15** (0.5 g, 1.06 mmol) in degassed dry THF (10 mL), biscyclene mono azide **2A** (0.567 g, 0.053 mmol), CuI (0.005 g, 6 mol %) and triethylamine (1 ml, 9.8 mmol) were added and the reaction mixture was stirred at room temperature for 12 h. The product was extracted from the reaction mixture with diethylether (3x10 mL). Then combined organic extract was evaporated under reduced pressure and the crude product was purified by column chromatography using 5% ethyl acetate in petroleum ether as eluent (yield: 85%)

1H NMR (300MHz, $CDCl_3$) δ [ppm]: 0.79 (t, $^3J = 7.3$ Hz, 3H), 1.16-1.20 (m, 32H), 1.40-1.34 (br, s, 108H), 1.96-1.94 (m, 2H), 3.36-3.77(m, br, 66H), 7.36 (d, $^3J = 9$ Hz, 2H), 8.01 (d, $^3J = 9$ Hz, 2H), 8.72 (s, 2H); **^{13}C NMR** (75MHz, $CDCl_3$) δ [ppm]: 14.1, 21.0, 22.6, 27.3, 28.5, 29.0, 29.3, 29.4, 29.6, 31.9,

50.9, 56.2, 60.3, 80.2, 109.0, 118.4, 121.5, 123.2, 124.5, 140.8, 148.2, 156.5, 160.13; **MS** (EI-MS) m/z (%) = 1298.0 (100) [(M+2H)²⁺], 1306.5 (45) [(MH⁺+ MH₄⁺)²⁺]; **MF**: C₁₃₂H₂₁₇N₂₉O₂₄, FW: 2594.32g/mol .



Synthesis of Compound Amp-1:

Boc-deprotection of Compound 16: Compound **16** (0.5 g, 0.19 mmol) was dissolved in DCM. Trifluoroacetic acid (2 ml, 0.02 mol) was added to it and the reaction mixture was stirred for 4h. Subsequently DCM was evaporated and the obtained TFA salt was dissolved in water and passed through a basic ion exchanger column resin. The elution of the product was controlled by pH indicator paper (pH > 10) and was completed when pH again was neutral. The eluate was concentrated and lyophilised to yield the Boc-deprotected compound (yield: quantitative).

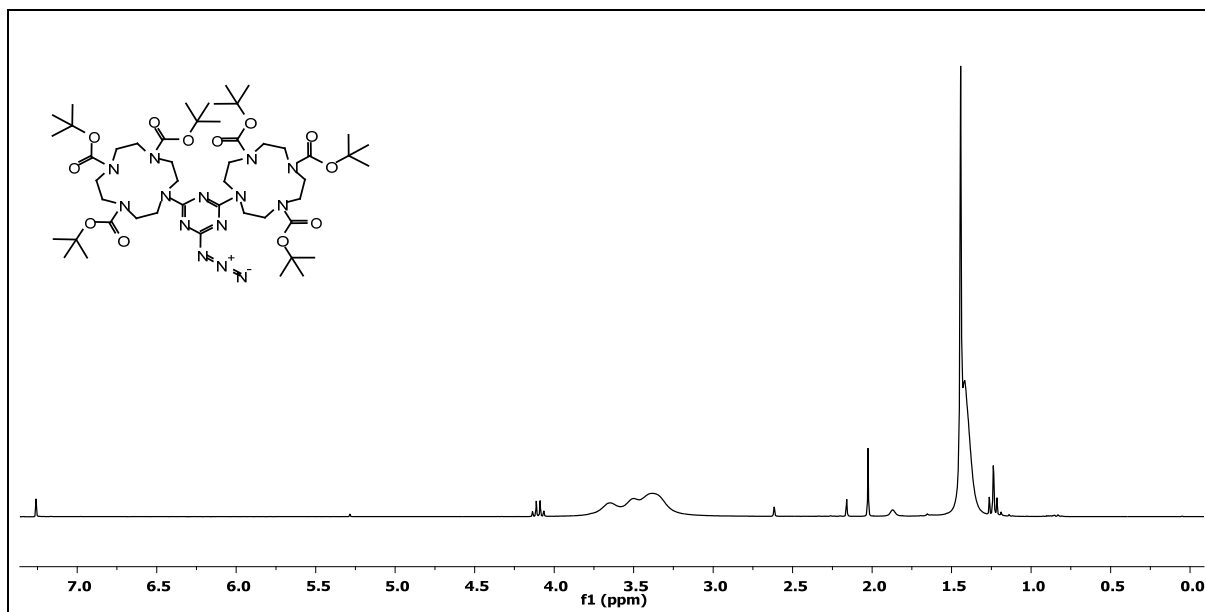
¹H NMR (300MHz, CDCl₃) δ [ppm]: 0.75 (t, ³J = 7.3 Hz, 3H), 1.18-1.23 (m, 32H), 1.98-2.01 (m, 2H), 3.31-3.58(m, br, 66H), 7.32 (d, ³J= 9Hz, 2H), 7.97 (d, ³J=9Hz, 2H), 8.71 (s, 2H); ¹³C NMR (75MHz, CDCl₃) δ [ppm]: 14.1, 22.6, 27.3, 29.2, 29.5, 29.6, 32.1, 58.2, 60.3, 80.5, 111.0, 119.4, 121.9, 123.2, 140.8, 148.3; **MS** (ESI-MS) m/z (%) =1391(100) [MH⁺]; **MF**: C₇₂H₁₂₁N₂₉, **FW**: 1392.93 g/mol

Metal complexation of Boc-deprotected compound 16: The Boc-deprotected compound (0.05g, 0.035 mmol), was dissolved in 3 mL acetonitrile and ZnClO₄.6H₂O (0.06g, 0.14 mmol) dissolved in methanol was added slowly. The reaction mixture refluxed overnight under vigorously stirring. The hot reaction mixture was filtered and the filtrate was evaporated under reduced pressure to get the complex **6** (yield: 99%).

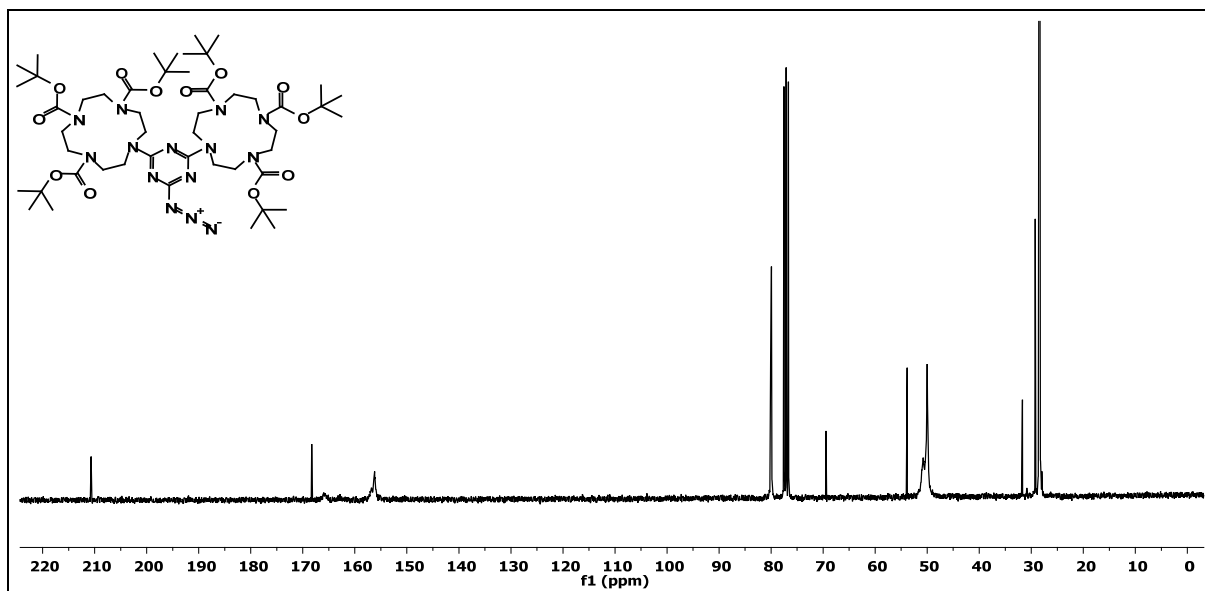
¹H NMR (300MHz, CDCl₃) δ [ppm]: 0.72 (t, ³J = 7.3 Hz, 3H), 1.19-1.24 (m, 32H), 1.97-2.01 (m, 2H), 3.29-3.50(m, br, 66H), 7.35(d, ³J= 9Hz, 2H), 7.93 (d, ³J=9Hz, 2H), 8.67 (s, 2H); ¹³C NMR (75MHz, CDCl₃) δ [ppm]: 14.2, 22.7, 27.3, 29.3, 29.7, 31.9, 50.1, 60.3, 80.1, 80.2, 111.0, 119.4, 120.9, 123.3, 141.0, 148.2; **MS** (ESI-MS) m/z (%) =1653.4 (80) [MH⁺]; **MF**: C₇₂H₁₂₁N₂₉Zn₄, **FW**: 1654.45g/mol

2.5 Supporting Data

^1H and ^{13}C spectra of synthesized compounds

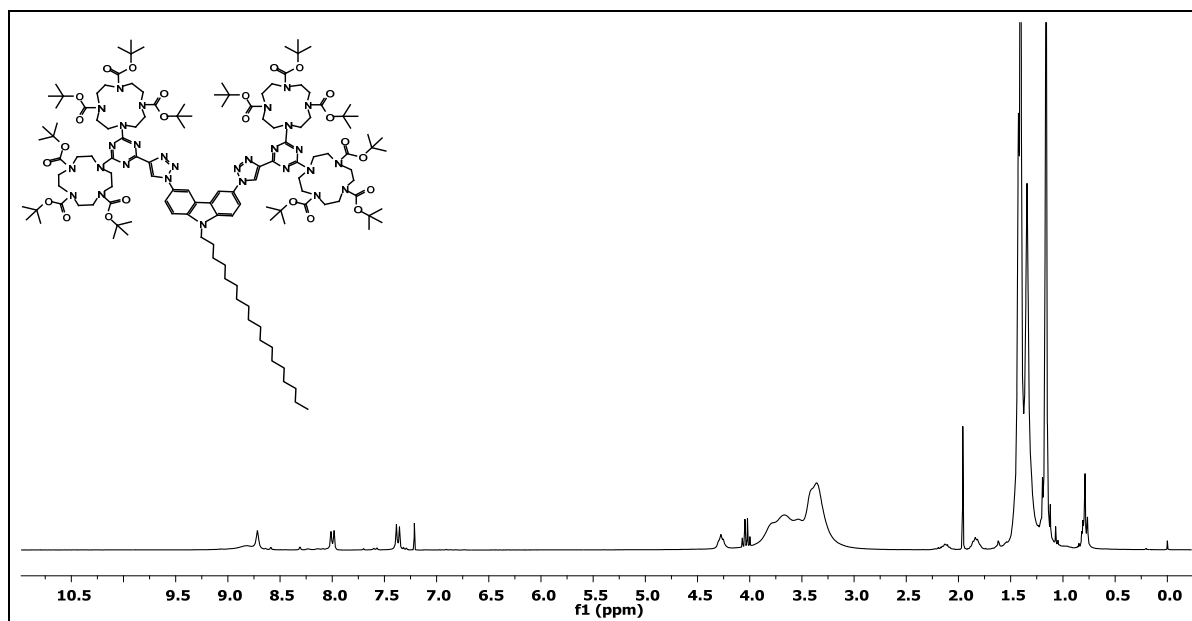


^1H -NMR spectrum of compound **4** (300 MHz, CDCl_3)

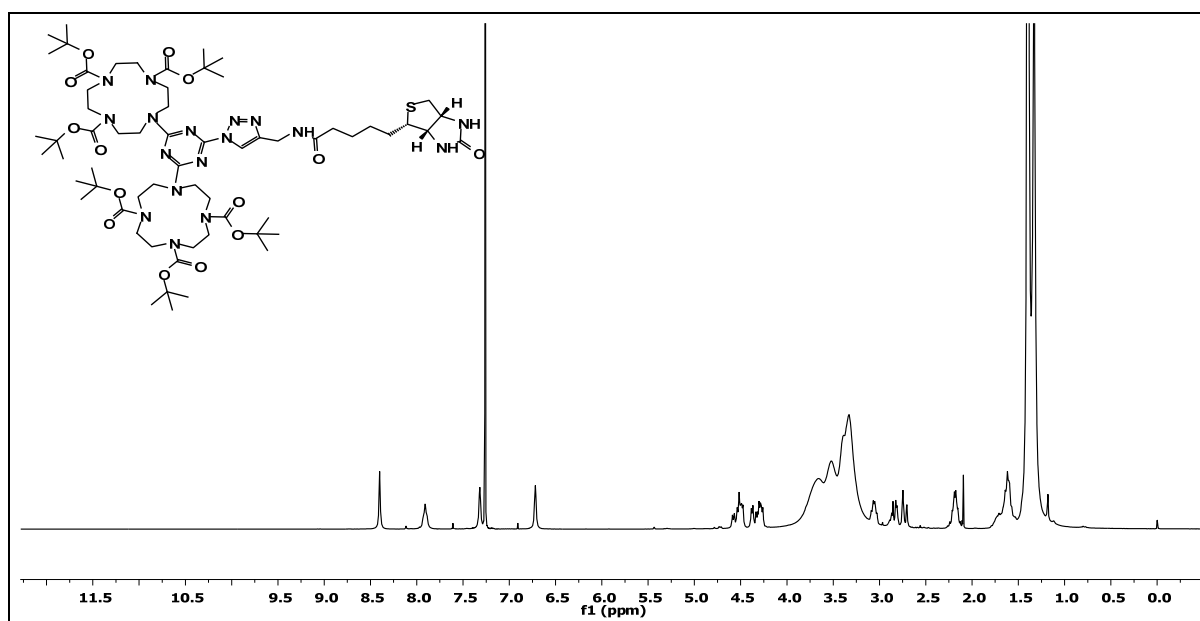


^{13}C -NMR spectrum of compound **4** (75 MHz, CDCl_3)

2. Rigid Amphiphilic Molecular receptors, Bioconjugates and Radiopharmaceuticals based on Metal-cyclen complexes via Click chemistry

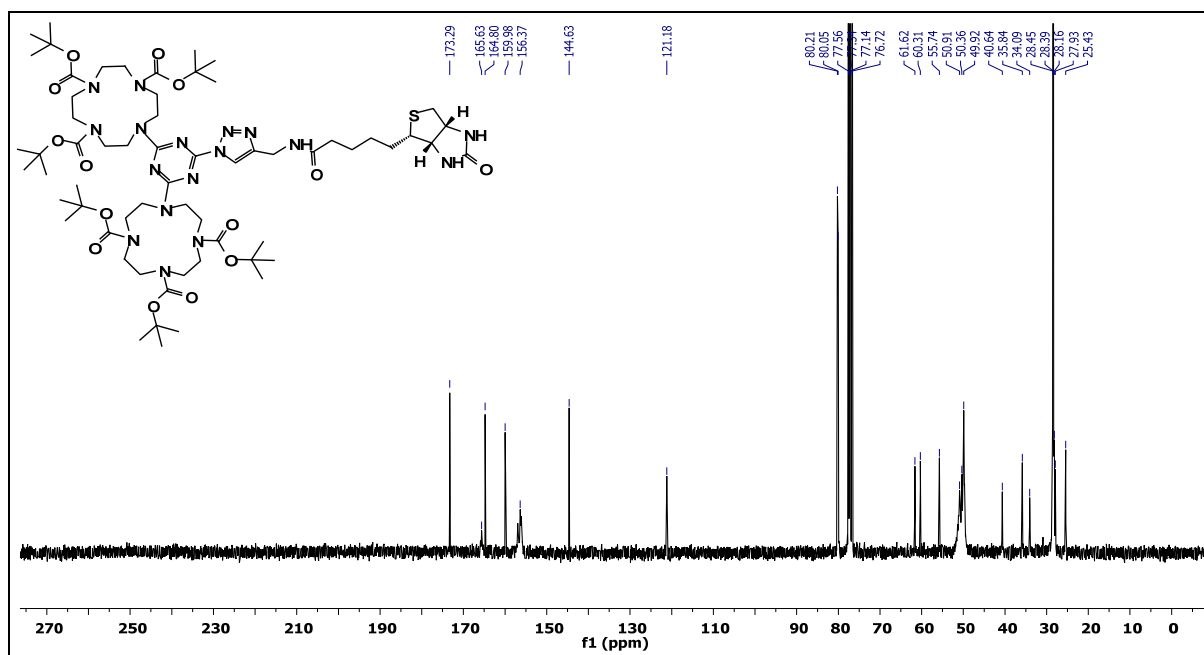


¹H-NMR spectrum of compound **16** (300 MHz, CDCl₃)

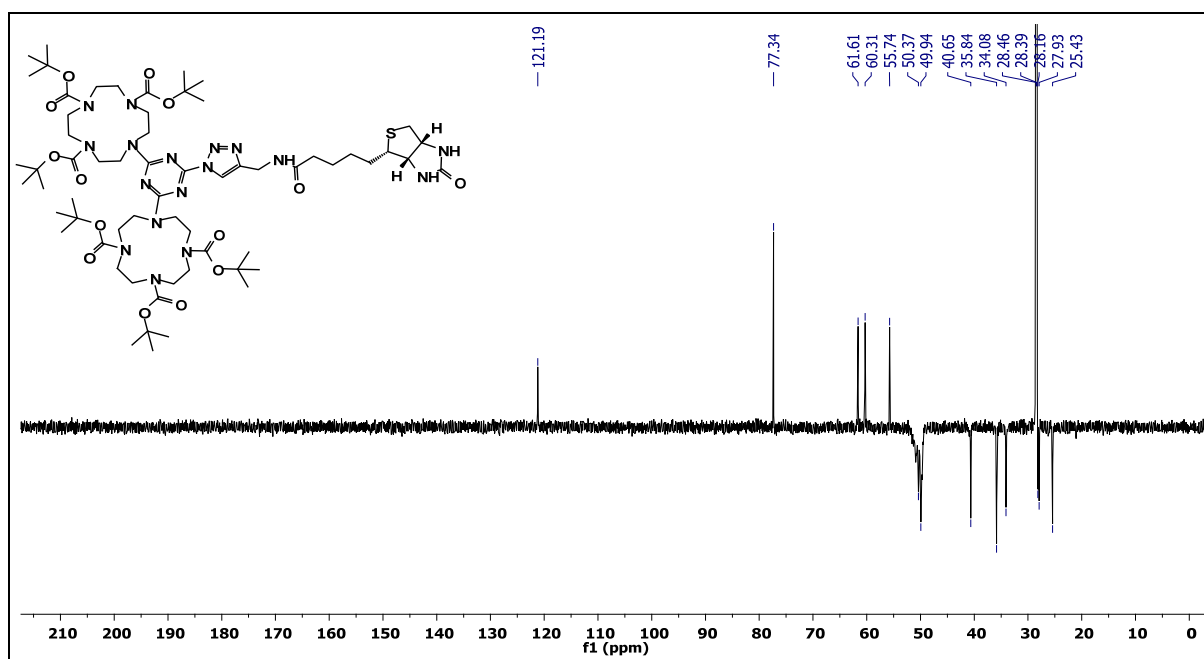


¹H-NMR spectrum of compound **5** (300 MHz, CDCl₃)

2. Rigid Amphiphilic Molecular receptors, Bioconjugates and Radiopharmaceuticals based on Metal-cyclen complexes via Click chemistry

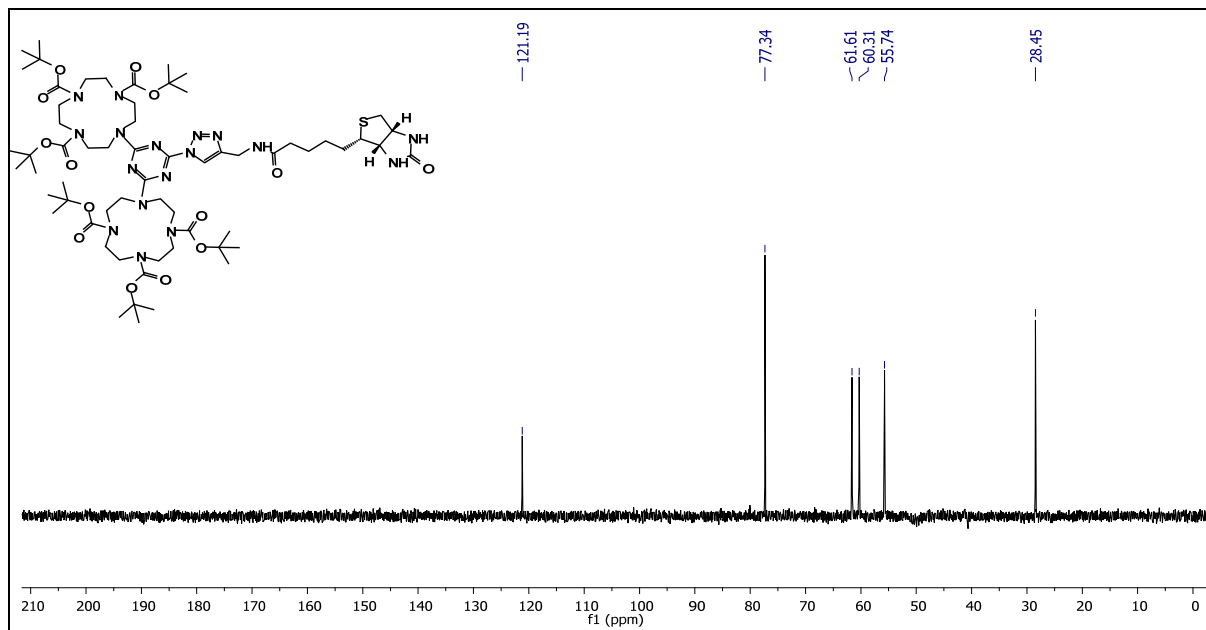


¹³C-NMR spectrum of compound **5** (75 MHz, CDCl₃)

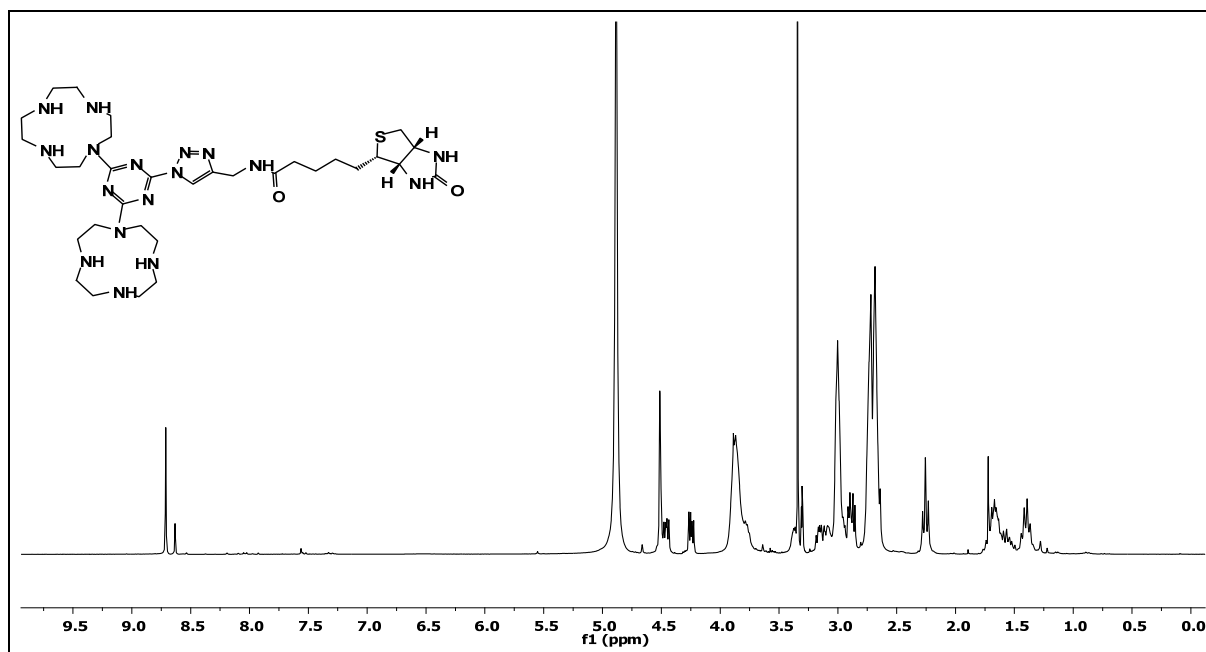


¹³C (DEPT 135)-NMR spectrum of compound **5** (150 MHz, CDCl₃)

2. Rigid Amphiphilic Molecular receptors, Bioconjugates and Radiopharmaceuticals based on Metal-cyclen complexes via Click chemistry

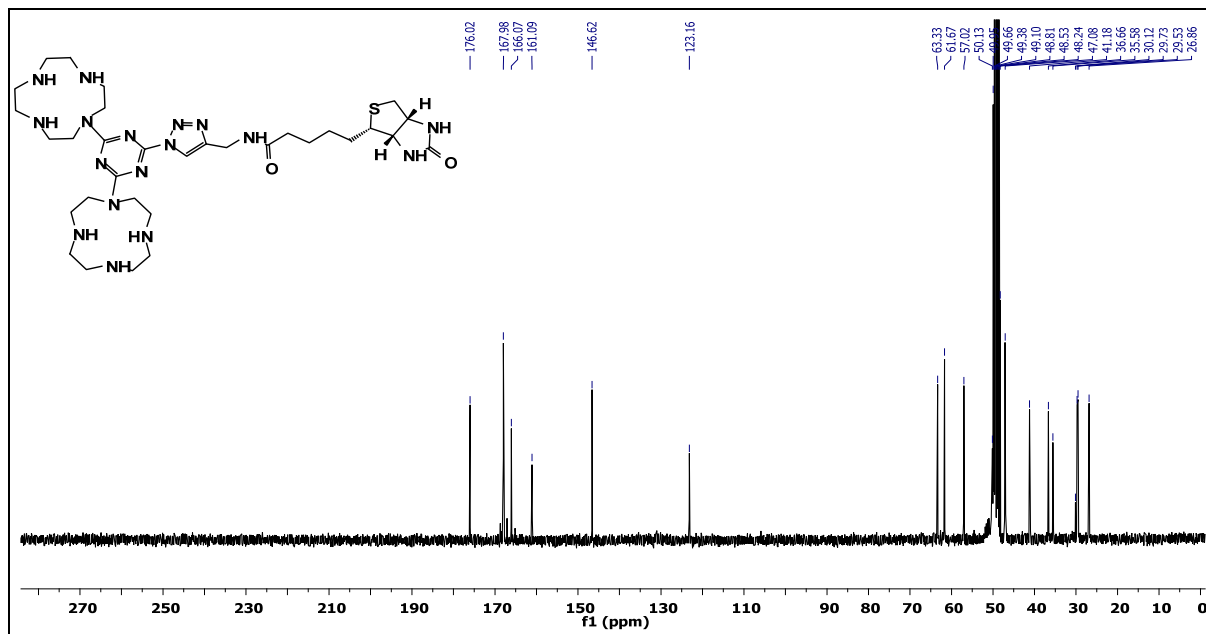


¹³C (DEPT 90)-NMR spectrum of compound 5 (150 MHz, CDCl₃)

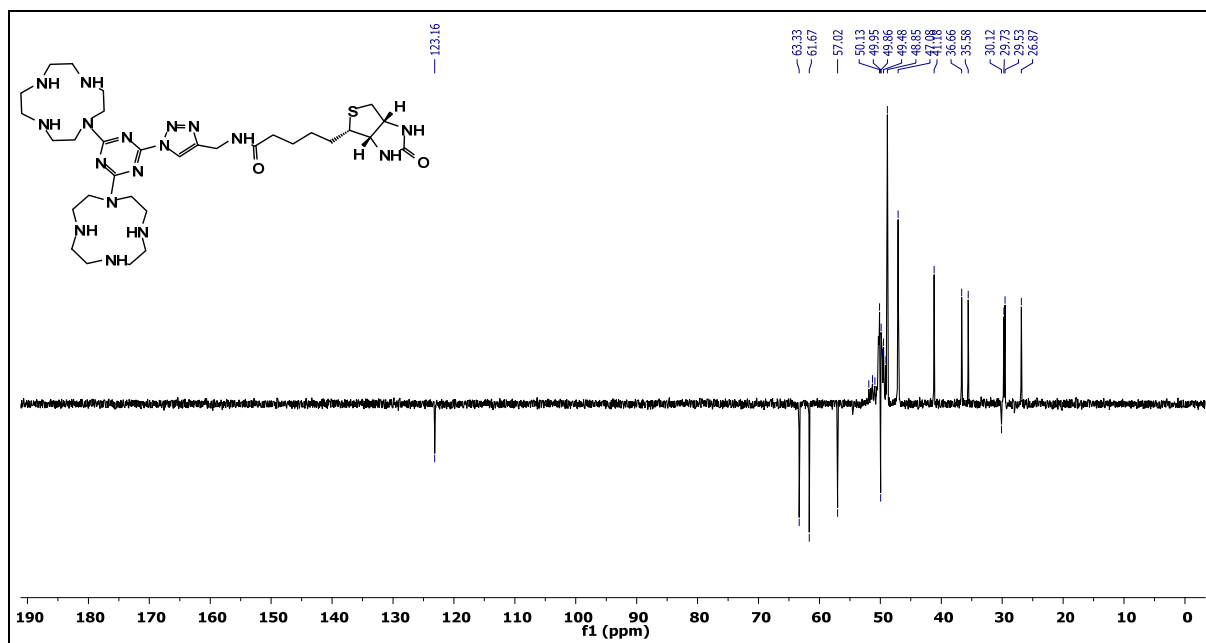


¹H-NMR spectrum of Boc-protected compound 5 (300 MHz, CDCl₃)

2. Rigid Amphiphilic Molecular receptors, Bioconjugates and Radiopharmaceuticals based on Metal-cyclen complexes via Click chemistry

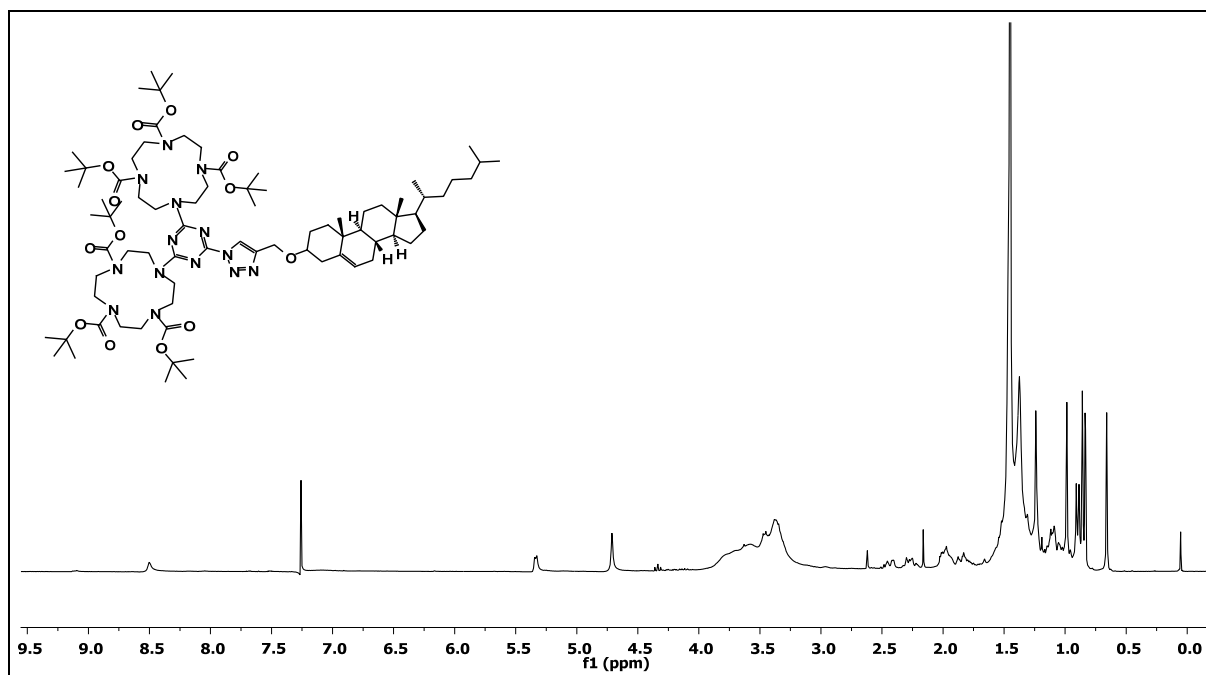


¹³C-NMR spectrum of Boc-protected compound **5** (75 MHz, CDCl₃)

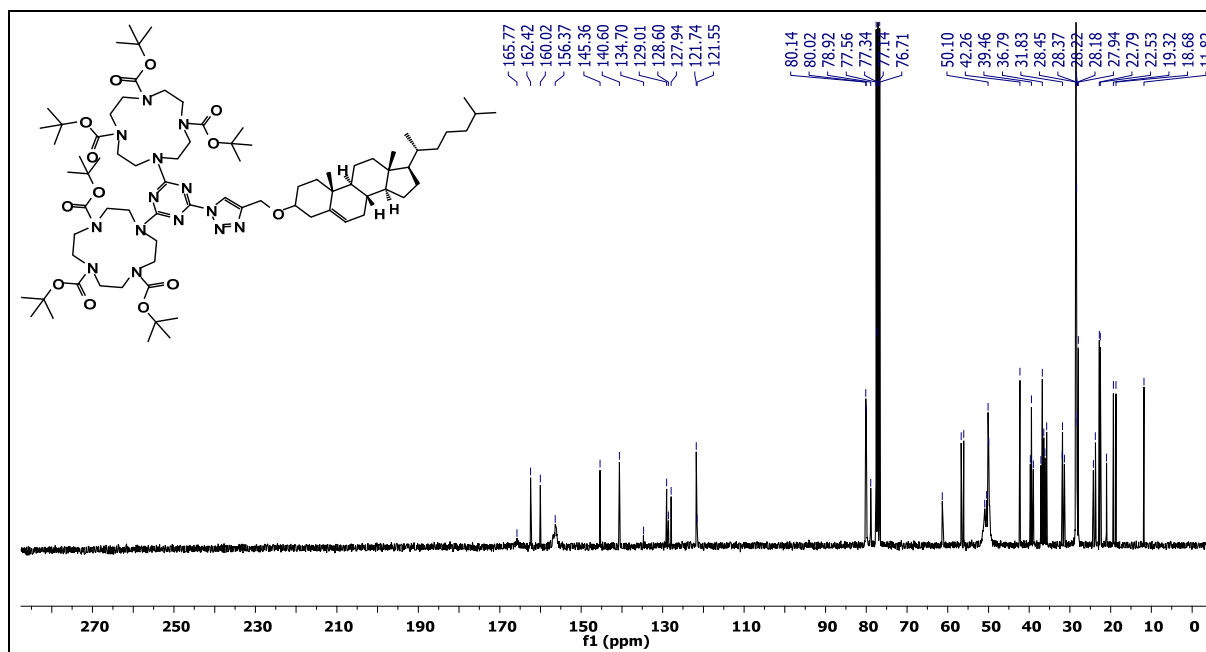


¹³C (DEPT 135)-NMR spectrum of Boc-protected compound **5** (150 MHz, CDCl₃)

2. Rigid Amphiphilic Molecular receptors, Bioconjugates and Radiopharmaceuticals based on Metal-cyclen complexes via Click chemistry



¹H-NMR spectrum of compound **11** (300 MHz, CDCl₃)



¹³C-NMR spectrum of compound **11** (75 MHz, CDCl₃)

2.6 References

- [1] H. C. Kolb, K. B. Sharpless *Drug Discov. Today* **2003**, *8*, 1128.
- [2] C. O. Kappe, E. Van der Eycken *Chem. Soc. Rev.* **2010**, *39*, 1280.
- [3] H. C. Kolb, M. G. Finn, K. B. Sharpless *Angew. Chem. Int. Ed.* **2001**, *40*, 2004.
- [4] R. Huisgen *J. Org. Chem.* **1976**, *41*, 403.
- [5] J. E. Moses, A. D. Moorhouse *Chem. Soc. Rev.* **2007**, *36*, 1249.
- [6] C. W. Tornøe, C. Christensen, M. Meldal *J. Org. Chem.* **2002**, *67*, 3057.
- [7] V. V. Rostovtsev, L. G. Green, V. V. Fokin, K. B. Sharpless *Angew. Chem. Int. Ed.* **2002**, *41*, 2596.
- [8] M. Meldal, C. W. Tornøe *Chem. Rev.* **2008**, *108*, 2952.
- [9] G. T. Hermanson *Bioconjugate Techniques, Vol. I*, **1996**.
- [10] R. Langer, D. A. Tirrell *Nature* **2004**, *428* 487.
- [11] S. S. van Berkel, M. B. van Eldijk, J. C. M. van Hest *Angew. Chem. Int. Ed.* **2011**, *50*, 8806.
- [12] E. M. Sletten, C. R. Bertozzi *Acc. Chem. Res.* **2011**, *44*, 666.
- [13] a)J.-F. Lutz, H. G. Börner *Prog. Polym. Sci.* **2008**, *33*, 1; b)L. Yi, J. Shi, S. Gao, S. Li, C. Niu, Z. Xi *Tetrahedron Lett.* **2009**, *50*, 759; c)Q. Wang, T. R. Chan, R. Hilgraf, V. V. Fokin, K. B. Sharpless, M. G. Finn *J. Am. Chem. Soc.* **2003**, *125*, 3192; d)K. Nwe, M. W. Brechbiel *Cancer Biother Radiopharm.* **2009**, *24*, 289.
- [14] J. W. Chin, S. W. Santoro, A. B. Martin, D. S. King, L. Wang, P. G. Schultz *J. Am. Chem. Soc.* **2002**, *124*, 9026.
- [15] C. W. Tornøe, C. Christensen, M. Meldal *J. Org. Chem.* **2002**, *67*, 3057.
- [16] A. J. Link, D. A. Tirrell *J. Am. Chem. Soc.* **2003**, *125*, 11164.
- [17] L. J. Cruz, C. Cuevas, L. M. Cañedo, E. Giralt, F. Albericio *J. Org. Chem.* **2005**, *71*, 3339.
- [18] J. Gierlich, G. A. Burley, P. M. E. Gramlich, D. M. Hammond, T. Carell *J. Org. Lett.* **2006**, *8*, 3639.
- [19] J. C. Walsh, H. C. Kolb *CHIMIA Int. J. Chem.* **2010**, *64*, 29.
- [20] S. Maschauer, J. Einsiedel, R. Haubner, C. Hocke, M. Ocker, H. Hübner, T. Kuwert, P. Gmeiner, O. Prante *Angew. Chem. Int. Ed.* **2010**, *49*, 976.
- [21] a)L. S. Campbell-Verduyn, L. Mirfeizi, A. K. Schoonen, R. A. Dierckx, P. H. Elsinga, B. L. Feringa *Angew. Chem. Int. Ed.* **2011**, *50*, 11117; b)T. L. Ross, M. Honer, P. Y. H. Lam, T. L. Mindt, V. Groehn, R. Schibli, P. A. Schubiger, S. M. Ametamey *Bioconjugate Chem.* **2008**, *19*, 2462.
- [22] a)C. M. Kam, A. S. Abuelyaman, Z. Li, D. Hudig, J. C. Powers *Bioconjugate Chem.* **1993**, *4*, 560; b)A. S. Abuelyaman, D. Hudig, S. L. Woodard, J. C. Powers *Bioconjugate Chem.* **1994**, *5*, 400.

- [23] A. B. Berger, P. M. Vitorino, M. Bogoy *Am J Pharmacogenomics* **2004**, *4*, 371.
- [24] W. Zhang, H. T. Liu *Cell Res* **2002**, *12*, 9.
- [25] E.J. McManus, K. Sakamoto, L.J. Armit, L. Ronaldson, N. Shpiro *EMBO J.* **2005**, *24*, 1571.
- [26] R. Hayes *Semin Nucl Med.* **1978**, *8*.
- [27] a)C. J. Anderson, M. J. Welch *Chem. Rev.* **1999**, *99*, 2219; b)S. Vallabhajosula, in *Molecular Imaging*, Springer Berlin Heidelberg, **2009**, pp. 179.
- [28] P. McQuade, D. W. McCarthy, M. J. Welch, in *Positron Emission Tomography: Basic Science and Clinical Practice* (Eds.: D. L. Bailey, D. W. Townsend, P. E. Valk, M. N. Maisey), Springer London, **2005**, pp. 237.
- [29] C. Burchardt, P. J. Riss, F. Zoller, S. Maschauer, O. Prante, T. Kuwert, F. Roesch *Bioorg. Med. Chem. Lett.* **2009**, *19*, 3498.
- [30] J. D. Badjić, A. Nelson, S. J. Cantrill, W. B. Turnbull, J. F. Stoddart *Acc. Chem. Res.* **2005**, *38*, 723.
- [31] L. J. Prins, D. N. Reinhoudt, P. Timmerman *Angew. Chem. Int. Ed.* **2001**, *40*, 2382.
- [32] M. Weisser, J. Käshammer, B. Menges, J. Matsumoto, F. Nakamura, K. Ijio, M. Shimomura, S. Mittler *J. Am. Chem. Soc.* **1999**, *122*, 87.
- [33] K. Kurihara, K. Ohto, Y. Honda, T. Kunitake *J. Am. Chem. Soc.* **1991**, *113*, 5077.
- [34] a)D. S. Turygin, M. Subat, O. A. Raitman, V. V. Arslanov, B. König, M. A. Kalinina *Angew. Chem. Int. Ed.* **2006**, *45*, 5340; b)J. C. Love, L. A. Estroff, J. K. Kriebel, R. G. Nuzzo, G. M. Whitesides *Chem. Rev.* **2005**, *105*, 1103; c)D. A. Offord, C. M. John, J. H. Griffin *Langmuir* **1994**, *10*, 761; d)W. A. Hayes, H. Kim, X. Yue, S. S. Perry, C. Shannon *Langmuir* **1997**, *13*, 2511.
- [35] a)M. Sugahara, M. Uragami, X. Yan, S. L. Regen *J. Am. Chem. Soc.* **2001**, *123*, 7939; b)D. Needham, R. S. Nunn *Biophys. J.* **1990**, *58*, 997; c)F. A. Nezil, M. Bloom *Biophys. J.* **1992**, *61*, 1176; d)M. Doxastakis, A. K. Sum, J. J. de Pablo *J. Phys. Chem. B* **2005**, *109*, 24173; e)R. K. Pandey, K. A. Suresh, V. Lakshminarayanan *J. Colloid Interface Sci.* **2007**, *315*, 528; f)K. Tu, M. L. Klein, D. J. Tobias *Biophys. J.* **1998**, *75*, 2147.
- [36] B. He, S. Velaparthi, G. Pieffet, C. Pennington, A. Mahesh, D. L. Holzle, M. Brunsteiner, R. van Breemen, S. Y. Blond, P. A. Petukhov *J. Med. Chem.* **2009**, *52*, 7003.
- [37] G. Godeau, C. Staedel, P. Barthélémy *J. Med. Chem.* **2008**, *51*, 4374.
- [38] G. V. Malkov, A. V. Shastin, Y. I. Estrin, E. R. Badamshina, Y. M. Mikhailov *Propellants Explos. Pyrotech.* **2008**, *33*, 431.

Chapter 3

Phosphorescent Small Unilamellar Vesicles with embedded Amphiphilic Lanthanide complexes

“Lanthanons – these elements perplex us in our researches, baffle us in our speculations, and haunt us in our very dreams. They stretch like an unknown sea before us; mocking, mystifying and murmuring strange revelations and possibilities.”

Sir William Crookes, in an address to the Royal Society, February 1887

3.1 General Introduction

3.1.1 Lanthanides: Relevance

Lanthanides occupy unique positions in the periodic table, which correspond to the first period of f-block elements from lanthanum to lutetium, and the electronic configuration $[\text{Xe}] 4f^n 5s^2 5p^6$ where n varies from 0 to 14. They are the subset of rare earth elements with rich photophysical and coordination chemistry.

The characteristic oxidation state of the lanthanide elements is +3. In addition to that, in reducing conditions, europium, samarium and ytterbium can be stable in +2 oxidation states; also, Ce^{3+} can lose its single f electron to form Ce^{4+} with the stable electronic configuration of xenon.^[1]

The trivalent lanthanides are hard acids and form stable ionic complexes with oxygen donor ligands rather than nitrogen donor ligands. The ionic character of bonding also leads to rapid ligand exchange in solution.^[2] The coordination number of $[\text{Ln}(\text{H}_2\text{O})_n]^{3+}$ where the anion is a poor ligand tends to be 9 for the early lanthanides (La-Eu) as shown by many X-ray studies. The nine water molecules in $[\text{Ln}(\text{H}_2\text{O})_9]^{3+}$ are typically found in a tricapped trigonal prismatic arrangement. The degree of hydration decreases in progression along the series.^[1]

The 4f electrons of lanthanides are well shielded from the environment, consequently the spectroscopic and magnetic properties of lanthanides are unaffected by the environment. The absorption spectra of lanthanide cations result from f - f transitions and are sharp and line like as opposed to the broad absorptions of transition metals, as broadening effect of ligand vibrations is minimized because of deeply buried 4f orbitals.

3.1.2 Sensitized Lanthanide Luminescence: Principles and Advantages

All tripositive lanthanide ions, except La(III) and Lu(III) are luminescent. The f - f emission lines of Ln(III) cover the entire spectrum ranging from UV (Gd(III)) to visible (e.g., Pr(III), Sm(III), Eu(III), Tb(III), Dy(III), Tm(III)) and near-infrared (NIR, e.g., Pr(III), Nd(III), Ho(III), Er(III), Yb(III)). An important parameter characterizing the emission of light from a Ln(III) ion is the lifetime of the excited state, τ_{obs} . Since the dipole strengths of f - f transitions are very small, lanthanide ions have very low molar absorptivities and can only be effectively excited by lasers; lanthanide luminescence can be significantly enhanced by chelating ligands in a process called 'sensitization'. In sensitized lanthanide luminescence, the chromophore is normally an aromatic or unsaturated organic molecule that is either anionic or has a strong dipole moment to coordinate to the Ln(III) ion. However intermolecular sensitization of lanthanide ions are also reported in gel matrix and also in micellar medium, which involves non covalent co-embedding of lanthanide ion and the sensitizing chromophore.^[3]

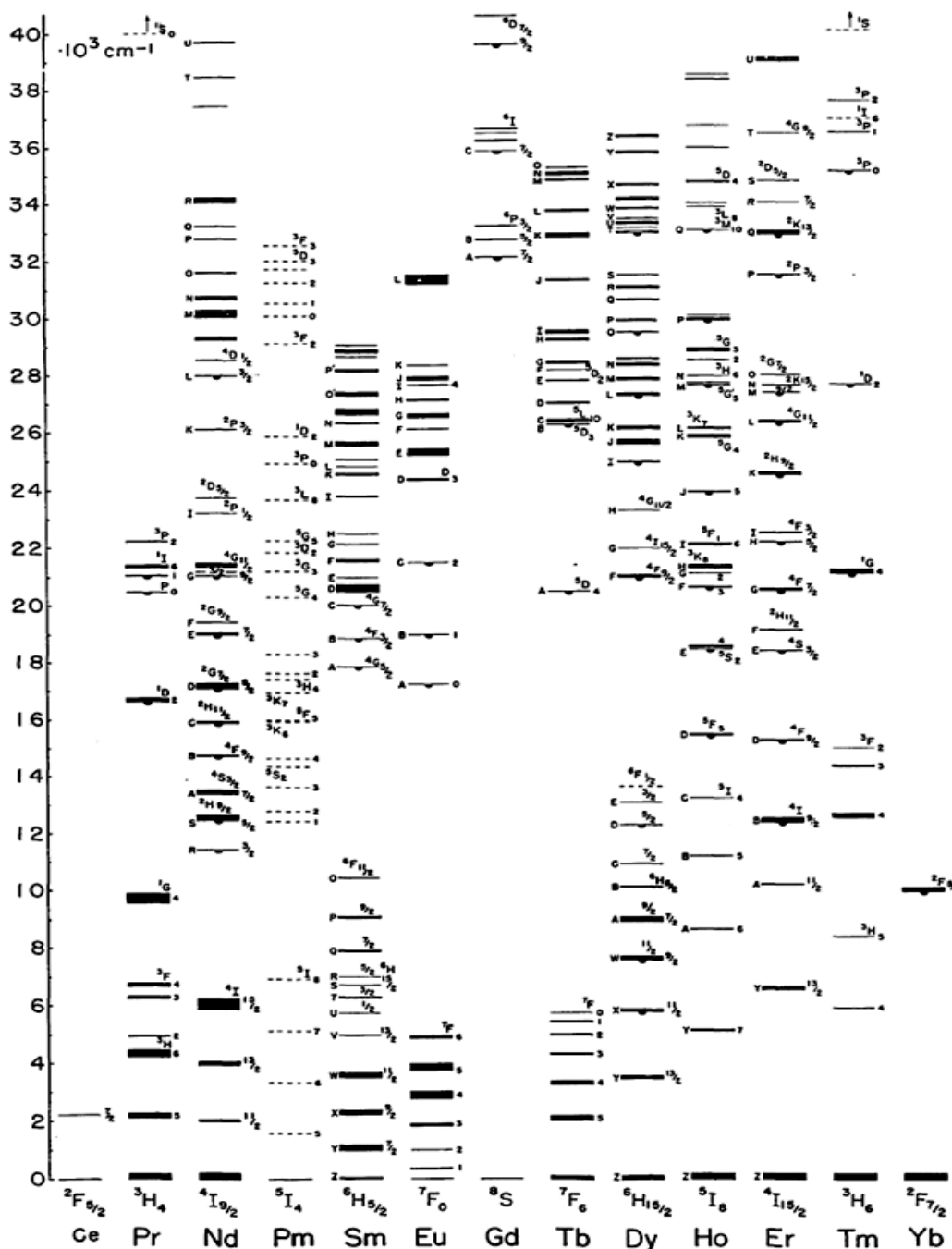


Figure 1: Energy level diagram, also known as a Dieke diagram, depicting the free ion energy levels of the trivalent lanthanide ions from Ce^{3+} ($4f_1$) to Yb^{3+} ($4f_{13}$). [Reprinted with permission from the quoted reference]^[4]

The sensitized luminescence of lanthanide complexes offers several advantages over the classical organic dyes for the use in complex biological medium.^[5]

1. The lanthanide emissions are Laporte forbidden and are therefore characterized by extremely long luminescence lifetimes. The emission life times of europium and terbium are in the millisecond range and that of samarium and dysprosium are in the microsecond range. Their

long lived excited states allow the short-lived background fluorescence to disperse before the lanthanide emission occurs.

2. The sensitised emission of a lanthanide complex gives rise to large Stokes shift between the absorption of the antenna and the emission of the lanthanide, hence avoiding the concentration dependent self absorption problems.

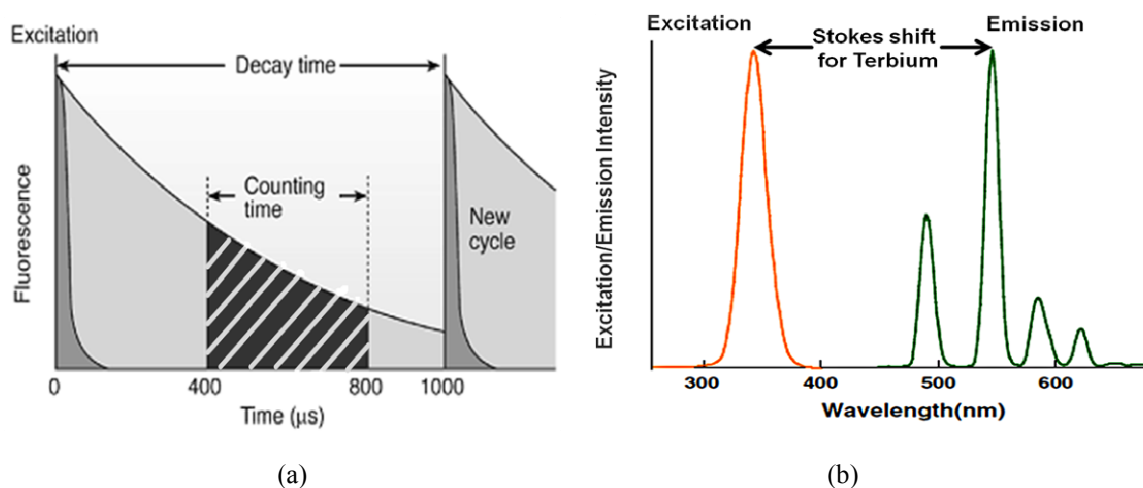


Figure 2: Unique fluorescence properties of lanthanides (a) long luminescence decay times [adapted from the quoted reference]^[6] (b) large Stokes' shift

3. The lanthanides have very narrow band emission spectra and these are insensitive to the environmental changes. The line like emission bands can also give a rise to better signal to noise ratio compared to fluorescent bands (several hundred nm).
4. The long wavelengths at which the lanthanides emit (480-620nm for Tb (III)) occur beyond the absorbance of body tissue, which is important for signal quality. Furthermore, ions such as Yb(III) and Nd(III) emit at even longer wavelengths in the near infrared part of the spectrum, which is particularly attractive for diagnostic applications.^[7]
5. The lanthanide emission spectra do not completely overlap with one another, hence multiple lanthanide probes can be employed for concurrent monitor of several analytes.

3.1.3 Phospholipid based Liposomes: Introduction

First described by the British haematologist Dr. Alec D Bangham in 1961^[8] at the Babraham Institute, Cambridge, liposomes are nano size artificial vesicles of spherical shape that can be produced from natural phospholipids and cholesterol. Since their discovery, they are versatile tool in many scientific disciplines like chemistry, biology, biochemistry, physics and medicine and have become paradigms for biomembranes, instructive models of selfassembling colloids, and vehicles for pharmaceutical, diagnostic, and cosmetic agents.

Liposomes are composed of natural phospholipids and may also contain mixed lipid chains with surfactant properties (e.g. phosphatidylethanolamine). Liposomes can be classified according to their lamellarity (uni-, oligo-, and multi-lamellar vesicles), size (small, intermediate, or large) and preparation method (such as reverse phase evaporation vesicles, VETs). Unilamellar vesicles are spherical concentric unilamellar (one layer) structures and generally have diameters of 50–250 nm. Multilamellar vesicles comprise several spherically concentric lipid bilayers and have diameters of 1–5 μm .^[9] These spherical nanoparticles (NPs) with unilamellar or multilamellar structures separate and encapsulate an aqueous interior from bulk aqueous solvent. The lamellae of liposomes are composed of a bilayer of either lipid with a hydrophobic midplane to separate the two aqueous volumes. Distearoylphosphatidylcholine is an example of a lipid material commonly used for assembling liposomes.^[10]

The properties of liposomes make them useful for different applications. They show structural stability on dilution, varying permeability of the bilayer to different molecules, ability to entrap both water soluble and insoluble substances and deliver them into desired environments.

The size, lamellarity (unilamellar or multilamellar) and lipid composition of the bilayers influence many of the properties like the fluidity, permeability, stability and structure -these can be controlled and customized to serve specific needs. The properties are also influenced by external parameters like the temperature, ionic strength and the presence of certain molecules nearby.^[11]

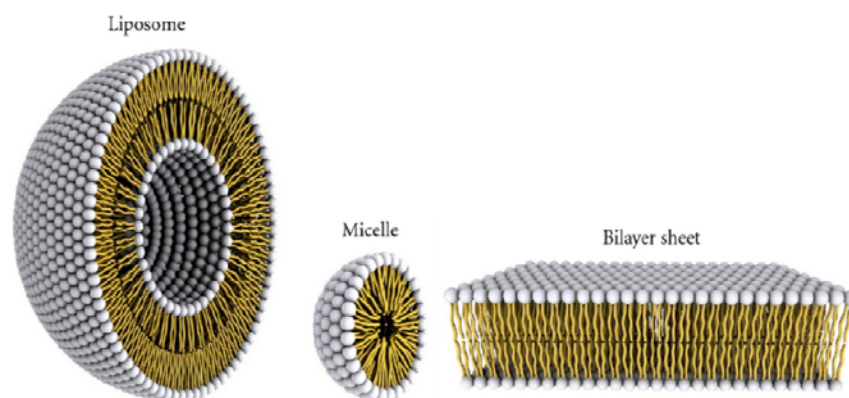


Figure 3: A representative diagram of the steric organization of a liposome (left) and a micelle (middle); Liposomes are constructed by lipid bilayer (right). [Reprinted with permission from the quoted reference]^[12]

3.1.4 Liposomal stability and surface modification chemistry

For the last five decades, the interest in the liposomes or amphiphilic nanoparticles arises from the combination of nanoscale size with the nearly infinite diversity of physical properties and chemical functionality that can be obtained through organic chemistry.^[10]

Liposomal stability: stealth liposomes

Liposomes have been investigated for many years in the biomedical field and their application in *in vivo* drug delivery,^[13] in gene therapy^[14] and as model systems for studying biological membranes^[15] are longstanding goals for many research projects. The main advantages of using liposomes include: i) the high biocompatibility, ii) the easiness of preparation, iii) the chemical versatility that allows the loading of hydrophilic, amphiphilic, and lipophilic compounds, iv) the simple modulation of their pharmacokinetic properties by changing the chemical composition of the bilayer components.^[16] For *in vivo* drug delivery and gene therapy, one of the most critical aspects is to improve liposome stability and enhance their circulation times in the blood. Conventional liposomes injected in blood stream are found to be unstable. The physicochemical properties of liposomes, such as net surface charge, hydrophobicity, size, fluidity, and packing of the lipid bilayers, influence their stability and the type of proteins that bind to them.^[17] To overcome these problems there had been many attempts towards surface modification of liposomes by manipulating the lipid contents. For example, including ganglioside GM1 into liposomes leads to significantly enhanced stability in serum. Another major improvement in increasing liposome stability was achieved by introducing polyethylene glycol (PEG) as polymeric stabilizer (Stealth liposomes).

PEG can be incorporated on the liposomal surface in different ways, but the most widely used method is by attaching polyethylene glycol (PEG) chains covalently to the polar head groups of phospholipids. Surface modification of liposomes with PEG has demonstrated several biological and technological advantages. One major advantage of using stealth liposomes in biology is its longer blood circulation time (hours) compared to conventional liposomes (minutes).^[18] PEG, which is a strongly hygroscopic synthetic polymer, strongly influences the physicochemical properties of the lipid bilayer. Some remarkable effects are

- (a) Upon incorporation in the phospholipid bilayer, PEG changes the thermotropic phase behaviour of the lipids. There are reports of increase in pre-transition (T_p) and transition (T_m) temperature of lipids in small unilamellar vesicles and multilamellar vesicles (MLV) with increase in concentration of the incorporated PEG.^[19] Based on DSC and ESR measurements, these changes were proposed to be due to the decrease in water content incorporated between phospholipid bilayer upon addition of poly-(ethylene glycol).^[20]
- (b) There are some reports of loss of pre-transition temperature of phospholipids upon incorporation of PEG into lipid bilayer.^[21]
- (c) Poly-(ethylene glycol) reduces the degree of the segmental lipid chain motion in the hydrocarbon region of some phospholipid layers in the gel phase. The motional restriction

of the labels due to PEG is reported to be more pronounced in ULVs than in MLVs of some phospholipids. These observations was explained in terms of the packing density of the hydrocarbon region of the phospholipid bilayers which increases with increase in concentration of incorporated high molecular weight PEG.^[21]

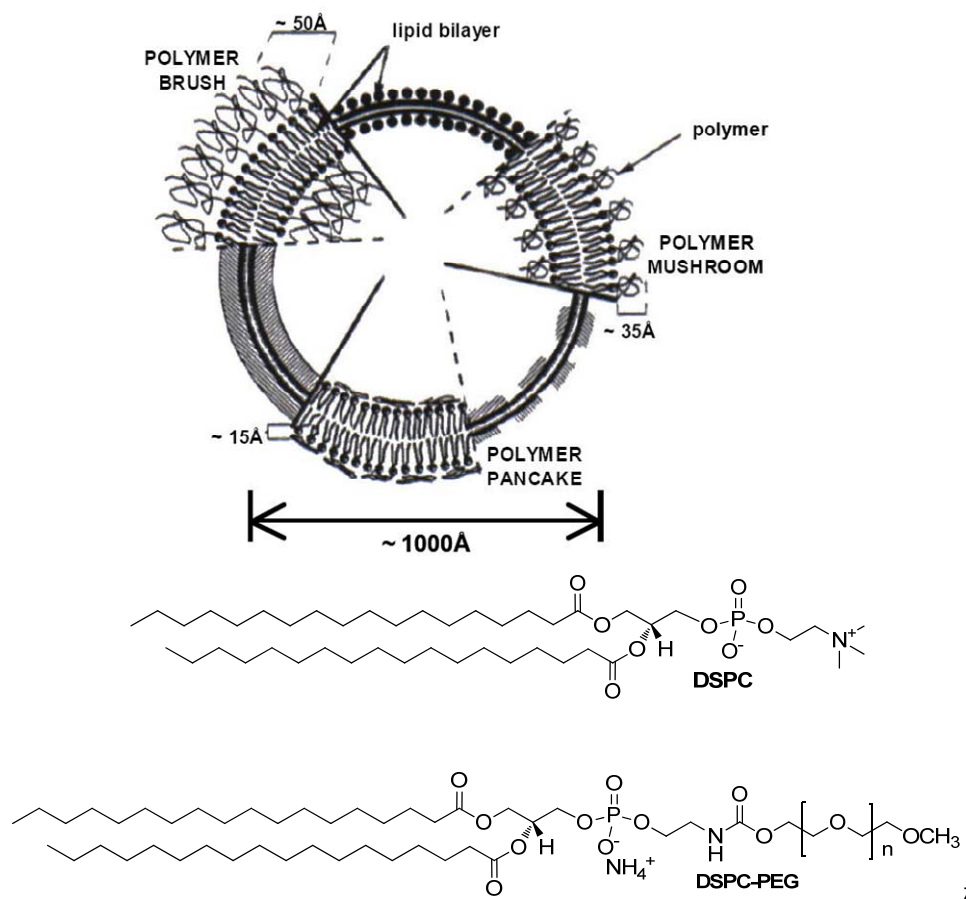


Figure 4: [Top] Schematic diagrams of poly-(ethylene glycol) (PEG) configurations regimes (mushroom, brush and pancake) for polymer grafted to the surface of liposome bilayer [Reprinted with permission from the quoted reference]^[9] [Bottom] Chemical structures of distearoylphosphatidylcholine (DSPC), distearoylphosphatidylethanolamine after conjugation with poly-(ethylene glycol) (PEG) (DSPE-PEG)

Liposomal surface modification

The introduction of functionalized amphiphiles into a liposomal surface has proven to be an effective strategy for developing liposomal conjugates via. Functional groups were introduced at the stage of liposome formation employing various lipids including the recognizable (e.g. biotin-labeled) ones by well established methods.^[22]

To prepare modified liposomes with controlled properties, proteins, peptides, polymers and other molecules are chemically conjugated to liposomes using standard crosslinking chemistry.^[23] The conjugation methodologies usually are based on three reactions: amide bond formation via activated

carboxyl groups and amines, thioether bond formation by reaction between maleimide derivatives and thiols, and disulphide bond formation via reaction between pyridyldithiols and thiols. Some other approaches involve the formation of carbamate bonds.^[24] Many of the activated lipids used in these processes are commercially available.^[25]

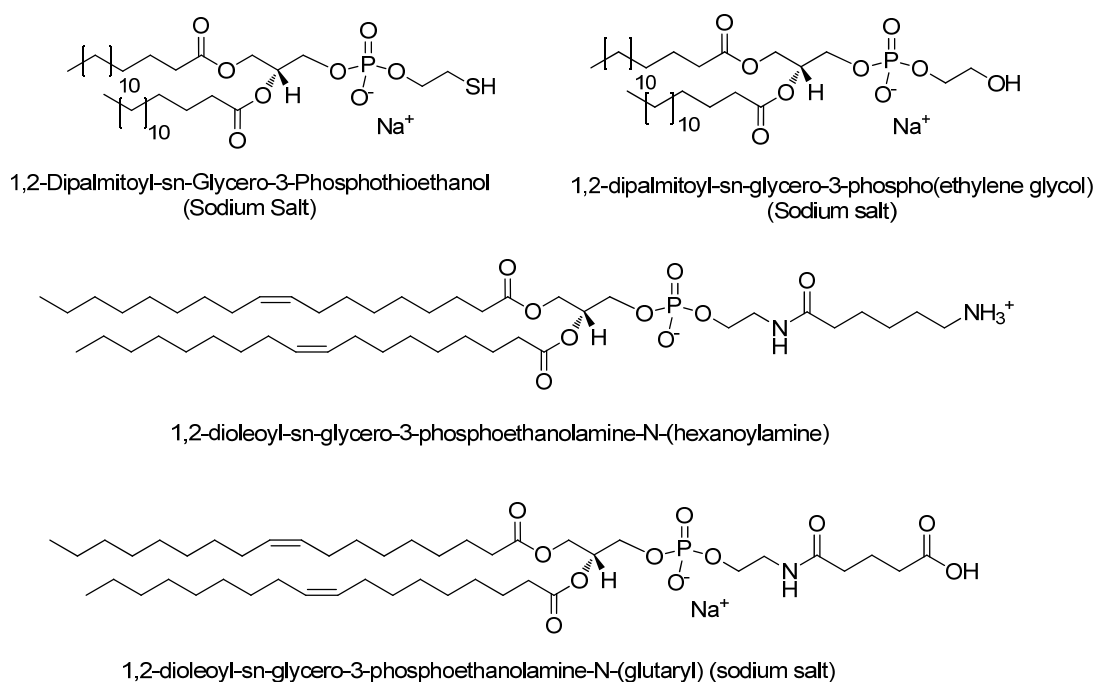


Figure 5: Some of the frequently used head group modified functionalized lipids

Functionalized vesicles or liposomes designed and prepared from different synthetic amphiphiles have been reported in the development of novel catalytic systems^[26] or nanoscale systems or biosensors for molecular recognitions.^[22, 27] Molecular recognition and sensing at interfaces are reported to be more effective relative to isotropic media, since the interacting groups are located at the organized liposomal surface. In fact, the binding constants between complementary moieties differ by some orders of magnitude for various types of molecular aggregates.^[28] Also, even less-catalytically active small molecules can be self-assembled to form bilayer vesicles and, in doing so, gain unique catalytic properties for a given molecular transformation.^[29] Incorporation of the recognition unit into the lipid bilayer^[30] by synthetic modification of lipids is one possible approach. Co-embedding of an amphiphilic recognition unit into lipids to form liposomes is an alternative.^[3a, 31] There are recent reports of incorporation of amphiphilic metal complexes in the liposome for effective molecular recognition and efficient catalysis.^[31]

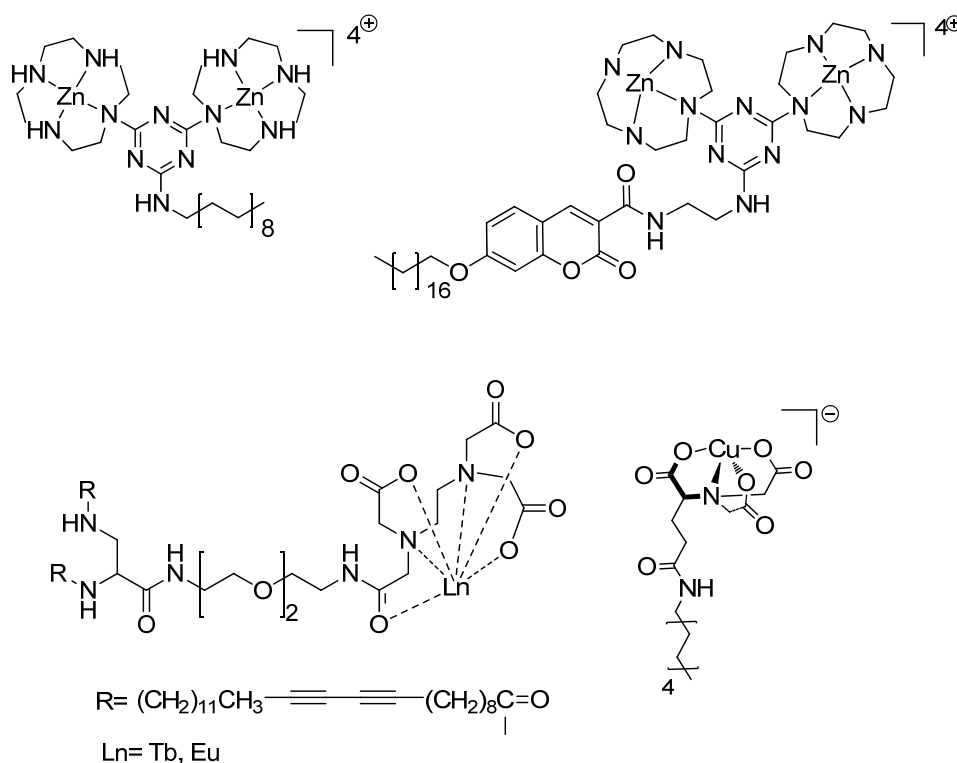


Figure 6: Amphiphilic metal complexes embedded in liposomes for molecular recognition and catalysis ^[31b, 32]

3.1.5 Lanthanide complexes and liposomes

Due to their rich photophysical properties, lanthanide complexes are in commercially applied as highly sensitive and selective probes in heterogeneous and homogeneous immunoassays, and in DNA assays.

Liposomes have been exploited to generate highly sensitive CEST (Chemical Exchange Saturation Transfer) agents named LipoCEST and it is an emerging area of research to develop new highly efficient CEST agents. There are several reports of the application of paramagnetic lanthanide complexes doped in liposomes to develop a novel class of LipoCEST agents for MRI (Magnetic Resonance Imaging), which allow a marked sensitivity enhancement and thus significantly contribute to the development molecular imaging protocols.^[33] Tm(III) and Dy(III) ions encapsulated in the liposomal cavity are used for developing LipoCEST agents.^[34] Liposomes incorporating Gd(III)-complexes have been successfully used in many *in vivo* MRI applications on animal models including the visualization of tumors either by passive^[35] or active^[36] targeting, detection of atherosclerotic plaques,^[37] lymph nodes,^[38] inflammation sites,^[39] and visualization of myocardium infarcted areas.^[40]

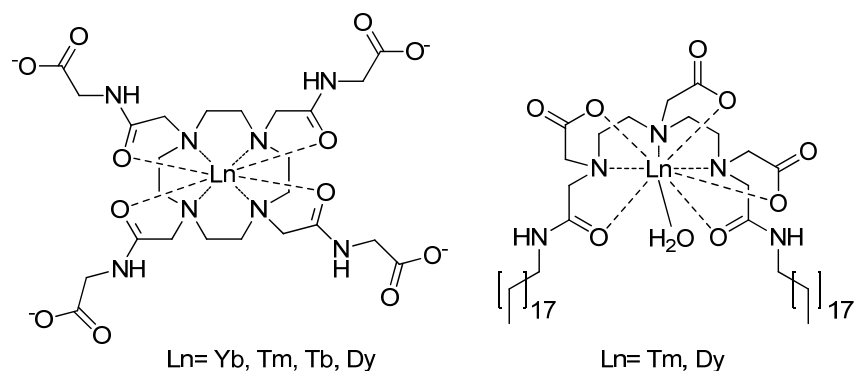


Figure 7: Some of lanthanide based complexes that were incorporated (either in liposomal cavity or on surface) into liposomes in the development of LipoCEST agents.^[41]

Lanthanide incorporated liposomes were also reported as selective biosensors. Elegbede et-al, in 2007, reported the application of lanthanide ion incorporated liposomes for selective recognition of carbonic anhydrase isozymes.^[42]

Liposomes have been used for *in vivo* drug delivery. For the necessary evaluation of the biodistribution of liposomes as drug carriers, lanthanide complexes (eg Eu(III)) were incorporated as alternative to the conventional fluorophores and radiolabeled tracers (¹⁴C, ¹H).^[43]

3.2 Outline of the chapter

This chapter describes the design, synthesis and applications of amphiphilic lanthanide complexes embedded in liposome surfaces. In the first part of this chapter (section 3.3), synthesis and embedding of an amphiphilic Tb(III) complex into liposomal surface and its potential applications as reporter for physiological temperature change are discussed. The second part of this chapter (section 3.4) summarizes attempts to use lanthanide based complexes as reporter dye non-covalently co-embedded with analyte binding sites in nano-sized vesicular membranes.

3.3 Temperature responsive phosphorescent small unilamellar vesicles¹

3.3.1 Introduction

Temperature is a fundamental physical property of matter important in everyday life and scientific and industrial applications. The methods to measure temperature can be divided into two main techniques: contact thermometry and non-contact thermometry. Contact methods include thermocouples, thermistors, and resistance temperature detectors (RTDs), whereas non-contact methods often use the spectral emittance of a material for readout.^[44]

Non-contact optical techniques have various advantages in terms of sensitivity and real-time monitoring over a wide range, from femtosecond to second.^[45] Among the available optical methods, infrared thermometers that use the principle of blackbody radiation are flexible and easy to use, but can only measure the temperature of surfaces, thus limiting their applications.^[46] Therefore luminescence based optical sensors have attracted much attention, because of their fast response, high spatial resolution, accurate usability even in strong electromagnetic fields^[47] and safety of remote handling.^[48] Such sensing probes use appropriate luminophores ranging from polycyclic aromatic hydrocarbons to metal complexes.^[45] Temperature sensitive probes were incorporated into nanogels for intracellular thermometry,^[49] and in sensor films or thermo-sensitive polymers to allow spatially resolved temperature imaging.^[50]

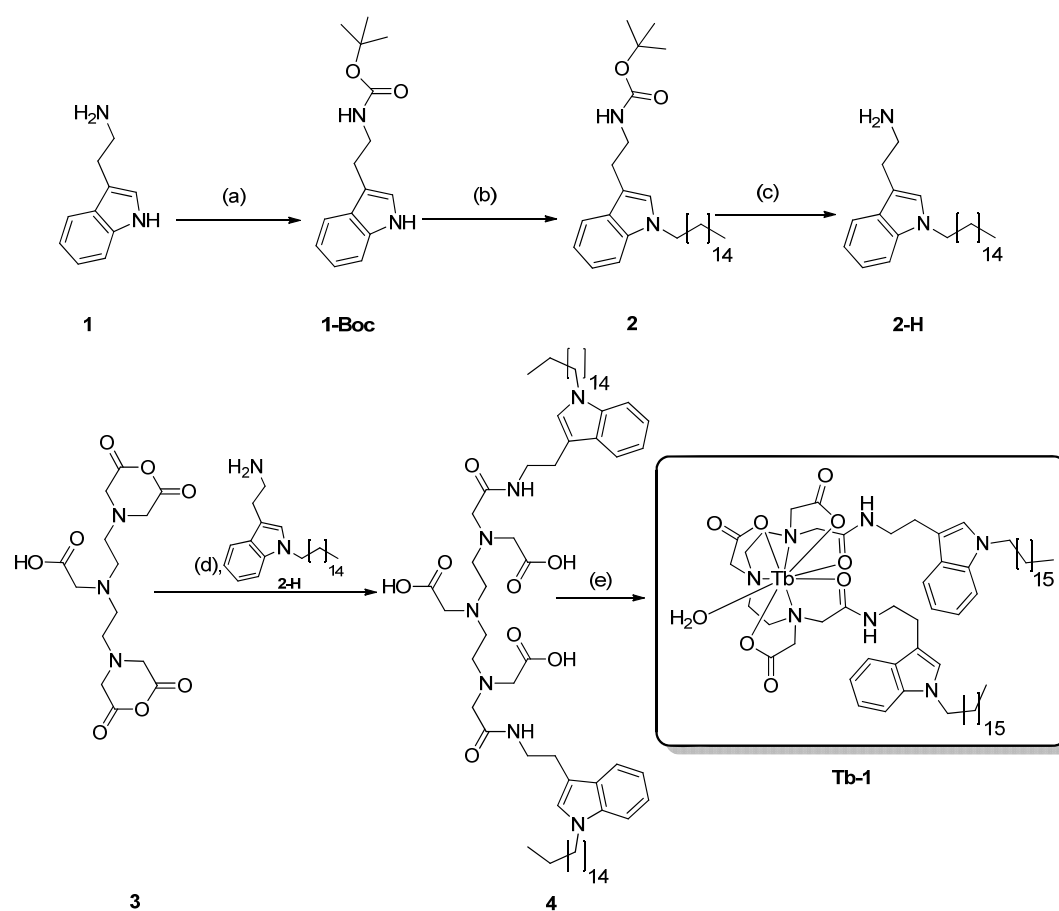
Recently lanthanide ion (Eu^{3+} and Tb^{3+}) complexes have been used for optical sensing of temperature.^[47, 50-51] The use of lanthanide complexes has several advantages over organic luminophores: (a) they have long emission wavelengths, (b) lanthanide emissions are Laporte forbidden and are therefore characterized by very long luminescence lifetimes, which is useful for applications in biological media; (c) 4f electrons of the lanthanides are highly shielded from the chemical environment by the 5s and 5p orbitals thus making them environment insensitive. Among the tripositive lanthanides, typically Eu^{3+} based complexes have been used as optical temperature sensors, while Tb^{3+} complexes are less explored. One reason is their smaller luminescence dependence on temperature.^[52] However, the longer luminescence lifetime of the Tb^{3+} ion compared to Eu^{3+} make terbium complexes the favored system for the lifetime based optical sensors of temperature.^[53] Having this in mind we considered using Tb^{3+} complexes as probes for optical sensing of temperature. By embedding the complex in different phospholipid based membranes we obtain reversible thermosensitive small unilamellar vesicles with an adjustable temperature range. Their luminescence is not affected by biological background fluorescence.

¹ Temperature responsive phosphorescent small unilammelar vesicles; M. Bhuyan, B. Koenig (*manuscript under preparation*)

3.3.2 Results and discussions

3.3.2.1 Synthesis of amphiphilic Tb(III) complex

The DTPA based amphiphilic Tb(III) complex was synthesized as shown in Scheme 1. Since the 4f electrons are well shielded by the 5s and 5p orbital, lanthanides depend on a sensitizer or antenna to show luminescence (Figure 8). The energy transfer between the excited triplet state of the sensitizing ligand and the emitting level of the Tb(III) ion is described by the Dexter mechanism^[54] We have chosen tryptophan as a known sensitizer for the Tb(III)-ion. Detailed experimental procedures and analytical data of the prepared compounds are provided in the Experimental and Supporting data section.



Scheme 1: Synthesis of **Tb-1**. (a) DCM, (Boc)₂O, NEt₃ [quantitative yield]; (b) DMF, 1-bromooctadecane, NaH [Yield: 93%]; (c) DCM, trifluoroacetic acid [Yield: 95%]; (d) DMF, CHCl₃, 40°C, 24h [Yield: 55%]; (e) CH₃OH, Tb(CF₃SO₃)₃, 24h [Yield: 98%]

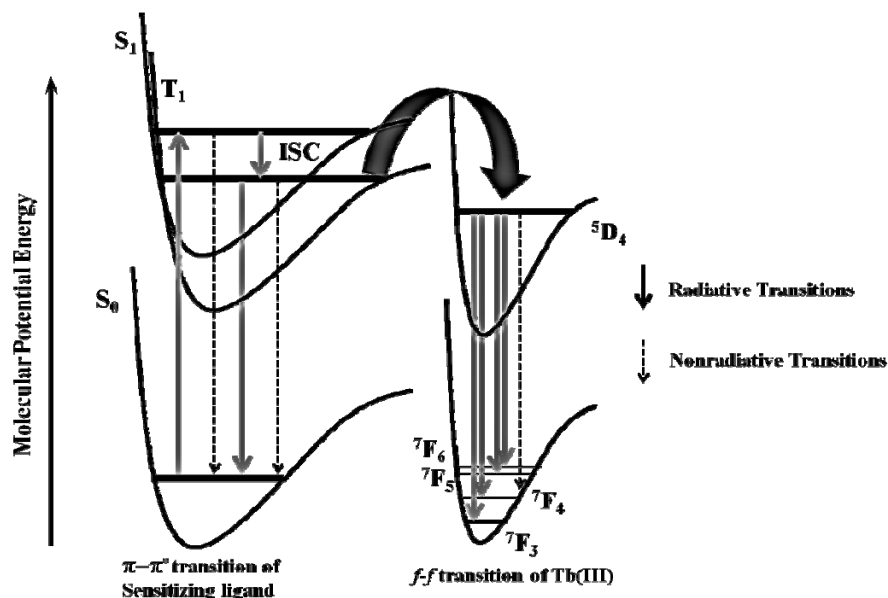


Figure 8: Energy Diagram of Tb(III) complexes with sensitizing ligand

3.3.2.2 Preparation of the Tb(III) containing vesicular systems (LNT)

Luminescent nanosized vesicular systems (LNT) with embedded Tb³⁺ complexes were prepared following the previously reported film-hydration method.^[55] The multilamellar vesicles were extruded through definite filters to get unilamellar vesicles of 90-100 (±5) nm in size. We have used different commercially available phospholipids for the preparation of LNT 1-7 (Table1).

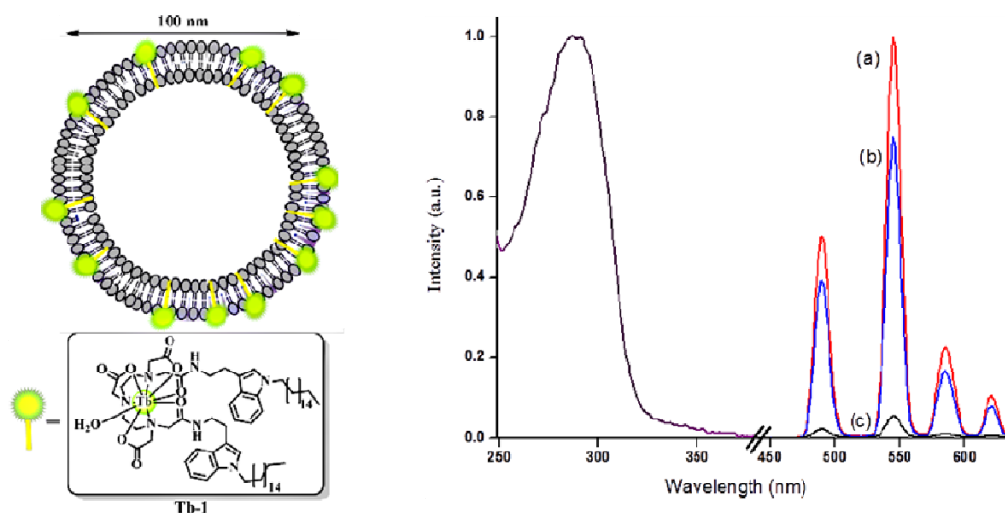


Figure 9: [Left] Schematic representation of LNT; [Right] excitation and emission spectra of LNT [excitation spectra: Tb(III) complex (5%)+DSPC vesicle at 25°C, conc. of Tb(III) = 5×10^{-6} M; emission spectra: (a) [Tb(III) complex (5%)+DSPC] vesicle at 25°C, conc. of Tb(III) = 5×10^{-6} M, (b) [Tb(III) complex (5%)+DOPC] vesicle at 25°C, conc. of Tb(III) = 5×10^{-6} M, (c) Tb(III) complex at 25°C, conc. of Tb(III) = 1×10^{-4} M]

Table 1: Composition, characterization and summary of applicability of prepared **LNTs**.

Luminescent Vesicle	Phospholipids used ^[56]	T_m ^[a] (°C) ^[56-57]	Size of Vesicles (nm) ^[b]	Effective Range (°C)	Most Sensitive Range (°C) ^[c]	Sensitivity (% °C ⁻¹) ^[c]
LNT1	18:0 PC (DSPC)	55	95	0-60	25-55	-3.5
LNT2	16:0 PC (DPPC)	41	98	0-40	20-40	-3.0
LNT3	14:0 PC (DMPC)	23	95	0-25	10-23	-4.2
LNT4	DSPE-PEG350	~60	90	0-60	25-55	-1.8
LNT5	18:1c9 PC (DOPC)	-20	92	n. a.	n. a.	n. a.
LNT6	PC(18:0/14:0) (SMPC)	30	95	0-30	15-30	-2.8
LNT4 ^[c] + BSA	DSPE-PEG350	~60	93	0-60	25-55	-1.4

[a] T_m = phase transition temperature of lipids; [b]Z-average(d. Nm.) with s.d.= ± 5 ; [c] the most sensitive temperature range and sensitivity per °C are based on the temperature dependent lifetime measurements carried out in HEPES buffer at pH 7.4, [c] the probable nonspecific interaction of the constituent lipids with protein (BSA)^[58] are minimised by shielding the vesicular surface by using DSPC-PEG350 having oligoethylene glycol residues attached to its polar head groups

The emission intensity of lanthanide complexes depend on their concentration. Due to clustering of the lanthanide ions a high concentration cross relaxation can lead to non-radiative decay from the 5D_3 to the 5D_4 level of a neighbouring ion.^[59] Therefore several different concentrations of **Tb-1** were used in the lipid membranes and in terms of emission intensity, 5 mol% of **Tb-1** with respect to the used lipids is the most suitable condition for these systems.

All vesicles (**LNT**) containing the Tb^{3+} complex exhibit a phosphorescence emission intensity at 488, 545, 584, 620 nm, which corresponds to the electronic transition from the 5D_4 state to 7F_3 , 7F_4 , 7F_5 , 7F_6 states of the Tb^{3+} ions. However, at 25°C, the emission intensity is significantly different for **LNT1** (DSPC lipids, $T_m=55$ °C) and **LNT5** (DOPC lipids, $T_m= -20$ °C), which indicates that the phase transition temperature of the lipids affects the emission intensity (Figure 9).

3.3.2.3 Temperature dependent measurements

The temperature dependent emission intensity and lifetime measurements of the vesicular systems **LNTs** were carried out in HEPES buffer at pH 7.4. All vesicles show a decrease in their emission intensity with increase in temperature and each system shows more than 85% decrease in luminescence intensity around the transition temperature of the constituent lipid used (Figure 10 and 11).

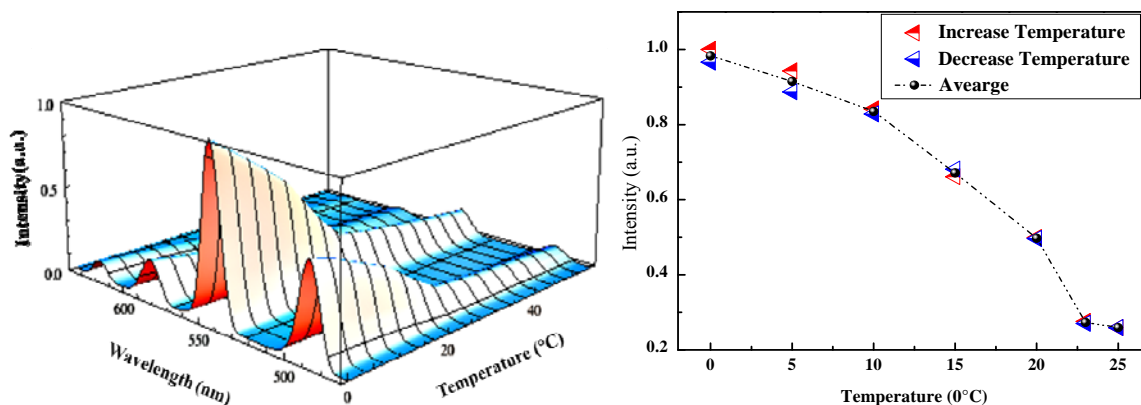


Figure 10: [Left] Temperature dependence of emission intensity measurements for **LNT3** (conc. of Tb(III) = 5×10^{-6} M); [Right] Reversibility of **LNT3** in the measured temperature range

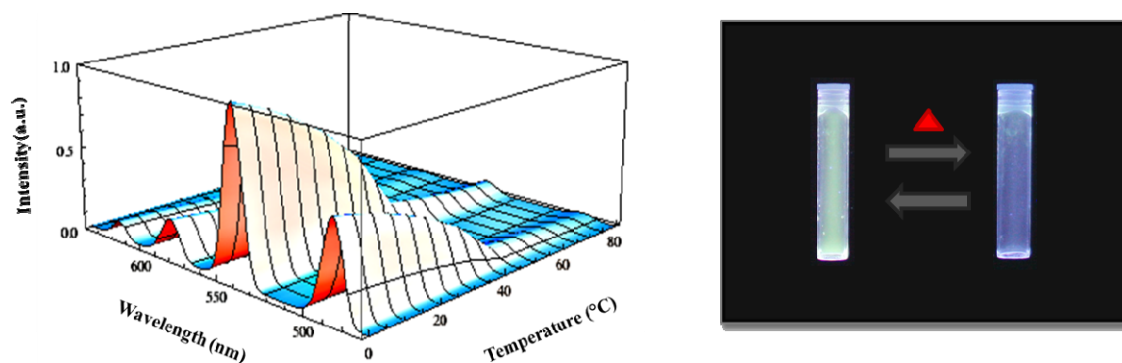


Figure 11: [Left] Temperature dependence of emission intensity measurements for **LNT2** (conc. of Tb(III) = 5×10^{-6} M); [Right] Photograph of change in emission intensity of **LNT2** (conc. 2mM, conc. of Tb(III) = 1×10^{-4} M) with temperature. Phosphorescence was recorded at different temperature by using a UV table ($\lambda_{\text{ex}} = 315$ nm)

The emission changes for the vesicular systems, **LNT1-6**, are reversible within the measured temperature range, as shown in Figure 10 (right) for **LNT3**.

However, the emission intensity based measurements often suffer from concentrations of sensors or drifts of the optoelectronic systems (lamps and detectors),^[51c] whereas decay lifetime based

data are free from these drawbacks and are more reliable. The synthesised luminescent vesicular systems, **LNT**, also show reversible change in decay lifetime with change in temperature. The luminescence decay vs. time curve follows first order exponential decay at every measured temperature (figure 12) and the average lifetime (τ) is determined by equation 1,

$$y = A_1 * \exp(-x/\tau) + y_0 \quad (1)$$

where, y = lifetime at time x ; y_0 = initial lifetime; x = time; $\tau = 1/(\text{decay constant})$, A_1 = pre exponential factor.

The lifetime vs. temperature plot shows that for every system, average lifetime (τ) decreases with increase in temperature and the system shows high sensitivity around the phase transition temperature (T_m) of the constituent lipid (Figure 12). Thus the most sensitive temperature range for these nano systems can be tuned by changing the constituent lipids. Table 1 shows the most sensitive temperature range and sensitivity per °C in that range for each particular system.

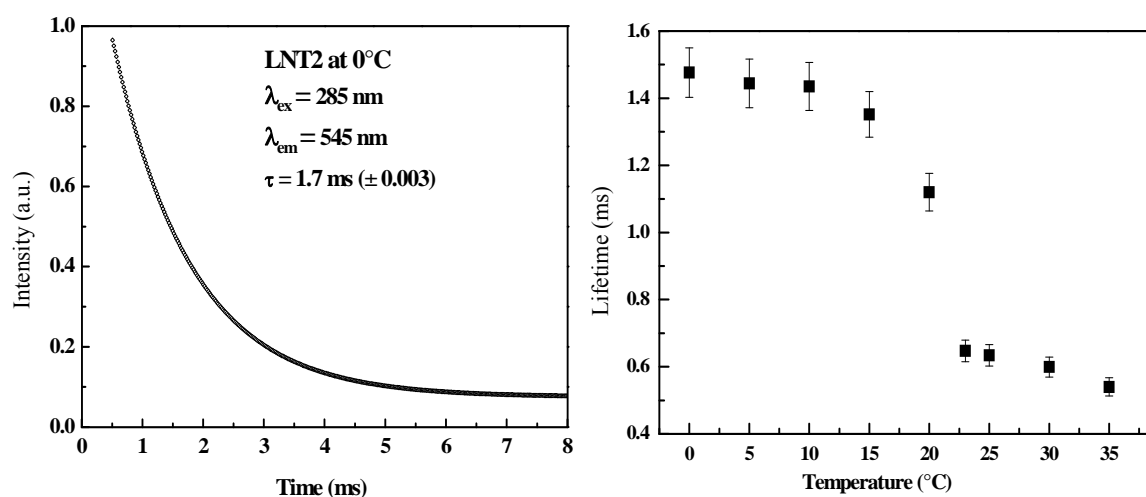


Figure 12: [Left] Luminescence decay vs. Time plot for **LNT2** at 0°C; [Right] Average lifetime (\pm s.d.) (ms) vs. Temperature (°C) plot for **LNT3**

The luminescence intensity and lifetime of lanthanides can be affected by many factors. The overall decay rate constant of the luminescence level can be expressed by the following equation,^[60] with k_r is the radiative rate constant and k_{nr} and $k_{nr}(T)$ are the non-radiative temperature independent and temperature dependent decay rate constants.

$$k = \frac{1}{\tau} = k_r + k_{nr} + k_{nr}(T) \quad (2)^{[60]}$$

The non-radiative transition consists of the vibrational excitation, back energy transfer (BET) to triplet excited state of the sensitizer attached from the 5D_4 state of Tb(III) and the concentration quenching. Temperature-dependence of the decay rate constant or $k_{nr}(T)$ is expected for the vibrational excitation and BET in the nonradiative transition from the 5D_4 level of the terbium(III) ion.^[52a] Decrease in luminescence intensity can be related to both the aforementioned factors, while decrease in luminescence lifetime is dependent only on the energy dissipation from the 5D_4 state of Tb(III). These facts give a rationale for the sensitivity of **LNT** near the transition temperature of the lipid. The constituent phospholipids are in a tightly packed gel phase below the transition temperature (T_m)^[61] and this leads to deactivation of vibrational excitation and hence a longer lifetime of the embedded Tb(III) ion. Near or above the phase transition temperature, the lipid bilayers are more or less in the liquid crystalline phase^[61c] with higher chain mobility of the constituent lipids consequently leading to drastic decrease in the luminescence lifetime by vibrational dissipation of energy from the 5D_4 state of the Tb(III) ion.

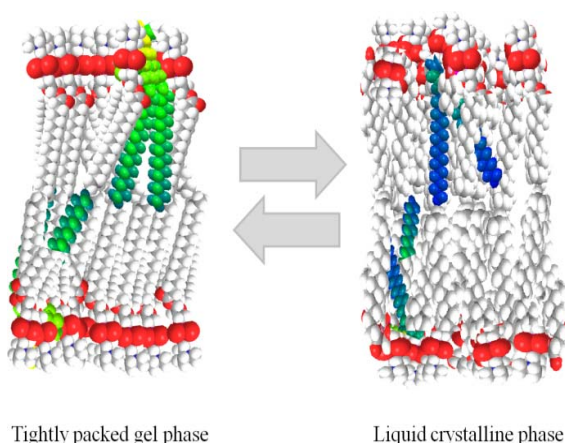


Figure 13: Schematic representation showing differences in gel and liquid crystalline phases in phospholipid bilayers with embedded amphiphilic Tb(III) ion

Above T_m of the corresponding lipids, the nano systems show negligible sensitivity towards increase in temperature.

The fully PEGylated vesicle, **LNT4**, shows reversible change in emission intensity with temperature. However, for a given wavelength, the intensity vs. temperature plot is convex for the non-PEGylated vesicles, while it is concave for the completely PEGylated vesicular system, **LNT4**, (Figure 14). The difference in the nature of the plot can be attributed to increased chain mobility of the PEGylated lipids compared to the non-PEGylated ones in gel, intermediate as well as in the fluid phase as shown by Belsito *et al* using spin-label ESR measurements.^[62]

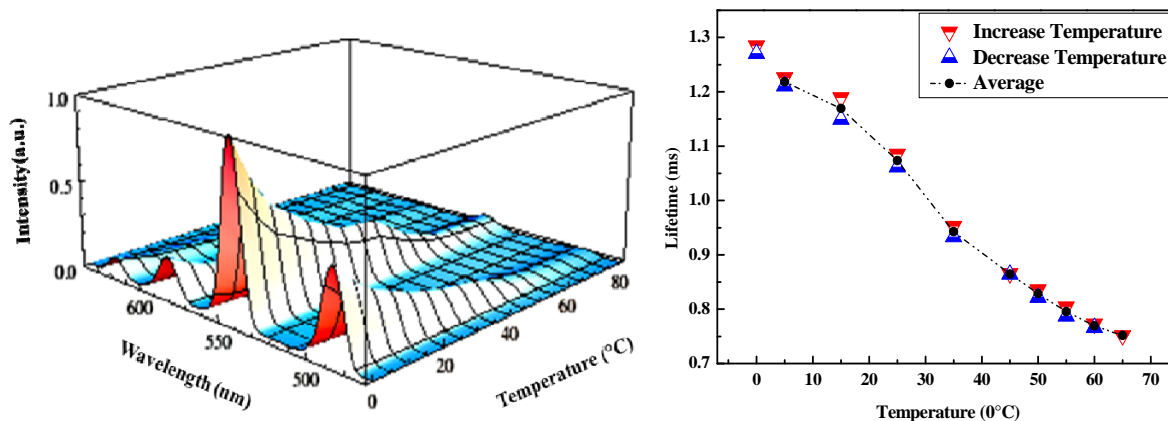


Figure 14: [Left] Temperature dependence of emission intensity measurements for **LNT4** (conc. of Tb(III) = 5×10^{-6} M); [Right] Lifetime reversibility of **LNT4** in the measured temperature range

The temperature dependent luminescence changes of **LNT4** is not affected by the presence of bovine serum albumin (BSA) (Table 1), which indicates potential applications of these kinds of systems in biological medium.

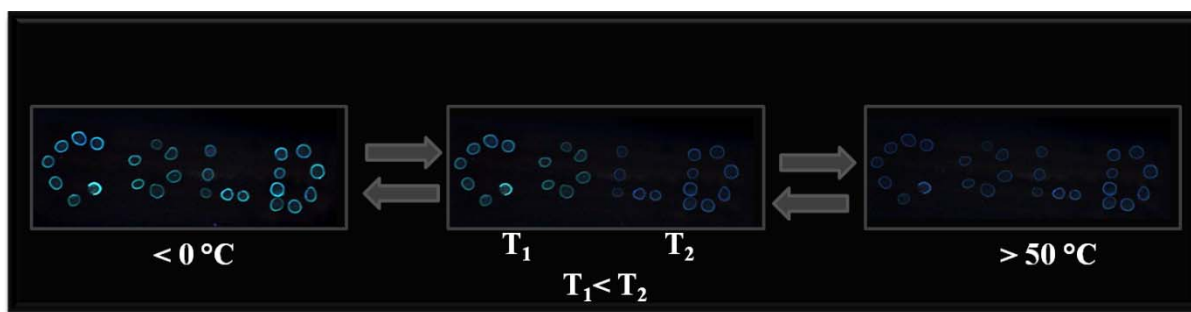


Figure 15: Photographs of the luminescent membranes at different temperature. The letters were written in a glass surface by using a solution of **LNT1** (2mM). The letters were dried by blowing a stream of air. Phosphorescence was recorded at different temperature by using a UV table ($\lambda_{\text{ex}} = 315$ nm).

3.3.3 Concluding remarks

In summary, we have developed a novel approach towards luminescence thermometry by using a self assembly of lipids and amphiphilic Tb(III) complexes. Such systems are useful for sensing and imaging of physiological temperatures by changes in their phosphorescence intensity and lifetime. The most sensitive temperature and sensitivity per $^{\circ}\text{C}$ can be tuned by merely playing with the phase transition temperature of the constituent lipids. As a proof of this principle, we have used lipids with different phase transition temperatures resulting in vesicles with their highest sensitivity in different temperature ranges. Membranes can be processed, e.g. by simple spreading on a glass surface without losing their sensing ability. Since Tb(III) has a very long luminescence lifetime,

interference of background fluorescence arising from proteins or cells can be avoided by delayed readout.

3.3.4 Experimental Section

General methods and material

All reagent-grade chemicals were used without purification unless otherwise specified. Diethylenetriaminepentaacetic dianhydride (DTPAA), tryptamine, $\text{Tb}(\text{CF}_3\text{SO}_3)_3$ were obtained from Aldrich and used as received.

NMR Spectra

NMR spectra were measured with Bruker Avance 600 (1H: 600.1 MHz, 13C: 150.1 MHz, T = 300 K), Bruker Avance 400 (1H: 400.1 MHz, 13C: 100.6 MHz, T = 300 K), Bruker Avance 300 (1H: 300.1 MHz, 13C: 75.5 MHz, T = 300 K). The chemical shifts are reported in δ [ppm] relative to external standards (solvent residual peak). The spectra were analysed by first order, the coupling **S-1** constants are given in Hertz [Hz]. Characterisation of the signals: s = singlet, d = doublet, t = triplet, q = quartet, m = multiplet, br = broad, dd = double doublet. Integration is determined as the relative number of atoms. The solvent used is reported for each spectrum.

Mass Spectra

Mass spectra were obtained with Varian CH-5 (EI), Finnigan MAT 95 (CI; FAB and FD), Finnigan MAT TSQ 7000 (ESI). Xenon serves as the ionisation gas for FAB.

IR Spectra

IR spectra were recorded with a Bio-Rad FTS 2000 MX FT-IR and Bio-Rad FT-IR FTS 155.

Absorption Spectroscopy

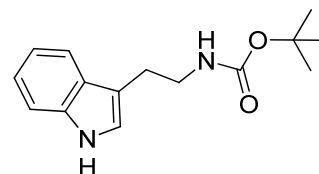
Absorption were recorded on a Varian Cary BIO 50 UV/VIS/NIR Spectrometer with temperature control by use of a 1 cm quartz cuvettes (Hellma) and aqueous buffered solution (HEPES 25 mmol, pH = 7.4).

Emission Spectroscopy

Luminescence intensity and lifetime measurements were performed with aqueous buffered solution (HEPES 25 mmol, pH = 7.4) in 1 cm quartz cuvettes (Hellma) and recorded on a Varian 'Cary Eclipse' fluorescence spectrophotometer with temperature control.

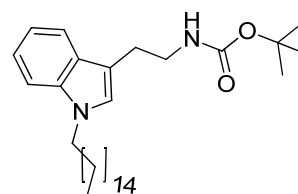
Dynamic light scattering

Photon correlation spectroscopy (PCS) measurements were performed on a Malvern Zetasizer 3000 at 25°C using 1cm disposable polystyrene fluorescence cuvettes (VWR). Three subsequent measurements of 60 s each were performed for each sample. Data analysis was performed using the Malvern PCS software.



Synthesis of compound 1-Boc: To a yellow suspension of tryptamine (1.00 g, 6.24 mmol) in 1, 4-dioxane (5 mL) was added Et₃N (1.80 mL, 12.9 mmol). A solution of (Boc)₂O (1.50 g, 6.87 mmol) in 1,4-dioxane (5 mL) then was added to the reaction mixture. This mixture was stirred for 1 h and the resulting yellow solution was concentrated to dryness under reduced pressure. The crude residue was purified by column chromatography on silica gel (30% ethylacetate in petrolether) to give the desired 1-Boc amine as an amorphous white solid (yield: quantitative).

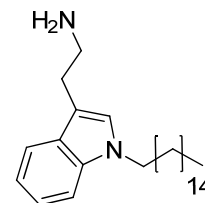
¹H NMR (300 MHz, CDCl₃) = 1.54 (s, 9H), 3.00 (t, 2H), 3.53 (d, 2H), 4.85 (br, s, 1H), 6.97 (s, 1H), 7.15-7.28 (m, 1H), 7.37 (d, 1H), 7.65 (d, 1H), 8.68 (br, 1H) ppm ¹³C NMR (75 MHz, CDCl₃) = 14.29, 21.16, 25.86, 28.57, 41.10, 60.60, 67.12, 111.45, 112.73, 118.80, 119.28, 121.99, 122.37, 127.44, 136.56, 156.33, 171.49 ppm **MS (EI MS)** m/z = 260.31 [M⁺] (Calc. =260.33)



Synthesis of compound 2: To a stirred suspension of NaH (60% dispersion in mineral oil, 0.05g, 2.37mmol) in THF (5mL), was added a solution of **1-Boc** (0.50 g, 1.97mmol) in THF (5mL). After stirring at room temperature for 10min, 1-bromooctadecane (0.76g, 2.37mmol) was added, and stirring was continued for 3h. Water was then added, and the mixture was extracted with ethylacetate. The organic layer was washed with brine, dried over MgSO₄, and concentrated under vacuum. The residue was chromatographed on silica gel, eluting with 10% ethylacetate in petrolether to give **2-Boc** as an amorphous solid (yield: 93%).

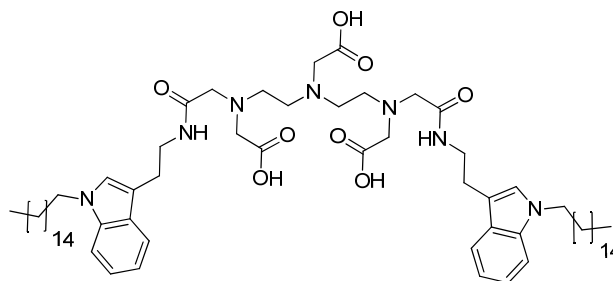
¹H NMR (300 MHz, CDCl₃) = 0.93 (t, 3H), 1.30 (s, 28H), 1.48 (s, 9H), 1.86 (t, 2H), 2.98 (t, 2H), 3.50 (t, 2H), 4.08 (2H), 6.96 (s, 1H), 7.10-7.16(m, 1H), 7.21-7.27 (m, 1H), 7.33 (d, 1H), 7.62(d, 1H) ppm. ¹³C NMR (75 MHz, CDCl₃) = 14.20, 22.77, 25.81, 27.12, 28.25, 28.85, 29.53, 29.57, 32.00, 44.96,

65.84, 109.34, 111.50, 118.73, 121.47, 125.69, 127.93, 136.42, 155.93, 161.00, 177.52 ppm. **MS (EI MS)** $m/z = 512.7 [M^+]$ (Calc. =512.81)



Synthesis of compound 2-H: Compound **2** (0.54g, 1.78mmol) was dissolved in dichloromethane (5ml). Trifluoroacetic acid (2ml 24.9mmol) was added and the solution was stirred for 6h. The solvent was then evaporated of under vacuum pressure. The colourless oil obtained, which is a trifluoroacetate salt was then dissolved in methanol: water mixture (1:1) and passed through basic ion exchange resin. The solvent was removed and the compound **2** was recovered as an amorphous white solid (yield: 95%).

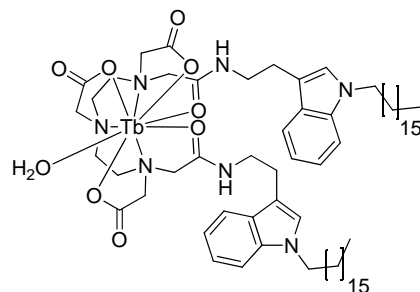
$^1\text{H NMR}$ (300 MHz, CDCl_3) = 0.82 (t, 3H), 1.20 (s, 28H), 1.68 (t, 2H), 2.86-2.96 (m, 4H), 3.96(t, 2H, 6.95-7.05 (m, 3H), 7.20 (d, 1H), 7.48(d, 1H) ppm. $^{13}\text{C NMR}$ (75 MHz, CDCl_3) =14.59, 23.81, 27.59, 28.01, 30.66, 31.34, 33.23, 42.16, 47.19, 110.61, 111.34, 119.87, 122.77, 127.34, 129.21, 138.20 ppm. **MS (EI MS)** $m/z = 412.7 [M^+]$ (Calc. =412.6)



Synthesis of compound 4: Diethylenetriaminepentaacetic dianhydride (**1**) (0.12g, 0.35 mmol) was dissolved in 5 mL of dry DMF. **Compound 2** (0.29 g, 0.69 mmol) was dissolved in 5 mL of dry chloroform; added drop wise to the solution and the mixture was left to stir at 40 °C for 24 h. On cooling to room temperature, a precipitate was formed, which was collected. The white solid was stirred in water at ~ 80 °C for one hour, isolated, stirred in diethyl ether for one hour and isolated. The crude product was recrystallised from 50:50 chloroform:methanol. On cooling a white solid was formed, which was isolated by filtration, washed with diethyl ether and dried under vacuum (yield: 55%).

$^1\text{H NMR}$ (400 MHz, $\text{CD}_3\text{OD}:\text{CDCl}_3= 1:1$) = 0.84 (t, 6H), 1.22 (s, 60H), 1.69 (t, 4H), 2.89-2.99 (m, 12H), 3.33-3.47 (m, 18H), 3.95 (t, 4H), 6.88(s, 2H), 6.99(m, 2H), 7.09(t, 2H), 7.22(d, 2H), 7.52(d, 2H) ppm $^{13}\text{C NMR}$ (100 MHz, $\text{CD}_3\text{OD}:\text{CDCl}_3= 1:1$) =14.49, 23.21, 27.29, 28.01, 30.34, 31.12,

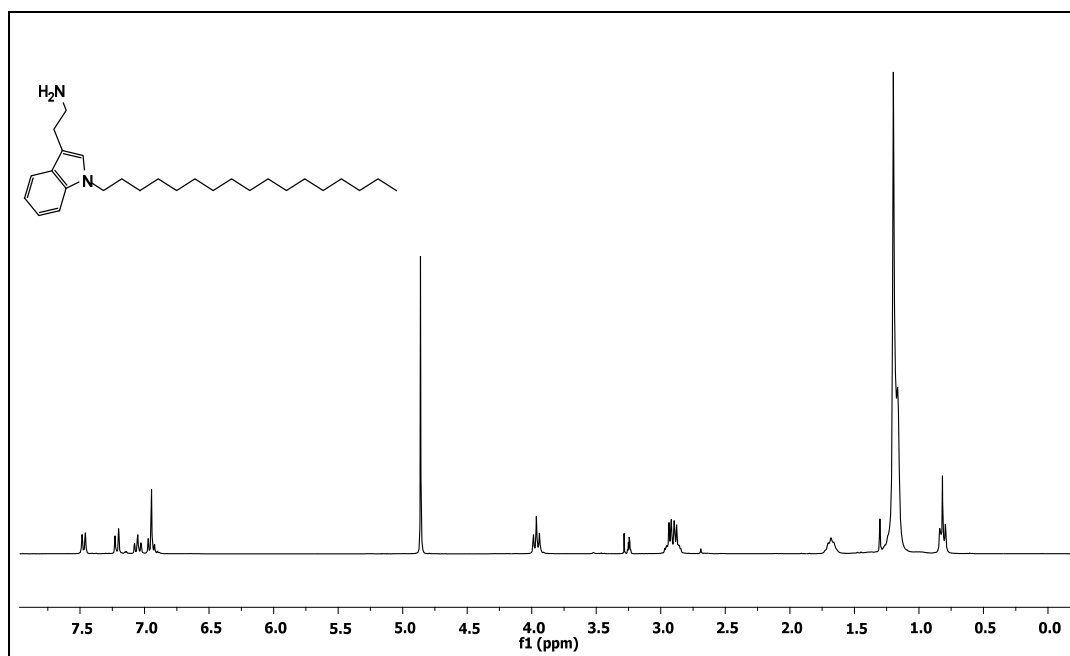
32.98, 42.02, 47.04, 50.10, 53.33, 55.08, 56.72, 58.59, 110.59, 111.34, 119.87, 122.35, 127.04, 129.01, 138.24 ppm **MS (EI MS)** $m/z = 1183.1 [M^+]$ (Calc. = 1182.7) ν_{\max} (KBr disc): 3303 b (OH), 2919 m , 2848 m (CH); 1625 w (C=O); 1468 w , 1373 m , 1236 m , 1098 w



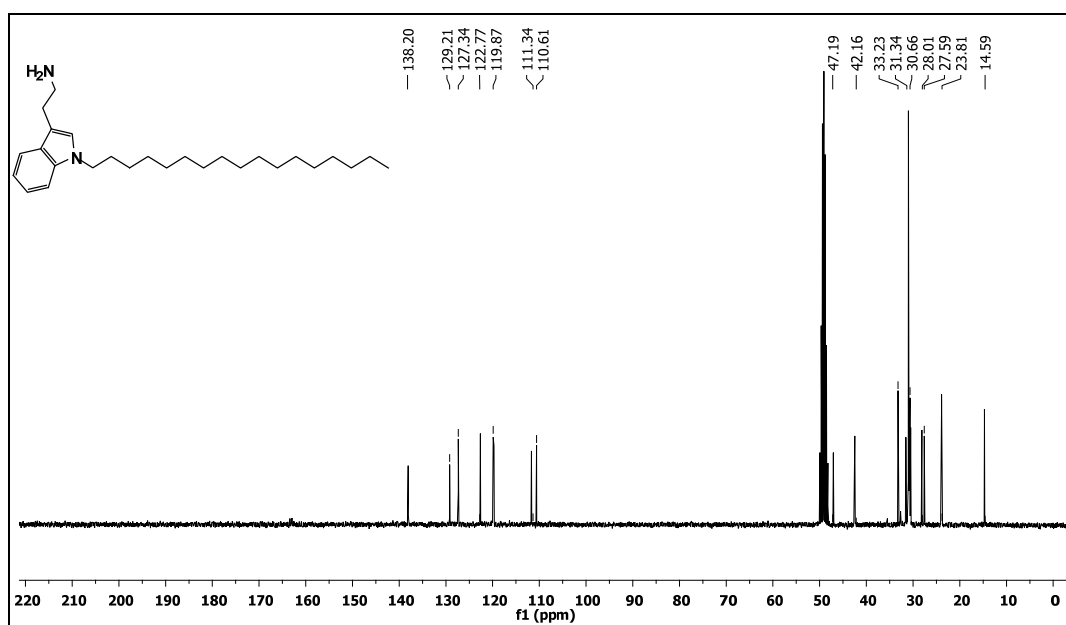
Synthesis of compound Tb-1: Compound **4** (0.1 g, 0.08 mmol) was dissolved in approximately 10 mL of a hot 1:1 CHCl₃/CH₃OH mixture. Tb(CF₃SO₃)₃ (0.05 g, 0.09 mmol), dissolved in 2 mL CH₃OH, was added and the mixture was stirred at 50 °C for 8 hours. The solvent was removed under vacuum and the white solid obtained was washed with water and dried (yield: 98%). **MS (EI MS)** $m/z = 1339.1 [M^+]$ (Calc. = 1340.8)

3.3.5 Supporting Data

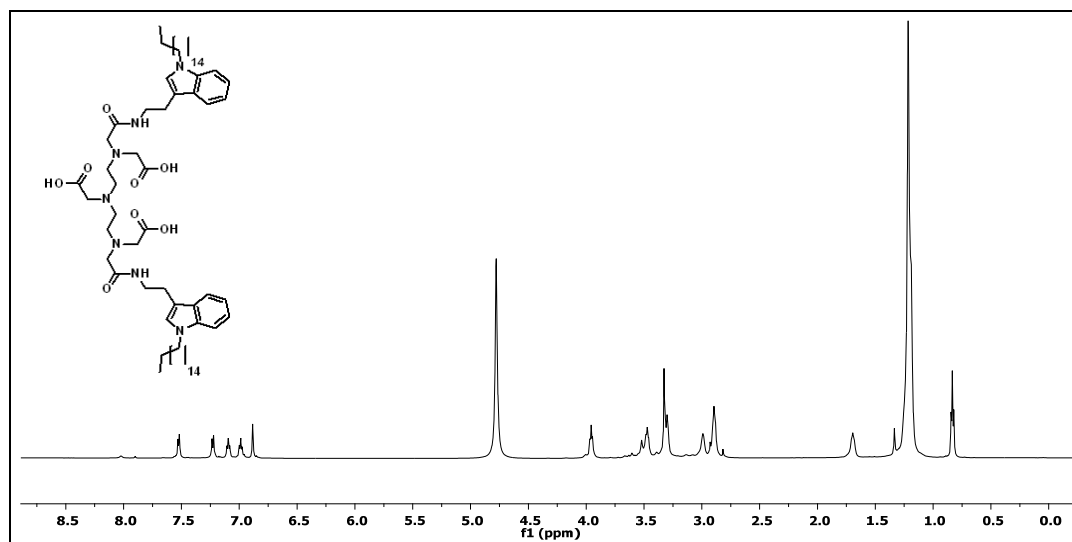
^1H and ^{13}C NMR of the synthesised compounds:



^1H NMR of compound **2** (300 MHz, CDCl_3)



^{13}C NMR of compound **2** (75 MHz, CDCl_3)



^1H NMR of compound **4** (400MHz, $\text{CD}_3\text{OD}:\text{CDCl}_3= 1:1$)

Dynamic light scattering measurements:

	Diam. (nm)	% Intensity	Width (nm)
Z-Average (d.nm): 95,42	Peak 1: 99,04	98,9	32,94
Pdl: 0,212	Peak 2: 5384	1,1	320,2
Intercept: 0,919	Peak 3: 0,000	0,0	0,000
Result quality Good			

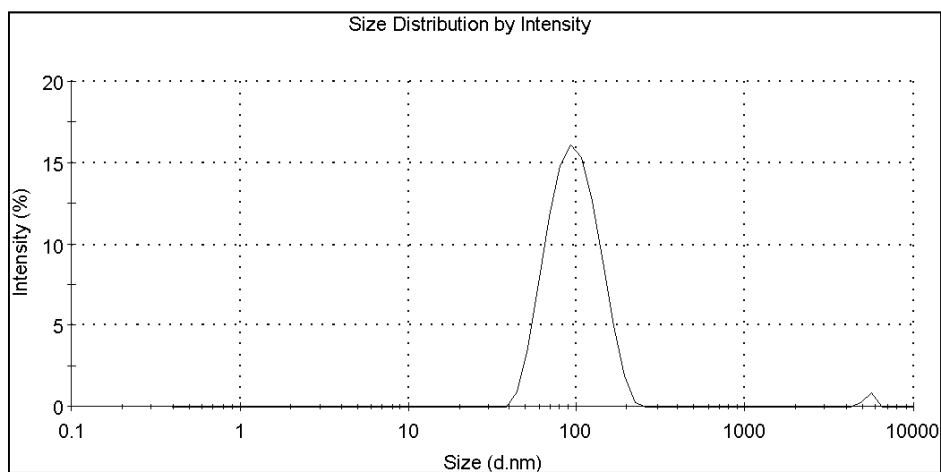


Figure 16: Dynamic light scattering measurements for **LNT3**

	Diam. (nm)	% Intensity	Width (nm)
Z-Average (d.nm): 89,86	Peak 1: 100,6	100,0	35,07
Pdl: 0,096	Peak 2: 0,000	0,0	0,000
Intercept: 0,912	Peak 3: 0,000	0,0	0,000

Result quality Good

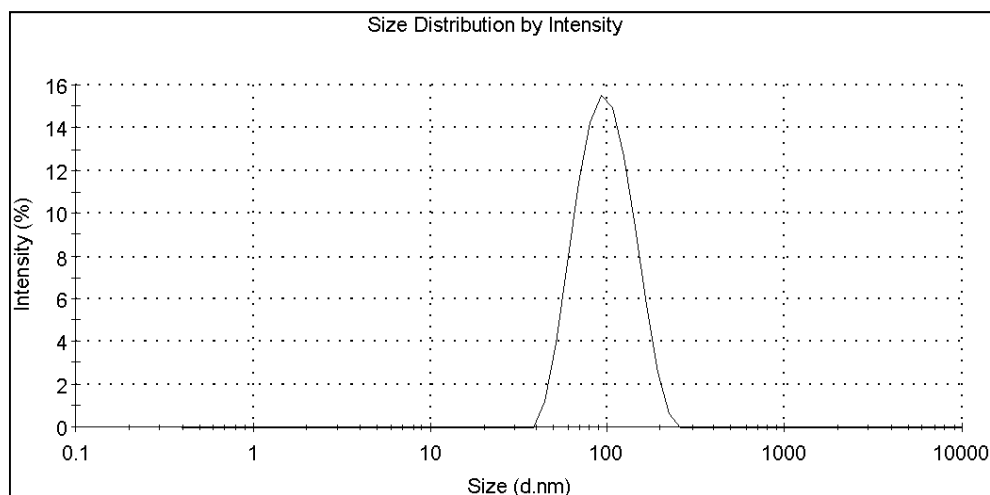


Figure 17: Dynamic light scattering measurements for LNT4

Temperature dependent emission intensity and lifetime measurements:

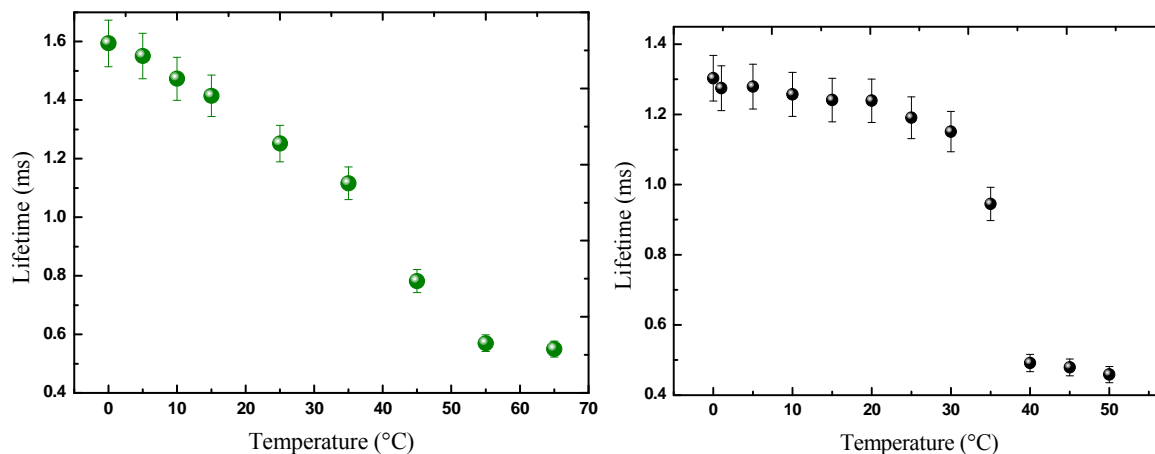


Figure 18: Change in lifetime (\pm s.d.) (ms) with change in temperature [left: LNT4, right: LNT2]

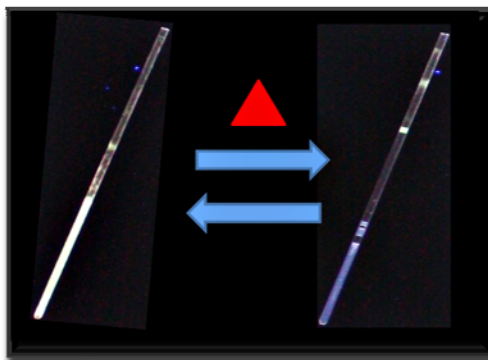


Figure 19: Photograph of change in emission intensity of **LNT1** (conc. 2mM, conc. of Tb(III) = 1×10^{-4} M) with temperature. Phosphorescence was recorded at different temperature by using a UV table ($\lambda_{\text{ex}} = 315$ nm).

3.4 Nano-sized Vesicular Membranes with Amphiphilic Binding Sites and Lanthanide complex with Delayed Luminescence as Reporter Dye

3.4.1 Introduction

Chemosensors, typically small abiotic molecules that can recognize the presence of a suitable analyte, have two main components: a recognition site that binds to the analyte and a readout system that signals the binding event.^[63] Although for the last two decades considerable attention in chemosensors was propelled by potential applications in biology, medicine, analytical chemistry, environmental and material science,^[64] the implementation of sensing probes in functional devices without the loss of sensitivity is still very challenging. For selective recognition of biologically relevant anions, transition metal complexes with vacant coordination sites are widely used as the recognition site and different chromophoric or luminophoric organic dyes are typical signaling units. The signaling unit can either be directly attached to the recognition site by covalent bond formation or it can be non-covalently attached as a part of a kinetically labile receptor complex and can easily be replaced by a suitable analyte. The later phenomenon is the basic principle of indicator displacement assays. Apart from these strategic approaches towards guest binding, which have the drawback of the difficult, laborious synthesis or non reversibility (indicator displacement assays), recently another alternate approach has been reported, which involves non-covalent co-embedding of the amphiphilic guest binding site and the reporter dye in a modulated vesicular membrane.^[31b] This approach has decreased the laborious effort for the synthesis of luminescent chemo sensors enormously and the system has been found to be quite effective for the detection of different biologically relevant analytes. However the usual reporter dyes that have been used for decades for the detection of biologically important analytes are typically organic dyes that have the limitation of having emission life times in nanosecond range, whereas those of biological matrix are typically in the submicrosecond range.^[5a] Hence these are practically not very effective as a part of an analytical tool to be used in complex biological medium. The use of extremely long luminescent lifetime of lanthanide based probes (for europium and terbium complexes life time is in millisecond range) can effectively overcome this limitation. Considering these advantages of lanthanide ions over organic dyes, we planned to use lanthanide based complexes as reporter dyes, which can be non-covalently co-embedded with analyte binding sites in nano-sized vesicular membranes.

3.4.2 Results and Discussions

3.4.2.1 Anion recognition site and reporter dye

The molecules that are used for the current studies are shown in Figure 1.

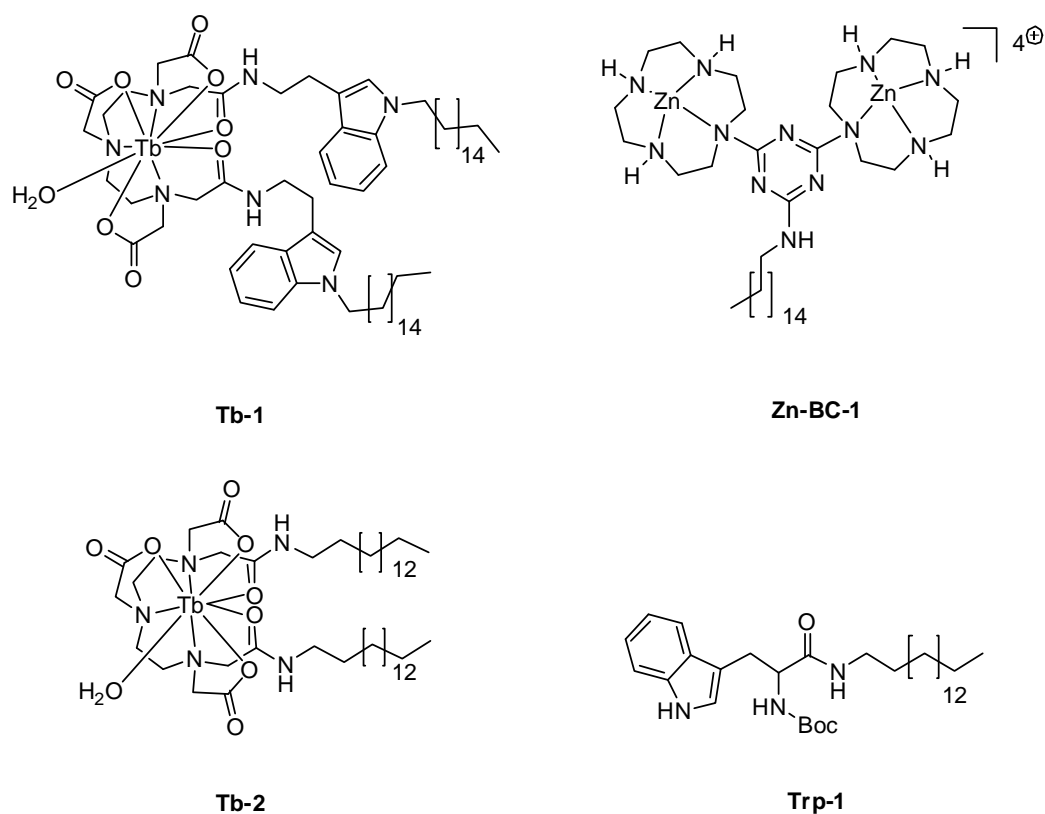


Figure 20: Molecules embedded in the vesicular membrane for anion recognition

The amphiphilic Zn(II)-bis cyclen complex (**Zn-BC-1**) was used as the guest recognition site. The Tb(III) complexes (**Tb-1**, **Tb-2**) were used as reporter dyes. However, as mentioned in part1 of this chapter (Chapter 3, Pat 1), like other lanthanides, Tb(III) depend on sensitizer or antenna molecules to show luminescence. Hence the tryptophan based modified amphiphile (**Trp-1**) was also incorporated into the vesicular membrane as antenna for **Tb-2**.

Synthesis of **Tb-1** is reported in Part1 of this chapter. The guest binding site **Zn-BC-1** and the reporter molecule **Tb-2** along with antenna **Trp-1** were synthesized following previously reported procedures.^[3a, 65]

3.4.2.2 Vesicle Preparation and Characterization of vesicle dispersions

The liposomes with embedded Tb(III) complex and sensitizer were prepared following the previously reported film-hydration method.^[55] The multilamellar vesicles were extruded through definite filters to get unilamellar vesicles of 90-100 (± 5) nm in size.

The modulated vesicular receptors (**LV-1**, **LV-2**, and **LV-3**) with phospholipid bilayer-embedded receptor and lanthanide complex as reporter dye were prepared following our previously reported procedure.

These are prepared from a mixture of commercially available synthetic phospholipid 1,2-distearoyl-sn-glycero-3-phosphocholine (DSPC), DSPC-PEG350, amphiphilic Zn(II)-cyclen complex (**Zn-BC-1**), and lanthanide complex (**Tb-1**) by the well-established film-hydration method.^[55] The resulting multilamellar vesicles (MLVs) were homogenized by extrusion to yield small unilamellar vesicles (SUVs) of a defined size of 80–100 nm.

The particle size, particle number and sample dispersity of the prepared vesicle dispersions were determined by dynamic light scattering (DLS) and the average hydrodynamic diameter of the functionalized vesicles was found to range from 80 to 90(±5) nm (Table 2). Generally, homogenized SUV dispersions are assumed to be free of impurities and thus no further purification is required. All prepared vesicle dispersions were stored as buffered aqueous solutions at 6°C and used within 2 weeks

3.4.2.3 Enhancement of lanthanide luminescence by self assembly

It is reported that lanthanide complexes can be sensitized by intermolecular energy transfer by a non-covalently bound sensitizer co-embedded in a micellar medium^[3a] or gel matrix.^[3b] Therefore the synthesized lanthanide complex **Tb-2** along with antenna **Trp-1** were incorporated into liposomes to check the energy transfer in different liposomal surfaces. Based on phase transition temperatures (T_m), we have chosen DSPC ($T_m = 55^\circ\text{C}$) and DOPC (-20°C) as phospholipids for two different liposomal surface. For similar concentrations of Tb(III) ion(**Tb-2**) and sensitizer (**Trp-1**) we could observe two drastically different emission maxima in these two different liposomal surface. Again from the Part 1 of this chapter, we know that the emission intensity observed for **Tb-1** with covalently attached sensitizer molecule in DSPC and DOPC lipids are also significantly different. However the emission maxima for **Tb-1** embedded in DOPC lipid based liposome is not comparable with that for **Tb-2** and **Trp-1** co-embedded in DOPC lipid based liposome. Since the sensitized emission of the lanthanide complex depends on the distance between the metal cation and the sensitizer,^[5a] the comparisons of the two different DOPC lipids based liposomes with **Tb-1** and **Tb-2** suggest that the packing of the complex molecules in DOPC liposomes at room temperature with very low phase transition temperature (-20°C) are similar to the solution phase.

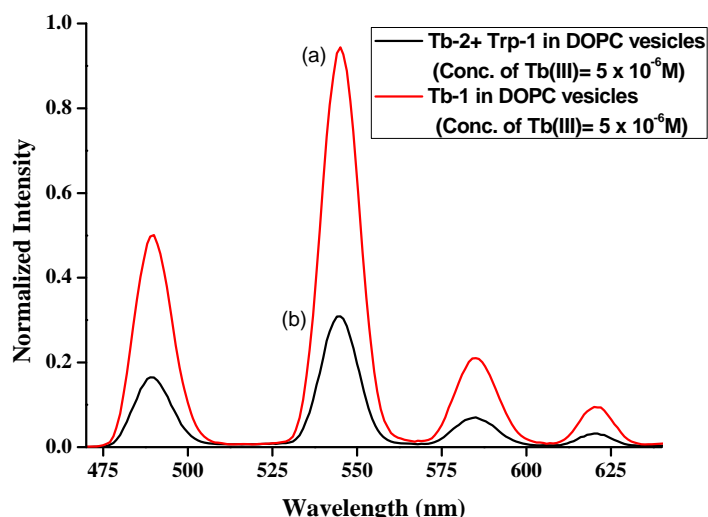


Figure 21: Emission spectra of (a) **Tb-1** and (b) **Tb-2** with **Trp-1** in DOPC lipid based liposomes

3.4.2.4 Attempts to use lanthanide based complex as reporter dye: Experimental observations

The synthesized lanthanide complex (**Tb-1**) was co-embedded as reporter dye with 1, 4, 7, 10-tetraazacyclododecane (cyclen)–zinc (II) complex (**Zn-BC-1**) as binding site in DSPC+DSPC-PEG350 vesicle. Upon excitation at 285nm the vesicle **LV-1** with phospholipid bilayer-embedded **Zn-BC-1** as receptor and **Tb-1** as reporter dye exhibit strong phosphorescence emission with four emission maxima at 490, 545, 585 and 620nm. These can be assigned to respective transitions from 5D_4 excited-state to the ground state 7F_J ($J = 3, 4, 5, 6$). The vesicular solution was titrated with oxoanions such as PPI and O-phospho-L-serine. In the presence of increasing amounts of phosphate anions, such as pyrophosphate (PPI) or phosphoserine (pSer), this emission intensity was decreased.

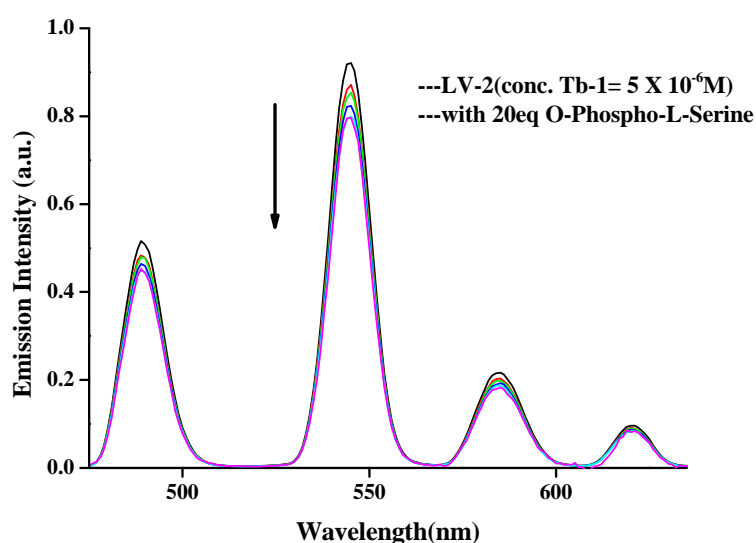


Figure 22: Change in emission intensity of **LV-2** with increasing concentration of O-phospho-L-Serine

Table2: Molar composition and size of the synthesized vesicles

Vesicle	Molar composition (+analyte)	Size(nm)
LV-1	Tb-1/DSPC/DSPC-PEG350/Zn-BC-1 1: 11.2: 8.8: 1	89 ± 5
LV-1+ BSA+ p-Ser	Tb-1/DSPC/DSPC-PEG350/Zn-BC-1 +BSA+p-Ser 1: 11.2: 8.8: 1+ 1eq BSA+2eq p-Ser	-----
LV-2	Tb-1/DSPC/DSPC-PEG350 1: 11.7: 9.3	92 ± 5
LV-2+ BSA	Tb-1/DSPC/DSPC-PEG350+BSA 1: 11.7: 9.3+ 2eq BSA	95 ± 5
LV-2+ α-Casein	Tb-1/DSPC/DSPC-PEG350+BSA 1: 11.7: 9.3+ 2eq α-Casein	117 ± 5
LV-2+ α-Casein (70% dephosphorylated)	Tb-1/DSPC/DSPC-PEG350+BSA 1: 11.7: 9.3+ 2eq α-Casein (70% dephosphorylated)	118± 5
LV-3	Tb-2/DSPC/Trp-1/Zn-BC-1 3:43:1:3	90± 5
LV-4	Tb-2/DSPC/Trp-1 3:46:1	95± 5

Similarly lanthanide complex **Tb-2** along with **Trp-1** and **Zn-BC-1** were incorporated into DSPC vesicles (**LV-3**). The vesicular solution was titrated with PPI. With increasing amount of PPI, the emission intensity corresponding to Tb(III) decreases and we could observe up to 25% decrease in intensity upon addition of 6eq of PPI.

The change in emission intensity of **Tb-1** upon phosphate binding to **Zn-BC-1** is also observed in presence of BSA. As a control experiment **Tb-1** was embedded in a vesicular membrane, **LV-2**, without any co-embedded receptor binding site and analysed for phosphate binding. With the

increasing amount of phosphate anions such as phosphoserin (pSer) there is some change in emission intensity. A similar control experiment was done with **Tb-2**. **Tb-2** with **Trp-1** were embedded into DSPC vesicles without **Zn-BC-1** to check if the Tb(III) complex has some interaction with the added analyte (**LV-4**). With increase in concentration of PPI (upto 6eq) we could observe some change (10%) in emission intensity (figure 23), which shows that the neutral Tb complex interacts with the oxo-anion.

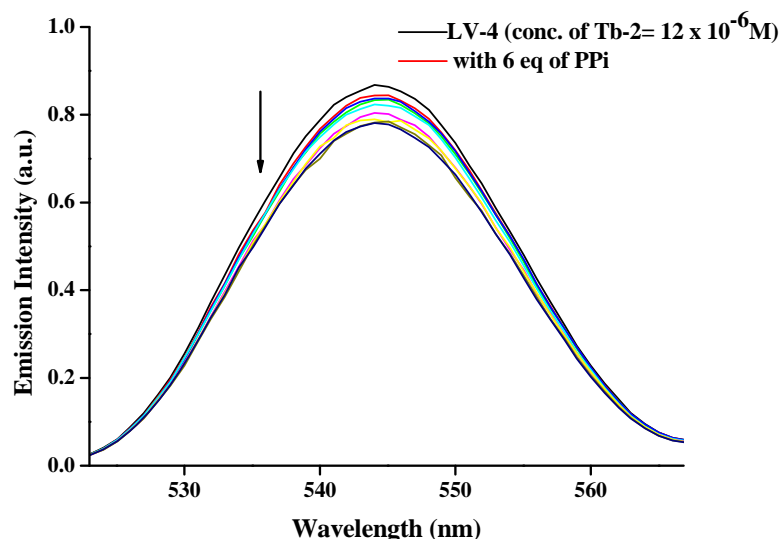


Figure 23: Change in emission intensity of **LV-4** with increasing concentration of PPI. (Emission change at only one wavelength, 545nm, is shown here)

Again, the prepared **Tb-1** embedded vesicular system, **LV-2** was found to be not responsive to an increasing amount of added BSA. However, with α -S1-Casein and dephosphorylated α -S1-Casein the results are found to inconclusive. In both cases with increasing amount of casein, there is a change in the terbium emission intensity.

3.4.3 Concluding remarks

In conclusions, we have synthesized neutral Tb(III) based complexes to explore applications of these complexes as reporter dye co-embedded with amphiphilic binding sites in a self-assembled vesicular membrane for the recognition of biologically relevant anions. Although in a control experiment, we could observe minor interactions of these neutral complexes with the added oxo-anions, co-embed complexes in vesicular membranes with amphiphilic Zn(II) complex as receptor molecule showed decrease in luminescence with increasing amount of oxo-anions as added analytes. These observations suggest a potential application of the complexes in the recognition of analytes. Future research includes modifying the structure of the Tb(III) complex to minimize its interaction with analytes.

3.5 References

- [1] J. E. Huheey, E. A. Keiter, R. L. Keiter *Inorganic Chemistry: Principles of Structure and Reactivity*, Fourth ed., HarperCollins College Publishers, **1993**.
- [2] F. A. Cotton, G. Wilkinson *Advanced Inorganic Chemistry*, John Wiley and Sons, New York, **1988**.
- [3] a) C. L. Davies, N. G. Housden, A.-K. Duhme-Klair *Angew. Chem. Int. Ed.* **2008**, *47*, 8856; b) S. Bhowmik, S. Banerjee, U. Maitra *Chem. Commun.* **2010**, 46.
- [4] A. Meijerink, R. T. Wegh *Materials Science Forum* **1999**, 315-317, 11.
- [5] a) A. Thibon, V. C. Pierre *Anal Bioanal Chem* **2009**, 394, 107; b) C. M. G. dos Santos, A. J. Harte, S. J. Quinn, T. Gunnlaugsson *Coord. Chem. Rev.* **2008**, 252, 2512.
- [6] <http://shop.perkinelmer.com/applicationsummary/applications/TRF-DELFLIA.htm>.
- [7] a) J. Coates, P. G. Sammes, R. M. West *J. Chem. Soc., Perkin Trans* **1996**, 2, 1275; b) E. F. Gudgin Dickson, A. Pollak, E. P. Diamandis *J. Photochem. Photobiol. B: Biol* **1995**, 27, 3.
- [8] a) A. D. Bangham, R. W. Horne *Nature* **1962**, 196, 952; b) R. W. Horne, A. D. Bangham, V. P. Whittaker *Nature* **1963**, 200, 1340; c) A. D. Bangham, R. W. Horne *J. Mol. Biol.* **1964**, 8, 660.
- [9] M. L. Immordino, F. Dosio, L. Cattel *Int. J. Nanomed.* **2006**, 1, 297.
- [10] W. R. Algar, D. E. Prasuhn, M. H. Stewart, T. L. Jennings, J. B. Blanco-Canosa, P. E. Dawson, I. L. Medintz *Bioconjugate Chem.* **2011**, 22, 825.
- [11] U. S. Huth, R. Schubert, R. Peschka-Süss *J. Controlled Release* **2006**, 110, 490.
- [12] D. Bitounis, R. Fanciullino, A. Iliadis, J. Ciccolini *ISRN Pharmaceutics* **2012**, 2012.
- [13] a) G. Mikhaylov, U. Mikac, A. A. Magaeva, V. I. Itin, E. P. Naiden, I. Psakhye, L. Babes, T. Reinheckel, C. Peters, R. Zeiser, M. Bogyo, V. Turk, S. G. Psakhye, B. Turk, O. Vasiljeva *Nat Nano* **2011**, 6, 594; b) O. P. Medina, Y. Zhu, K. Kairemo *Curr. Pharm. Des.* **2004**, 10(24), 2981; c) J. Huwyler, J. Drewe, S. Krähenbühl *Int. J. Nanomedicine* **2008**, 3(1), 21; d) M. Danquah, T. Fujiwara, R. I. Mahato *Biomaterials* **2010**, 31 (8), 2358.
- [14] a) A. S. Narang, L. Thoma, D. D. Miller, R. I. Mahato *Bioconjug. Chem.* **2005**, 16 (1), 156; b) L. Huang, S. Li *Nat. Biotechnol.* **1997**, 15, 620; c) N. Zhu, D. Liggitt, Y. Liu, R. Debs *Science* **1993**, 261, 209; d) A. R. Thierry *Proc. Natl. Acad. Sci.* **1995**, 92, 9742; e) D. D. Lasic *Liposomes in gene delivery*, CRC Press, **1997**.
- [15] a) G. Sessa, G. Weissmann *J Lipid Res.* **1968**, 9(3), 310; b) Y.-H. Chan, B. S.G. *Curr. Opin. Chem. Biol.* **2007**, 11, 581; c) D. Papahadjopoulos, H. K. Kimelberg *Prog. Surf. Sci.* **1974**, 4, 141.
- [16] E. Terreno, D. Delli Castelli, C. Cabella, W. Dastrù, A. Sanino, J. Stancanello, L. Tei, S. Aime *Chem. Biodivers.* **2008**, 5, 1901.

- [17] a)H. Harashima, K. Sakata, H. Kiwada *Pharm Res* **1993**, *10*, 606; b)A. Chonn, S. Semple, P. R. Cullis *J Biol Chem* **1992**, *267*, 18759; c)C. D. Oja, S. C. Semple, A. Chonn, P. R. Cullis *Biochim Biophys Acta* **1996**, *1281*, 31.
- [18] a)G. Blume, G. Cevc, M. D. J. A. Crommelin, I. A. J. M. Bakker-Woudenberg, C. Kluff, G. Storm *Biochim. Biophys. Acta.* **1993**, *1149*, 180; b)A. L. Klibanov, K. Maruyama, A. M. Beckerleg, V. P. Torchilin, L. Huang *Biochim. Biophys. Acta.* **1991**, *1062*, 142.
- [19] M. Yamazaki, M. Ohshika, N. Kashiwagi, T. Asano *Biophys. Chem.* **1992**, *43*, 29.
- [20] K. Arnold, L. Pratsch, K. Gawrisch *Biochim. Biophys. Acta- Biomembranes* **1983**, *728*, 121.
- [21] R. Bartucci, G. Montesano, L. Sportelli *Colloids and Surfaces A: Physicochemical and Engineering Aspects* **1996**, *115*, 63.
- [22] C. M. Paleos, Z. Sideratou, D. Tsiourvas *ChemBioChem* **2001**, *2*, 305.
- [23] J. T. P. Derksen, G. L. Scherphof *Biochim. Biophys. Acta* **1985**, *814*, 151.
- [24] V. P. Torchilin *Nat Rev Drug Discov* **2005**, *4*, 145.
- [25] V. P. Torchilin, A. L. Klibanov, in *Phospholipid Handbook* (Ed.: G. Cevc), Marcel Dekker, New York, **1993**, pp. 293.
- [26] G. Hamasaka, T. Muto, Y. Uozumi *Angew. Chem.* **2011**, *123*, 4978
- [27] K. P. McNamara, N. Rosenzweig, Z. Rosenzweig *Microchim. Acta* **1999**, *131*, 57.
- [28] M. Onda, K. Yoshihara, H. Koyano, K. Ariga, T. Kunitake *J. Am. Chem. Soc.* **1996**, *118*.
- [29] a)M. S. Goedheijt, B. E. Hanson, J. N. H. Reek, P. C. J. Kamer, P. W. N. M. v. Leeuwen *J. Am. Chem. Soc.* **2000**, *122* 1650 ; b)M. Ferreira, H. Bricout, N. Azaroual, C. Gaillard, D. Landy, S. Tilloy, E. Monflier *Adv. Synth. Catal.* **2010**, *352* 1193
- [30] a)N. Garelli, P. Vierling *Biochim. Biophys. Acta.* **1992**, *1127*, 41; b)T. Parac-Vogt, K. Kimpe, S. Laurent, C. Piérart, L. Elst, R. Muller, K. Binnemans *Eur Biophys J* **2006**, *35*, 136.
- [31] a)B. Gruber, E. Kataev, J. Aschenbrenner, S. Stadlbauer, B. König *J. Am. Chem. Soc.* **2011**, *133*, 20704; b)B. Gruber, S. Stadlbauer, A. Späth, S. Weiss, M. Kalinina, B. König *Angew. Chem. Int. Ed.* **2010**, *49*, 7125.
- [32] B. C. Roy, M. A. Fazal, A. Arruda, S. Mallik, A. D. Campiglia *Org. Lett.* **2000**, *2*, 3067.
- [33] a)E. Terreno, C. Boffa, V. Menchise, F. Fedeli, C. Carrera, D. D. Castelli, G. Digilio, S. Aime *Chem. Commun.* **2011**, *47*; b)D. D. Castelli, E. Gianolio, S. G. Crich, E. Terreno, S. Aime *Coord. Chem. Rev.* **2008** *252*, 2424; c)E. Terreno, A. Barge, L. Beltrami, G. Cravotto, D. D. Castelli, F. Fedeli, B. Jevasingh, S. Aime *Chem. Commun.* **2008**.
- [34] a)S. Aime, D. Delli Castelli, E. Terreno *Angew. Chem.* **2005**, *117*, 5649; b)E. Terreno, D. Delli Castelli, C. Cabella, W. Dastrù, A. Sanino, J. Stancanello, L. Tei, S. Aime *Chem. Biodiversity* **2008**, *5*, 1901; c)S. Aime, D. D. Castelli, S. G. Crich, E. Gianolio, E. Terreno *Acc. Chem. Res.* **2009**, *42*, 822.

- [35] I. Bertini, F. Bianchini, L. Calorini, S. Colagrande, M. Fragrai, A. Franchi, O. Gallo, C. Gavazzi, C. Luchinat *Magn. Res. Med.* **2004**, 52
- [36] D. A. Sipkins, D. A. Cheresch, M. R. Kazemi, L. M. Nevin, M. D. Bednarski, K. C. Li *Nat. Med.* **1998**, 4 623.
- [37] W. J. M. Mulder, K. Douma, G. A. Koning, M. A. v. Zandvoort, E. Lutgens, M. J. Daemen, K. Nicolay, G. J. Strijkers *Magn. Reson. Med.* **2006** 55.
- [38] V. S. Trubetskoy, J. A. Cannillo, A. Milshtein, G. L. Wolf, V. P. Torchilin *Magn. Reson. Imaging* **1995**, 13
- [39] D. A. Sipkins, K. Gijbels, F. D. Tropper, M. Bednarski, K. C. Li, L. Steinman *J. Neuroimmunol.* **2000**, 104
- [40] W. J. Chu, T. Simor, G. A. Elgavish *NMR Biomed.* **1997**, 10
- [41] a)A. C. L. Opina, K. B. Ghaghada, P. Zhao, G. Kiefer, A. Annapragada, A. D. Sherry *PLoS ONE* **2011**, 6, e27370; b)D. Burdinski, J. A. Pikkemaat, M. Emrullahoglu, F. Costantini, W. Verboom, S. Langereis, H. Gröll, J. Huskens *Angew. Chem. Int. Ed.* **2010**, 49, 2227.
- [42] A. I. Elegbede, M. K. Haldar, S. Manokaran, S. Mallik, D. K. Srivastava *Chem. Commun.* **2007**.
- [43] N. Mignet, D. Scherman *Methods Mol Biol.* **2010**, 606, 509.
- [44] a)R. E. Bentley *Temperature and Humidity Measurement*, Springer, Singapore, **1998**;
b)<http://www.temperatures.com>.
- [45] M. Mitsuishi, S. Kikuchi, T. Miyashita, Y. Amao *J. Mater. Chem.* **2003**, 13, 2875.
- [46] E. F. J. Ring *Infrared Phys. Technol* **2007**, 49, 297.
- [47] S. M. Borisov, O. S. Wolfbeis *Anal. Chem.* **2006**, 78, 5094.
- [48] R. Schorer, E. Friess, K. Eberl, G. Abstreiter *Phys. Rev. B* **1991**, 44, 1772.
- [49] S. Uchiyama, A. Prasanna de Silva, K. Iwai *J. Chem. Educ.* **2006**, 83, 720.
- [50] G. E. Khalil, K. Lau, G. D. Phelan, B. Carlson, M. Gouterman, J. B. Callis, L. R. Dalton *Rev. Sci. Instrum.* **2004**, 75, 192.
- [51] a)H. Lam, G. Rao, J. Loureiro, L. Tolosa *Talanta* **2011**, 84, 65; b)Y. Ohishi, S. Takahashi *Appl. Opt.* **1986**, 25, 720; c)H. Peng, M. I. J. Stich, J. Yu, L. Sun, L. H. Fischer, O. S. Wolfbeis *Adv. Mater.* **2010**, 22, 716; d)Y. Dwivedi, S. B. Rai *Sensors and Actuators A: Physical* **2010**, 163, 37; e)H. Sakaue, C.-Y. Huang, J. P. Sullivan *Sensors and Actuators B: Chemical* **2011**, 155, 372.
- [52] a)S. Katagiri, Y. Tsukahara, Y. Hasegawa, Y. Wada *Bull. Chem. Soc. Jpn.* **2007**, 80, 1492;
b)L.-N. Sun, J. Yu, H. Peng, J. Z. Zhang, L.-Y. Shi, O. S. Wolfbeis *J. Phys. Chem. C* **2010**, 114, 12642.

- [53] a)M. D. Chambers, D. R. Clarke *Surf. Coat. Technol.* **2007**, *202*, 688; b)D. R. Clarke, M. M. Gentleman *Surf. Coat. Technol.* **2007**, *202*, 681.
- [54] D. L. Dexter *J. Chem. Phys.* **1953**, *21*, 836.
- [55] J. Lasch, V. Weissig, M. Brandl in *Liposomes*, ed. V. Torchilin and V. Weissig, 2nd ed., Oxford University Press, **2003**.
- [56] <http://avantilipids.com>.
- [57] G. Boheim, W. Hanke, F. J. Barrantes, H. Eiblo, B. Sakmann, G. Fels, A. Maelicke *Proc. Natl Acad. Sci.* **1981**, *78*, 3586.
- [58] O. D. Velev *Adv. Biophys.* **1997**, *34*, 139.
- [59] a)D. de Graaf, S. J. Stelwagen, H. T. Hintzen, G. de With *J. Non-Cryst. Solids* **2003**, *325*, 29; b)J. Hölsä, M. Leskelä, L. Niinistö *Mater. Res. Bull.* **1979**, *14*, 1403.
- [60] N. Sabbatini, M. Guardigli, J.-M. Lehn *Coord. Chem. Rev.* **1993**, *123*, 201.
- [61] a)J. H. Crowe, A. E. Oliver, F. A. Hoekstra, L. M. Crowe *Cryobiology* **1997**, *35*, 20; b)W. F. Wolkers, H. Oldenhof, B. Glasmacher *Cryobiology* **2010**, *61*, 108; c)M. Caffrey, J. Hogan *Chem. Phys. Lipids* **1992**, *61*, 1.
- [62] S. Belsito, R. Bartucci, G. Montesano, D. Marsh, L. Sportelli *Biophys. J.* **2000**, *78*, 1420.
- [63] *Fluorescent Chemosensors for Ion and Molecule Recognition*, Vol. 538, American Chemical Society, **1993**.
- [64] R. Ziessel *J. Inclusion Phenom. Macrocyclic Chem.* **1999**, *35*, 369.
- [65] D. S. Turygin, M. Subat, O. A. Raitman, V. V. Arslanov, B. König, M. A. Kalinina *Angew. Chem. Int. Ed.* **2006**, *45*, 5340.

Summary

Chapter 1 of this thesis deals with synthesis of a series of water soluble bis- and tetrakis-Zn(II)-cyclen complexes with rigid structures and their applications in recognition of biologically relevant analytes. Boc-protected 6-chloro-1, 3, 5-triazine-bis cyclen was coupled to several aryl and alkyl moieties by using Suzuki cross coupling in moderate to high yields and subsequently converted into the corresponding bis- or tetrakis-Zn(II)-cyclen complexes. Some of the arene substituted modified bis- and tetra-Zn(II)-cyclen complexes were luminescent and those were studied by absorption and luminescence spectroscopy for their response to phosphate anions at physiological conditions. Also, tetra-Zn(II)-cyclen complexes were found to have significant affinity to genetically encodable oligo-aspartate and glutamate sequences (D₄- and E₄-tag). The rigid structures of the compounds enhance the electronic coupling between the metal complex binding site and the reporter dye leading an increased anion binding response in homogeneous aqueous solution.

Chapter 2 is a report of synthesis and potential applications of rigid amphiphilic molecular receptors, bioconjugates and radiopharmaceuticals based on metal-cyclen complexes via click chemistry. Using bioorthogonal click reaction, we have synthesized biotinylated Zn(II)-bis-cyclen and showed its promising application in activity based proteomics. Cholesterol and long alkyl chain conjugated modified Zn(II)-cyclen complexes were synthesized for a template guided cooperative self-assembly of nucleotides at interfaces fabricated by combination of self-assembled monolayer technique (SAM) and Langmuir Blodgett technique (LB). These complexes can act as binding sites at interfaces prepared by a combination of SAM and LB film approaches or in vesicular surfaces. Investigations of the binding properties of these new amphiphilic complex embedded surfaces are in progress.

Chapter 3 involves design, synthesis and applications of amphiphilic lanthanide complexes embedded in liposomal surface. We have synthesized amphiphilic Tb(III) complex and embedded into liposomal surface. This phosphorescent nanosystem has a potential application as a reporter for change in physiological temperature. We have also attempted to use lanthanide based amphiphilic complexes as reporter dyes non-covalently co-embedded with analyte binding sites in nano-sized vesicular membrane

Zusammenfassung

Kapitel 1 dieser Dissertation befasst sich mit der Synthese von wasserlöslichen Bis- und Tetrakis-Zn(II)-Cyclen Komplexen mit starren Strukturen und deren Anwendung in der molekularen Erkennung von Analyten biologischer Relevanz. Boc-geschütztes 6-Chloro-1,3,5-Triazin-Biscyclen wurde per Suzuki-Kreuzkupplung in mittelmäßigen bis hohen Ausbeuten an verschiedene Aryl- und Alkyleinheiten geknüpft und davon ausgehend die jeweiligen Bis- oder Tetrakis-Zn(II)-Cyclen Komplexe hergestellt. Die Lumineszenten unter den Aren substituierten Bis- und Tetra-Zn(II)-Cyclen Komplexen wurden durch Absorptions- und Lumineszenzspektroskopie im Hinblick auf deren Antwort gegenüber Phosphationen unter physiologischen Bedingungen getestet. Es wurden außerdem Tetra-Zn(II)-Cyclen Komplexe entdeckt, die eine signifikante Affinität gegenüber genetisch kodierbare Oligoaspartat- und Glutamatsequenzen (D₄- und E₄-Tag) aufweisen. Die starren Strukturen der Substanzen verstärken die elektronische Kupplung zwischen der Metallkomplexbindungsstelle und dem Reporter-Farbstoff, was zu einem verbesserten Signal der Anionenbindung in homogener wässriger Lösung führt.

Kapitel 2 beschäftigt sich mit der Synthese und der potentiellen Anwendung von starren amphiphilen molekularen Rezeptoren, Biokonjugaten und Radiopharmaka, die auf Metall-Cyclen Komplexen basieren und per „Click-Chemie“ synthetisiert wurden. Mittels der bioorthogonalen Click-Reaktion haben wir biotinylierte Zn(II)-bis-Cyclen Komplexe synthetisiert und ihre vielversprechende Anwendung in der aktivitätsbasierten Proteomik gezeigt. Cholesterin und mit langkettigen Alkylresten substituierte Zn(II)-Cyclen Komplexe wurden synthetisiert, um eine Templat gesteuerte kooperative Selbstorganisation von Nukleotiden an Grenzflächen zu erreichen, welche durch Kombination von selbstorganisierender Monoschicht (SAM) und Langmuir Blodgett Technik (LB) erzeugt wurden. Eine Anwendung dieser Komplexe ist der Einsatz als Bindungsstellen an Grenzflächen, die durch eine Kombination von SAM und LB Film Methoden oder in vesikularen Oberflächen entstehen. Die Bindungseigenschaften dieser neuen amphiphilen mit Komplexen funktionalisierten Oberflächen werden gerade untersucht.

Kapitel 3 beinhaltet das Design, die Synthese und die Anwendungen von amphiphilen Lanthanidkomplexen, die in liposomale Oberflächen eingebettet sind. Wir haben Tb(III) Komplexe synthetisiert und in liposomale Oberflächen integriert. Dieses phosphoreszente Nanosystem hat eine potentielle Anwendung als Sensor für physiologische Temperaturänderungen. Weiterhin haben wir erreicht, Lanthanid basierte amphiphile Komplexe als Reporter-Farbstoffe nichtkovalent zusammen mit Analytbindungsstellen in Vesikelmembrane im Nanomaßstab einzubetten.

Abbreviations

abs	Absolute	HSQC	heteronuclear single quantum coherence
ADP	Adenosine di phosphate	IR	Infrared
ATP	Adenosine tri phosphate	LB	Langmuir- Blodgett
Boc	tert-butyloxycarbonyl	MeCN	acetonitrile
br	broad	MeOH	methanol
BSA	Bovine Serum Albumin	MLV	multilamellar vesicle
COSY	Correlation spectroscopy	MS	Mass spectrometry
CuAAC	Copper catalyzed Azide Alkyne Cycloaddition	MW	Molecular weight
DCM	Dichloromethane	NP	Nanoparticle
DFT	Density Functional Theory	NMR	Nuclear Magnetic Resonance
DIPEA	Diisopropyl ethylamine	o/n	over night
DLS	Dynamic Light Scattering	PEG	polyethylene glycol
DMF	N,N-dimethylformamide	PET	Positron Emission Tomography
DMPC	1,2-dimyristoyl- <i>sn</i> -glycero-3-phosphocholine	PPi	pyrophosphate
DNA	Deoxyribonucleic acid	p-Ser	O-phospho-L-serine
DOPC	1,2-dioleoyl- <i>sn</i> -glycero-3-phosphocholine	rt	room temperature
DPPC	1,2-dipalmitoyl- <i>sn</i> -glycero-3-phosphocholine	UV	Ultraviolet

DSC	Differential Scanning Calorimetry	SAM	self assembled monolayer
DSPC	1,2-distearoyl- <i>sn</i> -glycero-3-phosphocholine	SDS-PAGE	sodium dodecyl sulfate polyacrylamide gel electrophoresis
DSPE-PEG350	1,2-distearoyl- <i>sn</i> -glycero-3-phosphoethanolamine-N-[amino(polyethyleneglycol)-350] (ammonium salt)	SMPC	1-stearoyl-2-myristoyl- <i>sn</i> -glycero-3-phosphocholine
DTPA	diethylene triamine pentaacetic acid	SUV	small unilamellar vesicle
ECL	enhanced chemiluminescent	TBTA	tris-(benzyltriazolymethyl)amine
eg	for example	TFA	trifluoroacetic acid
eq	equivalents	THF	tetrahydrofuran
ESI	Electron spray ionization	TLC	thin layer chromatography
HEPES	4-(2-hydroxyethyl)-1-piperazineethanesulfonic acid	TMS	trimethylsilyl
HBTU	<i>O</i> -(1-benzotriazolyl)- <i>N,N,N',N'</i> -tetramethyluronium hexafluorophosphate	T_m	transition temperature
HMBC	heteronuclear multiple bond correlation	T_p	pre-transition temperature

Appendix

Curriculum Vitaé

Mouchumi Bhuyan

CONTACT INFORMATION c/o Prof. Dr. Burkhard Koenig
Institut für Organische Chemie,
Universität Regensburg
Universitätsstr. 31, 93040 Regensburg, Germany
E-mail: mouchumi.bhuyan@yahoo.co.in

PERSONAL DATA Date of Birth: 5th November 1981
Sex: Female
Marital status: Married
Nationality: Indian

EDUCATION PhD in Organic Chemistry Oct'08-Present
University of Regensburg, Germany

MSc. in Chemistry Aug'04-May'06
Indian Institute of Technology, Guwahati, India

BSc. in Chemistry Aug'00-Jul'03
B. Barooah College, Guwahati, India

SCIENTIFIC EXPERIENCE **University of Regensburg, Germany,** Oct'08-Present
Supervisor: Prof. Dr. Burkhard Koenig

Indian Institute of Technology, Kanpur, India Jul'07-Aug'08
Supervisor: Late Dr. B. D. Gupta
"Synthesis of modified Organocobaloximes as model compounds for Vitamin B12 and their Co-C bond reactivity studies"

Indian Institute of Technology, Guwahati, India Jan'06-May'06
Supervisor: Dr. Gopal Das
"Synthesis, Characterization and Fluorescence Studies of Tripodal Ligands"

PUBLICATIONS

Temperature responsive phosphorescent small unilamellar vesicles M. Bhuyan, B. Koenig (*manuscript under preparation*)

Rigid Luminescent Bis-Zinc(II)-Bis-Cyclen Complexes for the Detection of Phosphate Anions and Non-Covalent Protein Labeling in Aqueous Solution M. Bhuyan, E. Katayev, S. Stadlbauer, H. Nonaka, A. Ojida, I. Hamachi, B. König *Eur. J. Org. Chem.* **2011**, 2807
doi: 10.1002/ejoc.201100103

Synthesis of rigidified flavin-guanidinium ion conjugates and investigation of their photocatalytic properties H. Schmaderer, M. Bhuyan, B. König. *Beilstein J. Org. Chem.* **2009**, 5(26)
doi: 10.3762/bjoc.5.26

Tripodal naphthalene ether ligand: Solidstate anion recognition and Fluorescence studies A. Pramanik, M. Bhuyan, R. Choudhury, G. Das *Journal of Molecular Structure* **2008**, 879, 88
doi:10.1016/j.molstruc.2007.08.016

Aromatic guest inclusion by a tripodal ligand: Fluorescence and Structural studies A. Pramanik, M. Bhuyan, G. Das *J. Photochem. Photobiol. A: Chem.* **2008**, 197,149
doi:10.1016/j.jphotochem.2007.12.020

Biphenyl-Bridged Dicobaloximes: Synthesis, NMR, CV, and X-Ray Study M. Bhuyan, M. Laskar, B. D. Gupta *Organometallics* **2008**, 27, 594
doi: 10.1021/om7009045

Co-C Bond Homolysis: Reactivity Difference between Alkyl- and Benzylcobaloximes D. Mandal, M. Bhuyan, M. Laskar, B. D. Gupta *Organometallics* **2007**, 26, 2795
doi: 10.1021/om070053q

Co-C Bond Reactivity and Cis Influence Relationship in Benzylcobaloximes with Glyoxime and Dimesitylglyoxime M. Bhuyan, M. Laskar, D.Mandal, B. D. Gupta *Organometallics* **2007**, 26, 3559
doi: 10.1021/om7003578

The interactions between axial and equatorial ligands in cobaloximes: NMR changes D. Mandal, P. Chadha, M. Laskar, M. Bhuyan, B. D. Gupta *Tetrahedron Lett.* **2007**, 48, 2377
doi: 10.1016/j.tetlet.2007.01.140

AWARDS AND ACHIEVEMENTS	Bavarian Research Scholarship, Germany (Bayerische Forschungs Stiftung)	2009-2011
	Degussa-Evonik Scholarship, Germany	2008-2009
	Best poster Award in MTIC-XII, IIT Madras, India	Dec'07
	Qualified in GATE'06, India GATE Rank: All India Rank 58; GATE Score: 508 Total no. of students appeared: 4542	Feb'06
	Merit-cum-Means Scholarship, IIT Guwahati, India	Apr'04-Apr'06
	Fifth rank in the B.Sc. examination with distinction, Gauhati University, India	Jul'03
CONFERENCES	4th International Summer School "Supramolecular Systems in Chemistry and Biology", Sept'11, Regensburg, Germany <i>Rigid Luminescent BisZinc(II)-BisCyclen Complexes and Non Covalent Protein Labelling in Aqueous Solution</i> (poster presentation)	
	2nd INDIGO PhD Research Conference and Intensive Course, Oct'10, Regensburg, Germany	
	3rd EuCheMS Chemistry Congress, Aug-Sept'10, Nuremberg, Germany <i>"Rigid Luminescent Zinc(II)-Bis-Cyclen Based Receptors for Recognition of Phosphate Anions in aqueous solution"</i> (poster presentation)	
	2nd German-Indian Symposium on Frontiers of Chemistry, Sept'09, University of Leipzig, Leipzig, Germany <i>"Luminescent Zinc(II)Bis-cyclen Receptors in Molecular Recognition"</i> (poster presentation)	
	V th International Symposium Supramolecular Systems in Chemistry and Biology, May'09, Kyiv, Ukraine <i>"Zinc(II)-cyclen Based Receptors for The Molecular Recognition of Phosphate Anions"</i> (poster presentation)	
	Modern Trends in Inorganic Chemistry (MTIC)-XII, Dec'07, Indian Institute of Technology Madras, India <i>"Biphenyl-Bridged Dicobaloximes: Synthesis, NMR, CV, and XRay Study"</i> (poster presentation)	

National Symposia on Organic and Inorganic Interface, Dec'04 Indian Institute of Technology Guwahati, Assam, India

LANGUAGES English (fluent, -TOEFL score 94/120 in Feb'08), German (basic), Assamese (native), Hindi, Bengali

ANALYTICAL NMR, UV-Visible spectrophotometer, FT-IR, Cyclic Voltametry, TECHNIQUES Fluorescence Spectrophotometer

KNOWN & Chem Draw, ISIS Draw, ChemCraft, Origin, ShelXl, WinGx, Mercury SOFTWARES 1.2.1, enCIFer

FAMILIER
